

ACADÉMIE ROUMAINE

COMITÉ DE RÉDACTION

Rédacteur en chef:

MIHAI BĂCESCU, membre de l'Académie Roumaine

Rédacteur en chef adjoint:

NICOLAE SIMIONESCU, membre de l'Académie Roumaine

Membres:

NICOLAE BOTNARIUC, membre de l'Académie Roumaine;
OLGA NECRASOV, membre de l'Académie Roumaine;
PETRU-MIHAI BĂNĂRESCU, membre correspondant de
l'Académie Roumaine; prof. dr. IRINA TEODORESCU; prof. dr.
RADU MEȘTER, secrétaire de rédaction.

La «Revue roumaine de biologie – Série de biologie animale» paraît
deux fois par an. Toute commande de l'étranger sera adressée à:

EDITURA ACADEMIEI ROMÂNE, Calea 13 Septembrie, nr. 13, Sector 5, P.O.Box 5-42,
București, Românie, RO-76117, Tel. 401-411 9008, 401-410 3200, Fax. 401-410 3983.

RODIPET S.A., Piața Presei Libere nr. 1, Sector 1, P.O.Box 35-37, București, Românie, Fax 401-
222 64 07, Tel. 401-618 5103; 401-222 4126.

ORION PRESS IMPEX 2000, P.O.Box 77-19, București 3, Românie, Tel. 401 653 7985, Fax 401-
324 0638.

Les manuscrits ainsi que toute correspon-
dance seront envoyés à la rédaction. Les
livres et les publications proposés en
échange seront envoyés à Institutul de
Biologie, Splaiul Independenței 296,
79651 Bucarest.

REVUE ROUMAINE DE BIOLOGIE
Série de biologie animale
Splaiul Independenței 296, P.O.Box 56-53
R-79651, București, Românie
Tél. 223 90 72

© 2000, EDITURA ACADEMIEI ROMÂNE
Calea 13 Septembrie nr. 13,
sector 5, RO-76117, București,
Tél. 401-410 32 00; 401-411 90 08
Fax: 401-410 39 83

REVUE ROUMAINE DE BIOLOGIE

SÉRIE DE BIOLOGIE ANIMALE

TOME 44, N° 1

janvier – juin 1999

SOMMAIRE

| | |
|---|-----|
| OTILIA ZĂRNESCU, RADU MEȘTER, Incorporation of vitellin-gold by ovarian follicles of <i>Carassius auratus gibelio</i> . I. <i>In vitro</i> studies..... | 3 |
| OTILIA ZĂRNESCU, RADU MEȘTER, Immunolocalization of clathrin in the vitellogenic oocytes of <i>Triturus vulgaris</i> | 15 |
| CĂLIN TESIO, IRINA TEODORESCU, Food analysis in <i>Bufo viridis</i> adults..... | 19 |
| LUCIA MOLDOVAN, OTILIA ZĂRNESCU, MARINELA BUNEA, OANA CRĂCIUNESCU, LIDIA CONSTANTINESCU, Comparative studies on <i>in vitro</i> fibrillogenesis of collagen from fish and pig cornea..... | 27 |
| C.-C. PRUNESCU, PAULA PRUNESCU, The genital system in <i>Lamyctes anderis</i> (Hemichordata, Aplousobranchia, Aplousobranchia)..... | 35 |
| N. MIRANCEA, DORINA MIRANCEA, Morphologic aspects and differentiation of some digestive tract segments during ontogenesis..... | 41 |
| ZORICA-ILEANA HERTZOG, F. MIXICH, R. HERTZOG, Chromosomal alterations in Rubinstein-Taybi syndrome..... | 53 |
| GETA RIȘNOVEANU, A. VĂDINEANU, GH. IGNAT, The structure of the benthic Oligochaeta communities in the aquatic ecosystems of the Danube Delta..... | 61 |
| GALINA NĂFORNIȚĂ, CARMEN POSTOLACHE, A. VĂDINEANU, The role of benthic bivalve Mollusc populations in the nitrogen and phosphorous cycles..... | 77 |
| IRINA TEODORESCU, DAN COGĂLNICEANU, CLEOPATRA STERGHIU, Arthropod diversity along an environmental gradient on the Sacalin Island, Danube Delta..... | 85 |
| MARIN FALCĂ, Numerical structure of earthworm populations in different forestry soil ecosystems..... | 93 |
| PAULA PRUNESCU, C.-C. PRUNESCU, Lésions du péritoine chez les rats intoxiqués avec du plomb..... | 101 |

REV. ROUM. BIOL. –BIOL. ANIM., TOME 44, N° 1, P. 1–108, BUCAREST, 1999

INCORPORATION OF VITELLIN-GOLD BY OVARIAN FOLLICLES OF *CARASSIUS AURATUS GIBELIO*

I. *IN VITRO* STUDIES

OTILIA ZĂRNESCU, RADU MEȘTER

Electron microscopy has been used to examine the crucian carp early vitellogenic follicles, *in vitro*, in the presence of electron-dense tracer.

Vitellin was adsorbed to colloidal gold, and the organelles traversed by internalized ligand were examined at various time intervals (30 minutes, 1, 3, 5 and 18 hours), after an initial incubation of follicle 2h at 1°C.

The gold particles appeared after an hour of incubation, in endocytotic compartments of internalization (vesicles) and transport (endosomes and multivesicular bodies). At 18 h after incubation with tracers the gold particles appeared at the periphery of primordial yolk globules.

Our results indicate that oocyte endocytosis, *in vitro*, is constitutive.

Moreover, *in vitro*, surface epithelial cells exhibit macropinocytosis instead of follicle cells that are little endocytotic.

During their development fish oocytes accumulate an insoluble lipoglycophosphoprotein complex, yolk, whose different components originate from a common precursor, vitellogenin (VTG) synthesized and secreted by the liver of vitellogenic females (13).

Many studies on the pathway of VTG transportation to the oocytes have been done by culturing vitellogenic oocytes of *Xenopus laevis* in media containing isotope-labeled VTG (1), gold conjugates (2, 14) or iron-conjugate VTG (9).

In teleosts, the largest group of vertebrates, the incorporation of VTG has not been studied so extensively. Selective incorporation and processing of VTG *in vitro* was studied by quantitative methods (5, 7, 10, 12).

In vitro culture system has been developed for studies on vitellogenin sequestration into vitellogenic oocytes in the mummichog (5, 16), rainbow trout (7, 12) and snook (15).

Our previous light microscopic observation has shown that in a short term culture system ovarian follicles of crucian carp survive well *in vitro* and sequestered FITC-Dextran from the culture medium (18).

In the present study we investigated at electron microscopic level the compartment of crucian carp, *Carassius auratus gibelio* early vitellogenic follicle *in vitro* used an electron-dense tracer, vitellin adsorbed with colloidal gold.

MATERIALS AND METHODS

Animals: The experiments were carried out on crucian carp, *Carassius auratus gibelio*, obtained from Fisheries Research Station, Nucet. The specimens were acclimatized to laboratory conditions for two or more weeks, at room temperature, in glass aquarium containing tap water.

Preparation of tracer - vitellin gold complex: Vitellin (from egg, Sigma) was adsorbed to 15 nm colloidal gold prepared by the tannic acid procedure of Slot and Geuze (11) using the protocol for protein adsorption described by these authors.

Follicle culture: Early vitellogenic follicles were manually dissected from ovary and maintained in protein free culture media (Leibovitz L-15, Sigma) for 1 hour before the incubations were started. After this time follicles were examined under a dissecting microscope and only those maintaining the appearance of freshly dissected follicles were used in the subsequent cultures (18).

Early vitellogenic follicles were incubated with vitellin gold conjugates diluted 1:10 with culture medium initially for 2 hours at 1°C and then for 30 minutes, 1, 3, 5 and 18 hours at room temperature. After incubation follicles were washed three times with culture medium containing 0.1% bovine serum albumin (BSA) and then fixed.

Electron microscopy: Ovarian follicles were fixed in 2.5% glutaraldehyde in 0.1 M Na-cacodylate, pH 7.4 with 1% dimethyl sulfoxide (DMSO), overnight, at 4°C, washing in the same buffer, overnight at 4°C and postfixed overnight in 1% OsO₄ also in cacodylate buffer. The follicles were then rinsed with cacodylate buffer, dehydrated in ethanol and embedded in Epon 812. Sections were stained with lead citrate and uranyl acetate after sectioning.

RESULTS

Early vitellogenic follicles were chosen for *in vitro* observation since these oocytes are in a rapid phase of vitellogenesis.

Electron micrographs have shown that cultured oocytes were surrounded by follicle and theca cells (Fig. 1A) or these cells are detached as sheets (Fig. 1B). Dissociation of follicle cells from the oocyte may be favored by cold incubation of ovarian follicles (2 h at 1°C) because after this treatment follicle microvilli are disorganized and retracted from pore channels of zona radiata (Fig. 1C).

The cells of the follicle surface epithelium show a macropinocytosis on luminal side. Ruffles form at the end of these epithelial cells (Fig. 2A) and macropinosomes have 0.577 µm in diameter (Fig. 2B). Moreover, the epithelial cells seem to uptake the molecules from culture medium through clathrin coated pits (Fig. 2C).

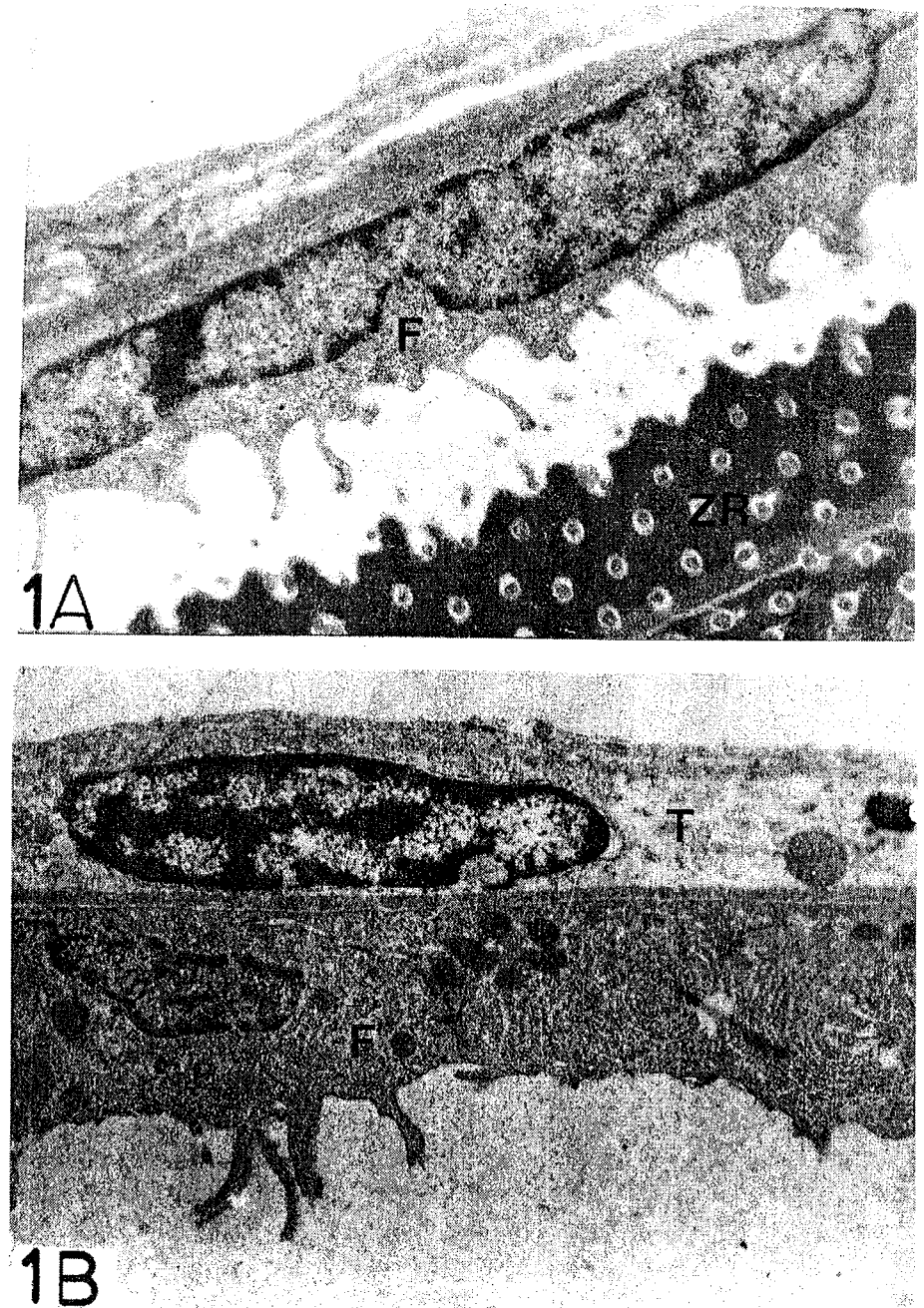


Fig. 1 A, B. Electron-micrographs of cultured ovarian follicles.

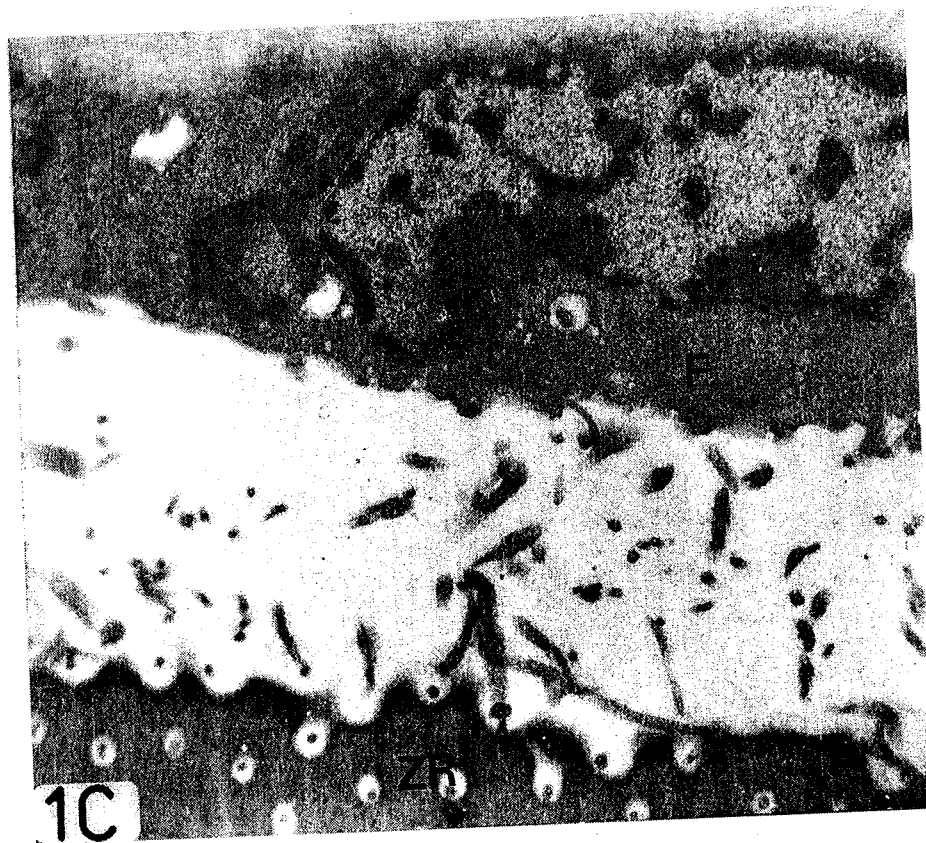


Fig. 1 A-C. Electron-micrographs of cultured ovarian follicles. Cultured oocytes were surrounded by follicle and theca cells (A) or these cells are detached as sheets (B). After cold incubation (2 h at 1°C) follicle microvilli are disorganized and retracted from pore channels of zona radiata (C). F-follicle cell; T-theca cell; ZR-zona radiata. A, B, C - × 10,000.

In the follicle cells surrounding the oocyte there were a few endocytic invaginations and vesicles (data not shown).

Following a 2h incubation at 1°C in the presence of vitellin-gold, periphery of the oocytes was devoid of any membranous vesicles. In addition, all transport compartments (endosomes, multivesicular bodies) were empty (Fig. 3A-C). Then, after incubation at room temperature, in the oocytes, all compartments of internalization (coated pits and vesicles) and transport were filled with an electron-dense material (Fig. 4A-D). The vitellin-gold conjugate was excluded from compartments filled with electron-dense material. The tracer was observed in endocytic pits (Fig. 5A) and vesicles (Fig. 5B-C), at 30 min of incubation and in endosomes fused with different size primordial yolk globules (Fig. 5D-E), after 5h of culture.

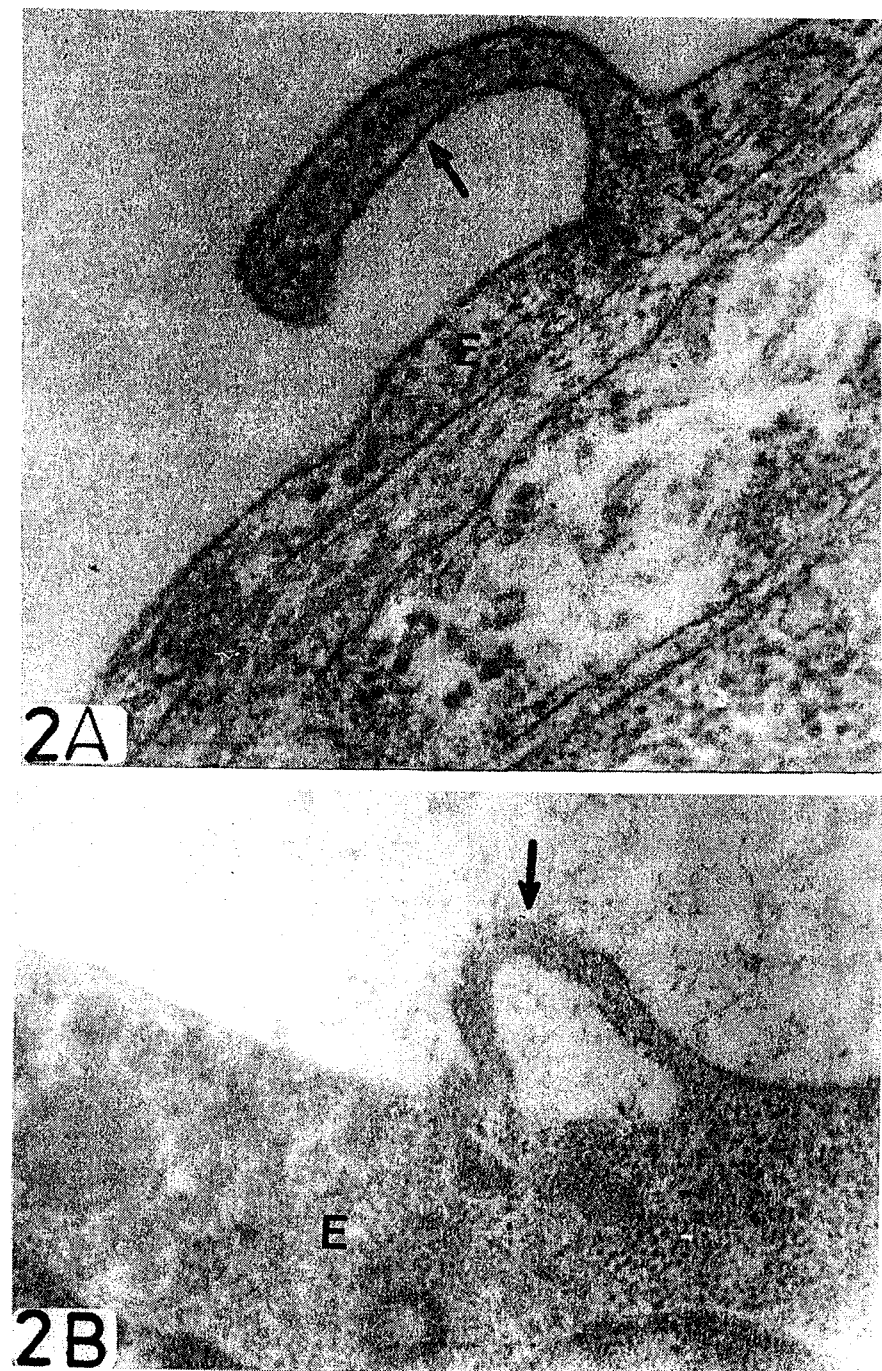


Fig. 2 A, B.

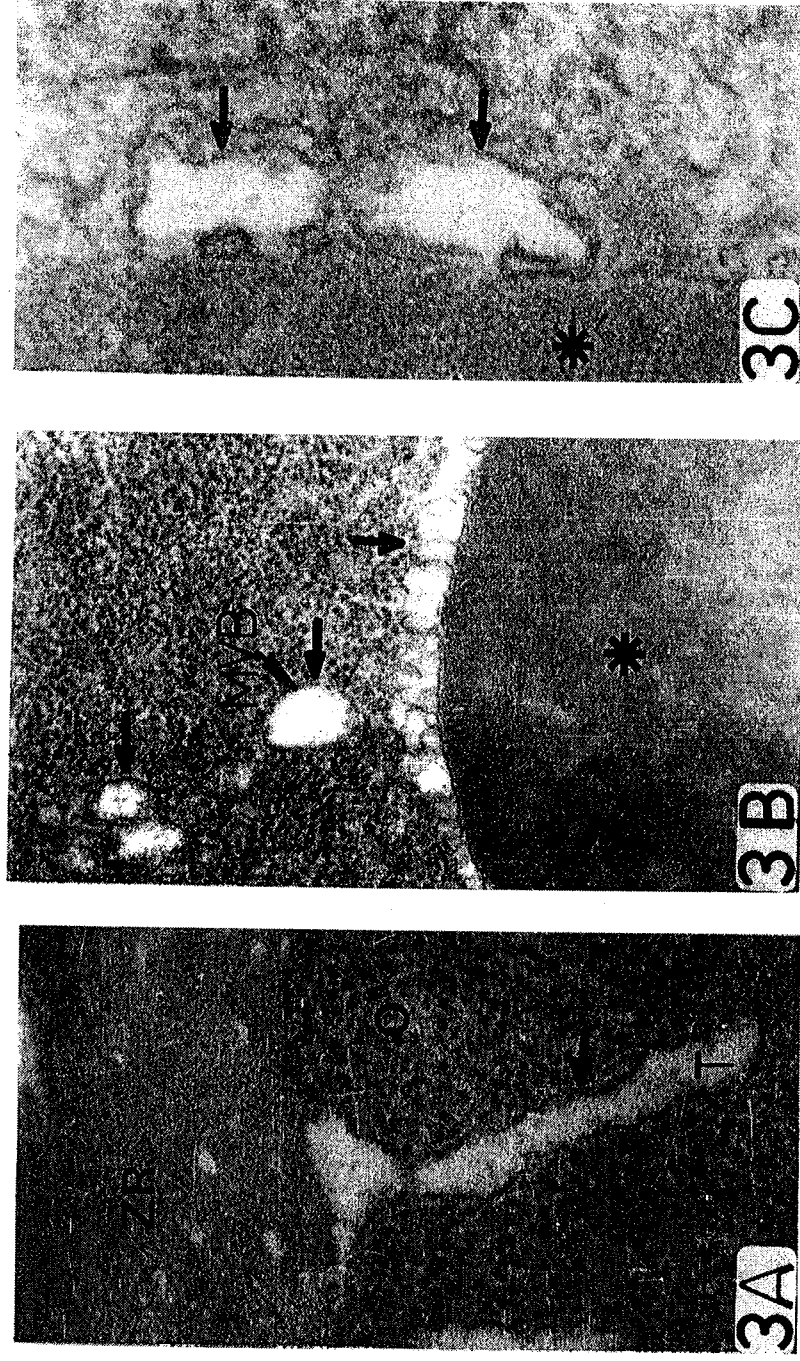


Fig. 3 A-C. Incubation of ovarian follicle at 1°C in presence of vitellin gold. The transport compartments (A-C) were empty (arrows). O-oocytic; T-tubules; MVB- multivesicular bodies; ZR-zona radiata; *-yolk globules. A- x75,000; B- x37,000; C- x150,000.

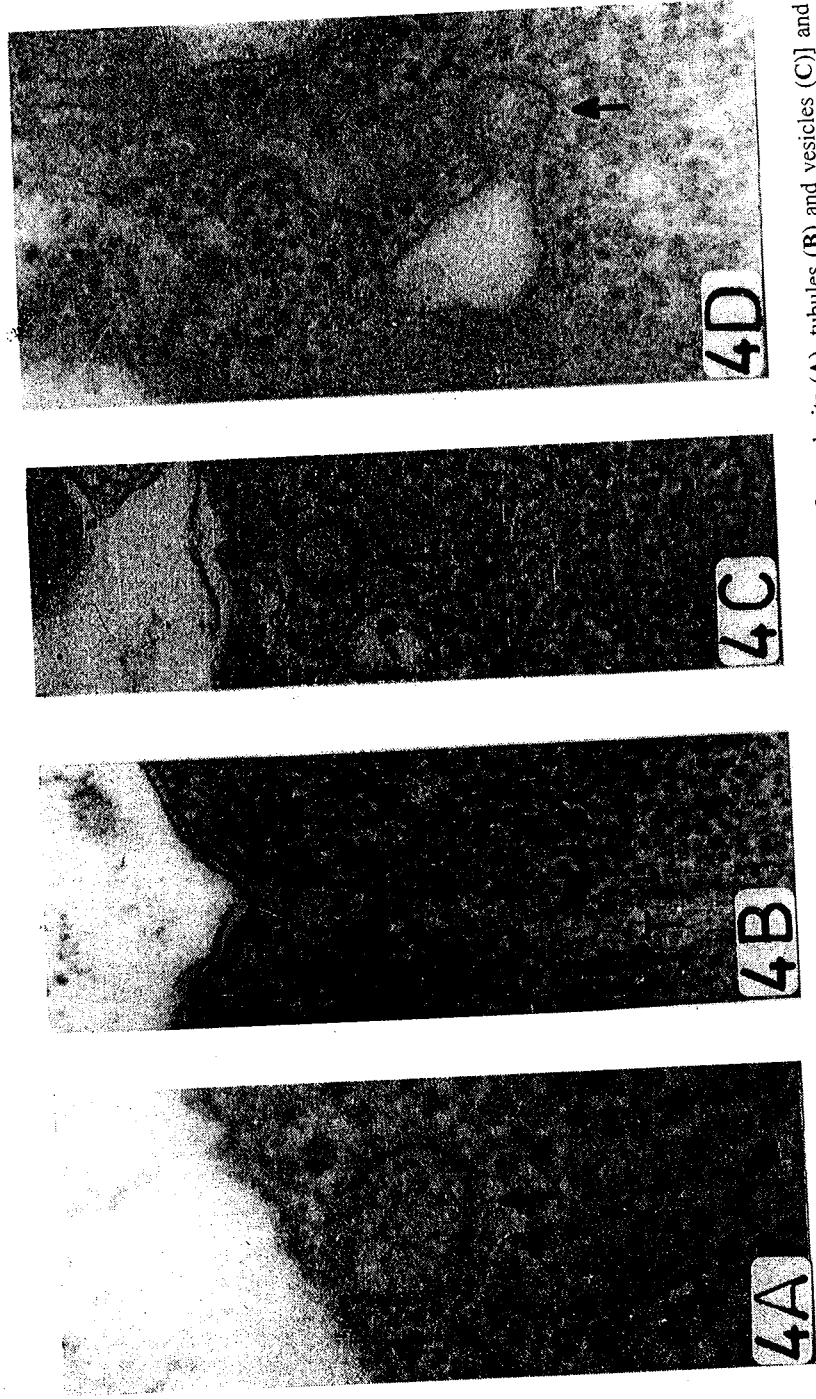


Fig. 4 A-D. After incubation at room temperature all compartments of internalisation [coated pits (A), tubules (B) and vesicles (C)] and transport (D) were filled with an electron-dense material (arrows). T-tubules; A- $\times 150,000$; B, C - $\times 75,000$; D- $\times 90,000$.

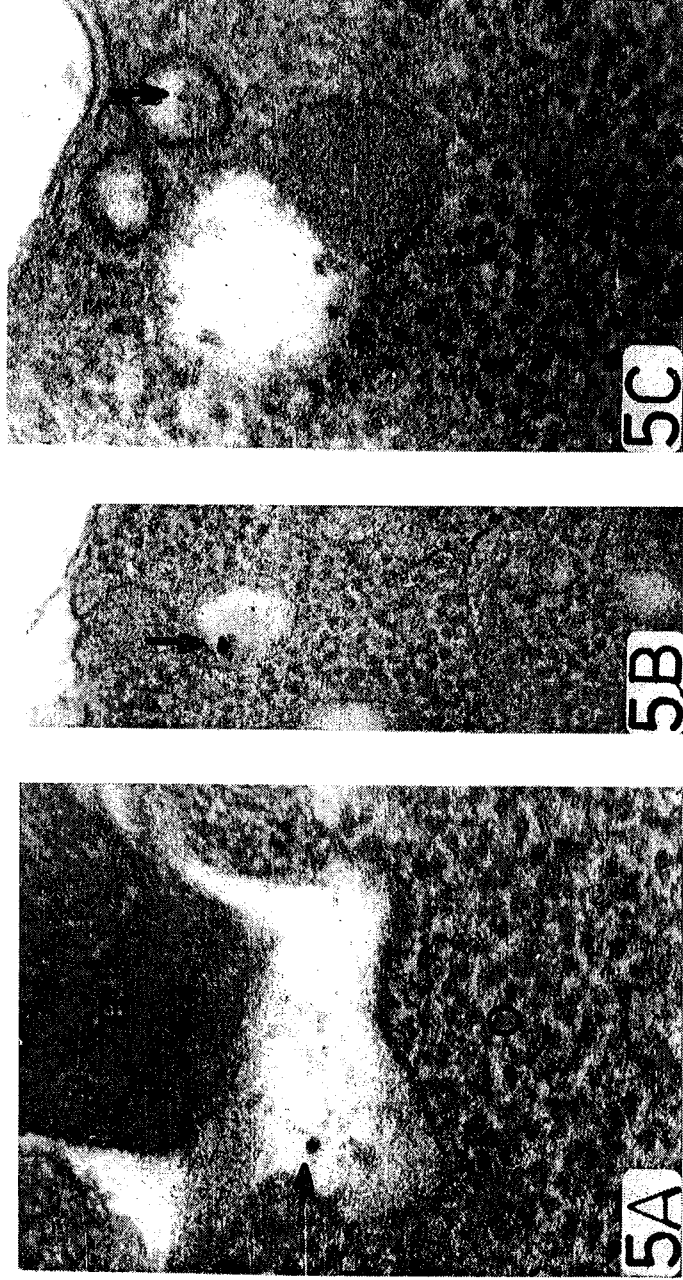


Fig. 5 A, B, C - Distribution of vitellin gold in endocytotic pathway of crucian carp oocyte.

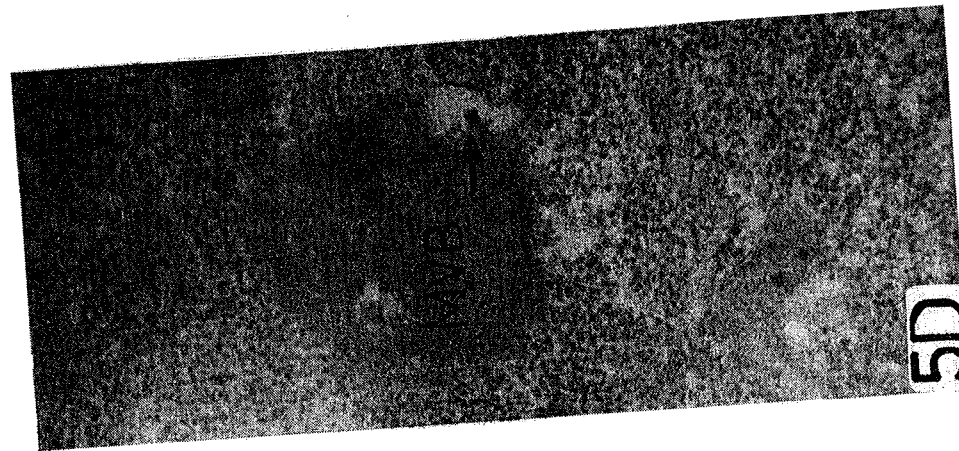
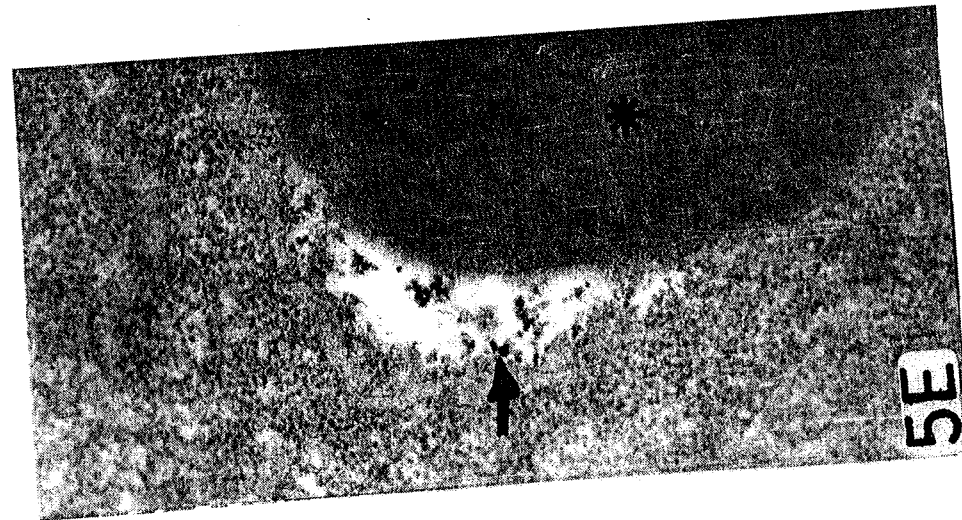
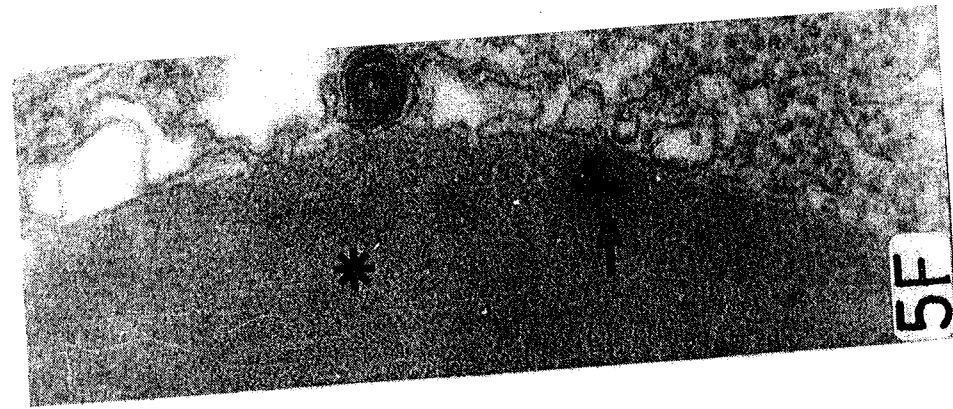


Fig. 5 A-F. Distribution of vitellin gold in endocytotic pathway of crucian carp oocyte. The electron-dense tracer was observed (arrows) in endocytic pits (A) and vesicles (B-C) after 30 min. of incubation and in endosomes fused with multivesicular bodies (D) and primordial yolk globules (E) after 5 h of culture. At 18 h of incubation the gold particles were present in superficial layers of primordial yolk globules (F). A, C - $\times 100,000$; B, F - $\times 75,000$; D, E - $\times 45,000$.

coated vesicles. Thus, the oocyte receptors are internalized at the same rate whether they are occupied or not (2).

The presence of tracers in a different endocytic compartment without electron dense material (originally from culture medium) present in other compartments indicates that vitellin-gold and electron-dense material was internalized through different endocytic pathways.

Our results indicate the presence of vitellin-gold conjugate in crucian carp primordial yolk globules after 18 h of incubation. Wall and Patel (14) postulate that vitellogenin internalized at low levels by the oocytes of *Xenopus laevis* is being shunted into an alternate (degenerative) pathway from which entry into yolk platelets is no longer possible after a certain period. Instead, other study (2) shows at the same species that vitellogenin internalized at low levels enters in mature yolk platelets only 7 h after the internalisation had begun.

Our observation also shows that cell surface epithelium could uptake molecules from culture medium by macropinocytosis, morphological aspects of this process being similar to those of other cells (3, 4).

In conclusion we used an electron-dense tracer for morphological characterization of endocytosis in the crucian carp early vitellogenic follicle *in vitro*.

REFERENCES

1. Brummett A.R., Dumont J.N. 1977, *Dev. Biol.*, **60**, 482-486.
2. Busson S., Ovtracht L., Gounon P., 1989, *Biol. Cell.*, **67**, 37-49.
3. Fawcett D.W., 1965, *J. Histochem. Cytochem.*, **13**, 75-90.
4. Hewlett L.J., Prescott A.R., Watts C., 1994, *J. Cell Biol.*, **124**, 689-703.
5. Kanungo J., Perino T., Wallace R.A., 1990, *J. Exp. Zool.*, **254**, 313-321.
6. Nagahama Y., 1987, *Zool. Sci.* **4**, 209-222.
7. Nagler J.J., Tyler C.R., Sumpter J.P., 1994, *J. Exp. Zool.*, **268**, 45-52.
8. Opresko L., Wiley H.S., Wallace R.A., 1980, *Cell* **22**, 47-57.
9. Richter H-P., Bauer A., 1990, *Eur. J. Cell Biol.*, **51**, 53-63.
10. Shibata N., Yoshikuni M., Nagahama Y., 1993, *Develop. Growth & Differ.*, **35**, 115-121.
11. Slot J.W., Geuze H.J., 1985, *Eur. J. Cell Biol.* **38**, 87-93.
12. Tyler C.R., Sumpter J.P., Bromage N.R., 1990, *J. Exp. Zool.*, **255**, 216-231.
13. Tyler C.R., Sumpter J.P., 1996, *Fish. Fisheries Rev.*, **246**, 171-179.
14. Wall D.A., Patel S., 1987, *Dev. Biol.*, **119**, 275-289.
15. Wallace R.A., Boyle S.M., Grier H.J., Selman K., Petrino T.R., 1993, *Aquaculture*, **116**, 257-273.
16. Wallace R.A., Hollinger T.G., 1979, *Exp. Cell Res.*, **119**, 277-287.
17. Wallace R.A., Opresko L., Wiley H.S., Selman K., 1983, In; *Molecular Biology of Egg Maturation*. (Ciba Found. Symp. 98), Pitman Books (London), p. 228-248.
18. Zărnescu O., Meșter R., 1997, *St. Cerc. Biol. Biol. Anim.*, **49**, 133-138.

Received September 30, 1998

Faculty of Biology
Bucharest, Spl. Independenței 91-95
E-mail: otilia@ibd.dbio.ro

IMMUNOLocalIZATION OF CLATHRIN IN THE VITELLOGENIC OOCYTES OF *TRITURUS VULGARIS*

OTILIA ZĂRNESCU, RADU MEȘTER

We used indirect immunoperoxidase to study the distribution of clathrin in vitellogenic oocytes of *Triturus vulgaris*.

Examination of vitellogenic follicles revealed that antigen was detected as a diffuse reaction under the plasma membrane. Furthermore, an accumulation of stain was observed as spots in the cortical cytoplasm. Moreover, in all vitellogenic oocytes immunolabeling was observed throughout the cytoplasm, around yolk platelets. Also, the localization of the antigen was associated with the surface epithelium of ovarian follicles.

Our observations revealed more unassembled than assembled clathrin in all vitellogenic oocytes.

Clathrin-coated vesicles mediate endocytosis of transmembrane receptors and transport of newly synthesized lysosomal hydrolases from the *trans*-Golgi network to the lysosome. Thus, two sets of coat proteins contain clathrin: one along with AP2 (adaptor protein) complexes, drives endocytic vesicle formation at the plasma membrane; other, along with AP1 complexes, drives transport vesicle formation at the *trans*-Golgi network (15).

Receptor-mediated endocytosis assures selective, efficient, and accumulative uptake of yolk components and mediates oocyte growth (16, 18). The role of extensive micropinocytotic activity at the surface of vitellogenic oocytes has been demonstrated by electron microscopy for several species of amphibians. Receptor-mediated endocytosis begins with binding of vitellogenins to receptors on the oolemma. This complex then clusters in clathrin-coated pits and, after endocytosis, intracellular vesicles appear. This process requires a considerable amount of ooplasmic clathrin.

Observation carried out on mosquito (6, 12), crucian carp (19) and *Xenopus laevis* oocytes (9) provide evidence suggesting that before the onset of endocytosis, the previtellogenic oocyte has the capacity to accumulate an extensive amount of clathrin. By contrast, in highly differentiated cells, including hepatocytes (4) and macrophages (17), the intracellular content of clathrin remains fairly constant and is independent of the endocytic activity of the cell.

In the present study, experiments were carried out to determine the distribution of clathrin in the vitellogenic oocytes of *Triturus vulgaris*.

MATERIALS AND METHODS

Fragments of *Triturus vulgaris* ovaries were fixed in 10% formaldehyde in 0.1M phosphate-buffered saline, pH-7.4 (PBS), with 1% dimethylsulphoxide (DMSO), overnight, at 4°C. After washing in PBS, the samples were then transferred in 2% glycine in PBS, to quench the free aldehyde groups, dehydrated and embedded in paraffin.

Slides were given several 10-min rinses in 0.1M PBS and sequentially incubated in methanol: H₂O₂ (9:1) to remove endogenous peroxidase (30 min), PBS plus 10% normal rabbit serum to remove non-specific background staining (1h), goat anti-clathrin, primary antibody (Sigma), diluted 1:40 (overnight, at 4°C), rabbit anti-goat IgG peroxidase conjugate (Sigma), diluted 1:200 (1h, at room temperature). Each incubation step was followed by four 5 min rinses in PBS. To visualize the primary antibody binding sites, the slides were incubated for 5-15 min in a solution of 3,3'-diaminobenzidine (0.05%) and 0.015% hydrogen peroxide, dissolved in 0.1M PBS.

RESULTS AND DISCUSSION

To determine the distribution of clathrin in vitellogenic oocytes, immunocytochemistry was carried out using the clathrin heavy chain antibody on tissue slices.

Examination of vitellogenic follicles revealed that antigen was detected as a diffuse reaction under the plasma membrane. Furthermore, an accumulation of stain was observed as spots in the cortical cytoplasm (Fig.1A). Moreover, in all vitellogenic oocytes immunolabeling was observed throughout the cytoplasm, around yolk platelets (Fig.1C). Also, the localization of the antigen was associated with surface epithelium of ovarian follicles (Fig.1E).

In controls (Fig. 1B, 1D, 1F), where tissue sections reacted with nonimmune serum, neither punctate nor diffuse reaction was detected.

Clathrin has been immunodetected previously in hemipteran previtellogenic oocytes (3) in the crucian carp oogenesis (19) and in amphibian oocytes (9). However, the distribution of clathrin during vitellogenic phase of urodeles oogenesis has not been extensively studied.

Previous studies have shown that the total cellular pool of clathrin can be either an assembled or a nonassembled form (4), and punctate reaction represents clathrin assembled in pits and coated vesicles (2). Meanwhile the diffuse staining was indicative of a reaction associated with an alternate nonassembled form of the molecule (8).

It is well established that developing oocyte has a great potential for biosynthetic activities. Observations reported previously (3, 6, 19) provide evidence suggesting that before the onset of endocytosis, the previtellogenic

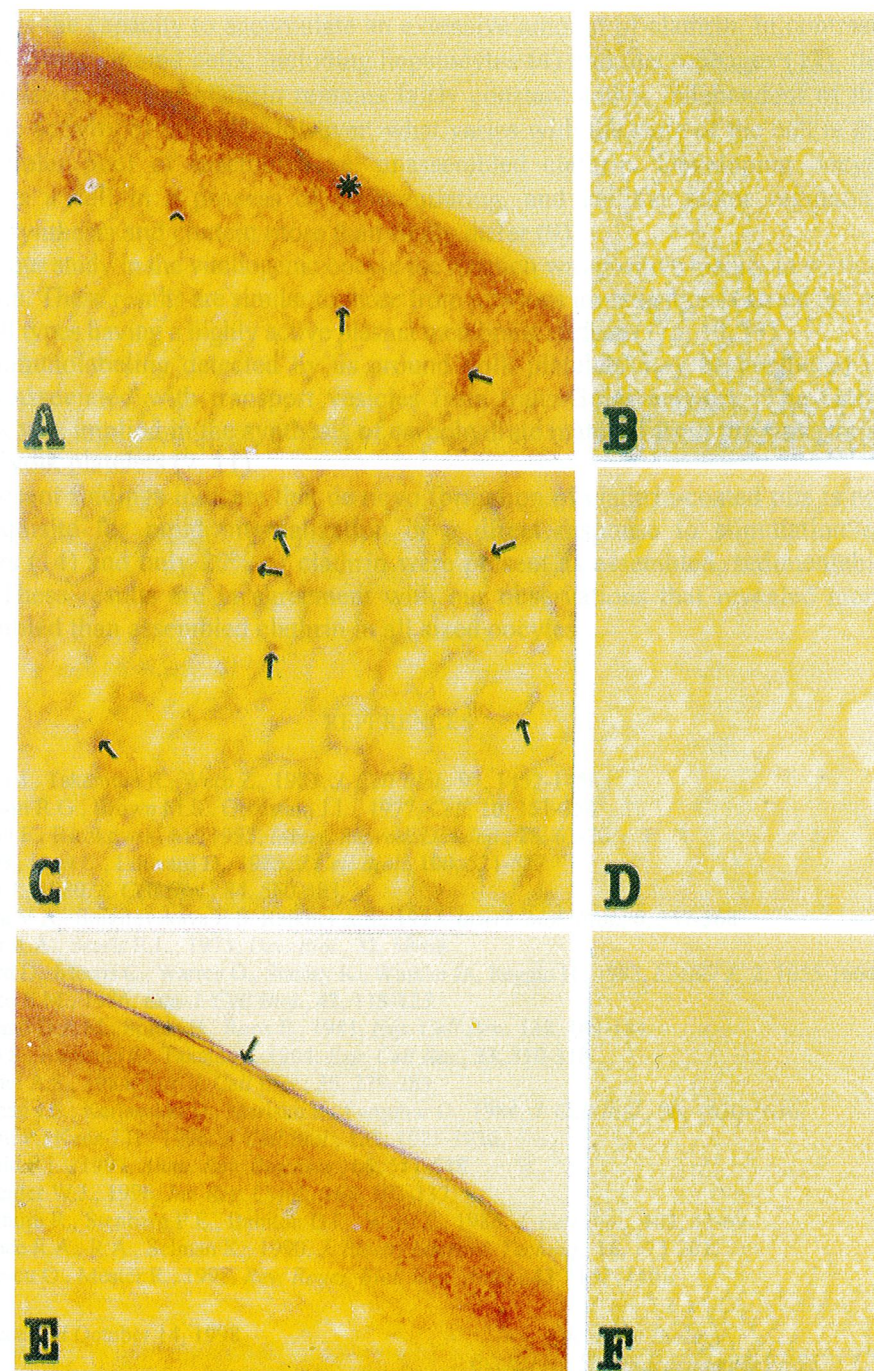


Fig. 1 A-F. Immunolocalization of clathrin in the vitellogenic follicles. In the cortical cytoplasm the antigen was detected as a diffuse subplasmalemmal band (A, *) and as spots (arrows). Also, the immunolabelling was associated with cytoplasm around yolk platelets (C, arrows) and surface epithelium of ovarian follicles (E, arrows). The specificity of the reaction was seen by the absence of stain in controls, sections reacted with nonimmune serum (B, D, F).

oocyte has the capacity to accumulate an extensive amount of clathrin. In contrast, in highly differentiated cells, including hepatocytes (4) and macrophages (17), the intracellular content of clathrin remains fairly constant and is independent of the endocytic activity of the cell. However, what varies with the state of the cell is the total cellular pool of assembled vs. unassembled clathrin. Developing oocyte represents a cell in a process of differentiating, and cellular factor regulating clathrin synthesis and content more than likely differ (9).

In our study in the vitellogenic oocyte the reaction was positive mainly in cortical cytoplasm. These results are similar to those from previous investigations carried out on other cell types having a highly active plasma membrane surface (1, 5, 10, 13).

Immunolabeling detected by us around yolk platelets may be attributed to clathrin associated with transport vesicles from trans-Golgi network. The Golgi complex was implied in the synthesis of carbohydrate material from the superficial layer of yolk platelets (7, 11).

Recent findings indicate that de novo formation of clathrin-coated pits is not a prerequisite for rapid internalization or a direct response to stimulation of receptors (14) and only 20% of clathrin were present as assembled, sedimentable forms. These results are in agreement with our observations that revealed more unassembled than assembled clathrin in all sized oocytes.

REFERENCES

1. Aggeler J., Takemura R., Werb Z., 1983, *J. Cell Biol.*, **97**, 1452-1458.
2. Anderson R.G., Brown M.S., Goldstein J.L., 1977, *Cell*, **10**, 351-364.
3. Dittman F., Biczkowski M., 1995, *Invert. Reprod. Develop.*, **28**, 63-70.
4. Goud B., Huet C., Louvard D., 1985, *J. Cell Biol.*, **100**, 521-527.
5. Heuser J., 1980, *J. Cell Biol.*, **84**, 560-583.
6. Kokoza V.A., Snigirevskaya E.S. Raikhel A.S., 1997, *Insect. Mol. Biol.*, **6**, 357-368.
7. Kosher R.A., Searls R.L., 1973, *Dev. Biol.*, **32**, 50-68.
8. Louvard D., Morris C., Warren G., Stanley K., Winkler D., Reggio H., 1983, *EMBO J.*, **2**, 1655-1664.
9. Merisko E.M., 1986, *Eur. J. Cell Biol.*, **42**, 118-125.
10. Mesland D.A.M., Spiele H., Roos E., 1981, *Exp. Cell Res.*, **132**, 169-184.
11. Ohno S., Karasaki S., Takata K., 1964, *Exp. Cell Res.*, **33**, 310-318.
12. Raikhel A.S., 1984, *Eur. J. Cell Biol.*, **35**, 279-283.
13. Rodman J.S., Kerjaschki D., Merisko E., Farquhar G., 1984, *J. Cell Biol.*, **98**, 1630-1636.
14. Santini F., Keen J.H., 1996, *J. Cell Biol.*, **132**, 1025-1036.
15. Schmid S.L., 1997, *Annu. Rev. Biochem.*, **66**, 511-548.
16. Schneider W.J., 1996, *Int. Rev. Cytol.*, **166**, 103-137.
17. Takemura R., Stenberg P.E., Bainton D.F., Werb Z., 1986, *J. Cell Biol.*, **102**, 55-69.
18. Wallace R.A., R.A., Selman K., 1990, *J. Electr. Microsc. Techniq.*, **16**, 175-201.
19. Zărnescu O., Meşter R., 1998, *Rev. Roum. Biol. Biol. Anim.*, **43** (137-140).

Received October 14, 1998

Faculty of Biology
Bucharest, Spl. Independenței 91-95
E-mail: otilia@ibd.dbio.ro

FOOD ANALYSIS IN *BUFO VIRIDIS VIRIDIS* ADULTS

CALIN TESIO*, IRINA TEODORESCU*

Analysis of stomach content of 55 specimens of *Bufo viridis viridis*, collected from an anthropic ecosystem in Bucharest area, gives information on food components in adults of this species.

Bufo viridis viridis adults consume *Insecta*, *Arachnida*, *Crustacea*, *Chilopoda*, *Diplopoda* and *Gastropoda* specimens.

The studies concerning the importance of amphibians in trophic networks have developed in the idea of understanding their populations' function in anthropic ecosystems. Among those who had contributions in this field, we mention: G. Portevin (1942), A. Bragg (1957-including *Bufo* species), F. B. Turner (1959), St. Vancea & collab. (1964), J. R. Zimka (1974), S. I. Medvedev (1974), G. Sin & collab. (1975), N. N. Scerbac & M. I. Scerbac (1980), M. Zarewski & E. Kepa (1981), J. M. Gutowski & L. Krzysztofiak (1988).

Food composition in *Bufo viridis* has been only occasionally taken into account, sometimes on very few specimens. The current study intends to estimate the role of this species in anthropic ecosystems (the parks in Bucharest).

MATERIAL AND METHODS

Investigations were performed on 55 specimens of *Bufo viridis viridis* (31 males and 26 females), collected around Balta Alba Lake in Bucharest, during June (20 specimens), July (17 specimens) and September (18 specimens), at night, between 7 p.m. - 9 p.m. and 10 p.m. - 12 a. m.

Animals were collected during night - torch survey - and were immediately killed with chlorophorm and injected in the body cavity with 3 cm³, 4% formalin, to stop the digestion of ingested preys. The stomach contents were dissected and the prey identified, where possible at the species level.

Several biometrical measurements were made (body length, femoral and tibial length, first finger length, tuberculus length and height).

RESULTS AND DISCUSSION

Qualitative and quantitative analyses of stomachal content of *Bufo viridis viridis* showed that the adults of this species consume almost exclusively

arthropods (*Insecta*, *Arachnida*, *Crustacea*, *Chilopoda* and *Diplopoda*), the few *Gastropoda* specimens were found to have an insignificant numerical weight.

Among arthropods, insects are dominant, as a result of the faunistic structure at the ground level, and not of the way the toads selected their food.

The comparison has been done between the food of the population in the Bucharest area, and the food of the populations from countries adjacent to Romania, established by the analysis of 2 specimens from Poland (Gutov), 23 specimens from Russia (Medvedev) and 28 specimens from Ukraine (Scerbac). The quantitative differences were induced by the variations in local faunistic structure and in the numerical abundance of different prey species (Table 1).

Table 1

Comparison between food composition of *Bufo viridis viridis*, in Romania and some adjacent countries

| Class | Orders and families | Russia | Poland | Ukraine | Romania |
|----------------------|----------------------|--------|--------|---------|---------|
| <i>Oligochaeta</i> | <i>Lumbricidae</i> | 3 | | 2 | |
| <i>Gasteropoda</i> | | | | 11 | 2 |
| <i>Arachnida</i> | | 17 | | 21 | 4 |
| <i>Crustacea</i> | <i>Isopoda</i> | | 2 | 4 | |
| <i>Chilopoda</i> | <i>Epimorpha</i> | | | 7 | 125 |
| <i>Diplopoda</i> | <i>Oniscomorpha</i> | | | | |
| <i>Insecta</i> | <i>Blattodea</i> | 1 | | 18 | 3 |
| | <i>Orthoptera</i> | 1 | | 9 | 39 |
| | <i>Forficulidae</i> | | 1 | | 20 |
| | <i>Heteroptera</i> | | | | 2 |
| | <i>Aphididae</i> | | | | 2 |
| | <i>Cicadellidae</i> | | | 96 | |
| | <i>Coleoptera</i> | | | 44 | 249 |
| | <i>Carabidae</i> | 68 | 4 | 8 | 1 |
| | <i>Staphylinidae</i> | 2 | | 4 | 1 |
| | <i>Elateridae</i> | 1 | | | 3 |
| | <i>Dermestidae</i> | | | | |
| | <i>Buprestidae</i> | 1 | | 6 | |
| | <i>Anobiidae</i> | | | | |
| | <i>Tenebrionidae</i> | 3 | | | 6 |
| | <i>Coccinellidae</i> | | 1 | | 4 |
| <i>Scarabaeidae</i> | 3 | | 4 | 2 | |
| <i>Chrysomelidae</i> | 1 | | 32 | 9 | |
| <i>Curculionidae</i> | 3 | | 42 | 519 | |
| <i>Formicidae</i> | 11 | 1 | 168 | 616 | |
| <i>Myrmicidae</i> | | | | 18 | |
| <i>Vespidae</i> | | | | 15 | |
| <i>Ichneumonidae</i> | 5 | | | | |
| <i>Braconidae</i> | | | | 2 | |
| <i>Diptera</i> | | 1 | 70 | 3 | |
| <i>Lepidoptera</i> | 20 | | 52 | | |
| | | 1 | | | |

| | <i>Noctuidae</i> | | | 51 | 2 |
|--------------------------|--------------------------|------|-----|-------|-------|
| | <i>Neuroptera-larvae</i> | | 1 | | |
| No toads | | 23 | 2 | 28 | |
| No. prey specimens | | 141 | 11 | 682 | 1620 |
| No prey specimens / toad | | 6.13 | 5.5 | 24.36 | 28.31 |

Coleoptera and *Formicoidea* were dominant in the samples, these being characteristic groups for ground level fauna.

Among the coleopterans, *Carabidae* species were dominant, especially in the samples from Russia (58.15%) and Poland (45.45%). Fewer *Carabidae* occurred in the material from Romania (17.10%), where *Formicoidea* (1135 specimens) and terrestrial *Crustacea* (125) were better represented.

The numerical weight of *Hymenoptera* in the samples from Romania, where they were represented exclusively by *Formicidae* and *Myrmicidae*, is very high (70.32 %). Other *Hymenoptera* species mentioned in adjacent countries were only accidentally found in the *Bufo viridis* adults' food, *Formicoidea* being also dominant.

It is also worth mentioning the presence of the terrestrial *Crustacea* in the samples from Romania, with a significant numerical weight (7.74 %).

The total number of *Oligochaeta*, *Gastropoda* and *Arthropoda* specimens was found in the stomachs of *Bufo viridis*, reported to the number of stomachs analysed for Romania and Ukraine, due to the greater number of samples and to the high numerical weight of *Formicoidea*, which are gravimetrically less important (Table 1).

The dynamics of the number and weight of *Bufo viridis* preys registered a higher value in July, when the numerical abundance increased 2.71 times and the species weight, 1.37 times, comparatively with June. In September, an important decrease in number (1.74 times) and weight (over 1.6 times) comparatively with July was observed (Table 2).

Table 2

Number and weight dynamics of invertebrate specimens in *Bufo viridis viridis* stomach

| Number and weight | June | July | September | Total |
|-------------------|-------|-------|-----------|--------|
| Specimens number | 307 | 834 | 479 | 1620 |
| Specimens weight | 29.26 | 39.89 | 24.008 | 93.158 |

The trophic structure of the identified fauna from the stomachs of the 55 *Bufo viridis* specimens comprises **primary consumers** (phytophagous), **secondary consumers** (predaceous and parasitoids), **coprophagous**, **necrophagous** and **detritophagous** (Table 3). Ants, which were not identified, have not been taken into consideration, their trophic category being not known.

By the number of species (29), but especially of specimens (253), primary consumers were dominant (Table 4), belonging to the *Insecta* (*Coleoptera*, *Orthoptera*, *Heteroptera*, *Homoptera* and *Lepidoptera* orders) and *Gastropoda* classes.

Table 3

Invertebrate trophic categories, numerical abundance and frequency in *Bufo viridis viridis* stomach

| Trophic categories | June | July | September | Total | Numerical abundance | Frequency |
|---------------------------|------------|------------|------------|-------------|---------------------|-----------|
| Primary consumers | 104 | 93 | 56 | 253 | 15.62 | 100 |
| Secondary consumers | 18 | 9 | 17 | 44 | 2.72 | 100 |
| Coprophagous | 1 | - | - | 1 | 0.06 | 33.33 |
| Necrophagous | 3 | - | - | 3 | 0.18 | 33.33 |
| Detritophagous | 12 | 46 | 67 | 125 | 7.72 | 100 |
| Formicidae and Myrmicidae | 134 | 672 | 329 | 1135 | 70.06 | 100 |
| Uncertain | 34 | 14 | 10 | 58 | 3.58 | 100 |
| Pollinators | 1 | - | - | 1 | 0.06 | 33.33 |
| Total | 307 | 834 | 479 | 1620 | | |

Table 4

Primary consumers groups in *Bufo viridis viridis* stomach

| Groups | Families | Species | | Specimens | |
|--------------------|-----------------------|-----------|-------|------------|-------|
| | | nr. | % | nr. | % |
| <i>Gasteropoda</i> | | 2 | 6.90 | 2 | 0.79 |
| <i>Orthoptera</i> | <i>Gryllotalpidae</i> | 1 | 3.44 | 3 | 1.18 |
| <i>Homoptera</i> | <i>Cicadellidae</i> | 1 | 3.44 | 2 | 0.79 |
| | <i>Aphididae</i> | 1 | 3.44 | 17 | 6.72 |
| <i>Heteroptera</i> | <i>Pyrrochoridae</i> | 1 | 3.44 | 2 | 0.79 |
| | <i>Lygaeidae</i> | 2 | 6.90 | 205 | 81.03 |
| <i>Coleoptera</i> | <i>Carabidae</i> | 9 | 31.03 | 1 | 1.58 |
| | <i>Elateridae</i> | 1 | 3.44 | 3 | 1.18 |
| | <i>Chrysomellidae</i> | 3 | 10.34 | 4 | 1.58 |
| | <i>Scarabaeidae</i> | 1 | 3.44 | 9 | 3.16 |
| | <i>Curculionidae</i> | 4 | 13.79 | 2 | 0.79 |
| <i>Lepidoptera</i> | <i>Noctuidae</i> | 1 | 3.44 | 2 | 0.79 |
| Total | | 29 | | 257 | |

Among the identified 224 specimens of coleopterans, *Carabidae* were dominant (81.03%), especially by *Harpalus* species (57.31% from total coleopterans and 78.83% from carabidae). *Harpalus* is a genus of ground polyphagous species, which consumes various seedlings.

As more important, specific or polyphagous pests, we mention *Zabrus tenebrionides*, *Oulema melanopus*, for wheat, *Phytodecta fornicata*, *Otiorrhynchus ligustici*, *Phytonomus variabilis*, *Apion apricans* for trefoil, *Sitona*, *Amphimallon solstitialis* for peas, *Gryllotalpa gryllotalpa* and *Agriotes* species as polyphagous. All pest species were represented by few specimens (Table 5).

Secondary consumers were represented by 16 species, with 44 specimens (Table 6), being 1.6 times fewer as species number and over 5 times as specimens

number, compared to the phytophagous ones. With the exception of 2 specimens of parasitoid *Braconidae* species, the secondary consumers (95.45%) are predaceous. Most of them are coleopterans, especially *Carabidae* (54.54%) and *Coccinellidae* (15.91%). Also important were *Chilopoda* (*Geophilidae* species, with 13.64% numerical abundance) (Table 7).

Table 5

Primary consumers' dynamics, abundance and frequency

| Nr. | Phytophagous species | VI | VII | IX | Total | Abundance | Frequency |
|-----|---------------------------------|------------|-----------|-----------|------------|-----------|-----------|
| 1 | <i>Gastropoda</i> | - | 1 | - | 1 | 0.39 | 33.33 |
| 2 | <i>Cochlicopa lubrica</i> | 1 | - | - | 1 | 0.39 | 33.33 |
| 3 | <i>Gryllotalpa gryllotalpa</i> | 1 | 1 | 1 | 3 | 1.18 | 100 |
| 4 | <i>Cicadellidae</i> | - | 1 | 1 | 2 | 0.79 | 66.66 |
| 5 | <i>Aphididae</i> | 2 | - | - | 2 | 0.79 | 33.33 |
| 6 | <i>Pyrrochoris apterus</i> | - | - | 17 | 17 | 6.72 | 33.33 |
| 7 | <i>Lygaeus equestris</i> | - | 2 | - | 2 | 0.79 | 33.33 |
| 9 | <i>Harpalus aeneus</i> | 44 | 57 | 4 | 105 | 41.50 | 100 |
| 10 | <i>Harpalus azureus</i> | 1 | - | 4 | 5 | 1.98 | 66.66 |
| 11 | <i>Harpalus distinguendus</i> | 3 | 1 | - | 4 | 1.58 | 66.66 |
| 12 | <i>Harpalus sp.</i> | 29 | 14 | 18 | 61 | 24.11 | 100 |
| 13 | <i>Amara crenata</i> | - | - | 2 | 2 | 0.79 | 33.33 |
| 14 | <i>Amara ovata</i> | 5 | 3 | 2 | 10 | 3.95 | 100 |
| 15 | <i>Anisodactylus signatus</i> | 2 | - | - | 2 | 0.79 | 33.33 |
| 16 | <i>Anisodactylus binottatus</i> | - | 4 | - | 4 | 1.58 | 33.33 |
| 17 | <i>Carabidae</i> | 7 | 3 | - | 10 | 3.95 | 66.66 |
| 18 | <i>Zabrus tenebrionides</i> | - | 1 | 1 | 2 | 0.79 | 66.66 |
| 19 | <i>Agriotes lineatus</i> | 1 | - | - | 1 | 0.39 | 33.33 |
| 20 | <i>Phytodecta fornicata</i> | 1 | - | - | 1 | 0.39 | 33.33 |
| 21 | <i>Lema melanopus</i> | 1 | - | - | 1 | 0.39 | 33.33 |
| 22 | <i>Chalcoides aurata</i> | - | - | 1 | 1 | 0.39 | 33.33 |
| 23 | <i>Amphimallon solstitialis</i> | 3 | 1 | - | 4 | 1.58 | 66.66 |
| 24 | <i>Phytonomus variabilis</i> | - | - | 2 | 2 | 0.79 | 33.33 |
| 25 | <i>Sitona lineata</i> | - | 3 | - | 3 | 1.18 | 33.33 |
| 26 | <i>Apion apricans</i> | - | 1 | - | 1 | 0.39 | 33.33 |
| 27 | <i>Otiorrhynchus ligustici</i> | - | - | 1 | 1 | 0.39 | 33.33 |
| 28 | <i>Curculionidae</i> | 1 | 1 | - | 2 | 0.79 | 66.66 |
| 29 | <i>Noctuidae</i> | - | - | 2 | 2 | 0.79 | 33.33 |
| | Total | 104 | 93 | 56 | 253 | | |

Table 6

Secondary consumers groups in *Bufo viridis viridis* stomach

| Groups | Families | Species number | Species % | Specimens number | Specimens % |
|-----------|--------------------|----------------|-----------|------------------|-------------|
| Aranea | | 2 | 12.50 | 4 | 9.10 |
| Chilopoda | <i>Geophilidae</i> | 1 | 6.25 | 6 | 13.64 |

| Groups | Families | Species number | Species % | Specimens number | Specimens % |
|-------------|---------------|----------------|-----------|------------------|-------------|
| Coleoptera | Carabidae | 6 | 37.50 | 24 | 54.54 |
| | Staphylinidae | 1 | 6.25 | 1 | 2.27 |
| | Coccinellidae | 5 | 31.25 | 7 | 15.91 |
| Hymenoptera | Braconidae | 1 | 6.25 | 2 | 4.54 |
| | Total | 16 | | 44 | |

From the other trophic categories, the detritophagous arthropods were better represented by *Diplopoda* (*Glomeris* species).

Table 7

Secondary consumers dynamics, abundance and frequency

| Nr. | Species | VI | VII | IX | Total | Abundance | Frequency |
|-----|--|-----------|----------|-----------|-----------|-----------|-----------|
| 1 | <i>Aranea</i> | - | 1 | 1 | 2 | 4.54 | 66.66 |
| 2 | <i>Phalangidae</i> | 2 | - | - | 2 | 4.54 | 66.66 |
| 3 | <i>Geophilus</i> | 3 | 3 | - | 6 | 13.64 | 66.66 |
| 4 | <i>Poecilus cupreus</i> | 6 | 2 | 5 | 13 | 29.54 | 100 |
| 5 | <i>Poecilus sp.</i> | - | - | 1 | 1 | 2.27 | 33.33 |
| 6 | <i>Bembidion sp.</i> | - | 1 | - | 1 | 2.27 | 33.33 |
| 7 | <i>Abax carinatus</i> | - | - | 3 | 3 | 6.82 | 33.33 |
| 8 | <i>Abax sp.</i> | - | 2 | 2 | 4 | 9.09 | 66.66 |
| 9 | <i>Calathus melanocephalus</i> | - | - | 2 | 2 | 4.54 | 33.33 |
| 10 | <i>Staphylinidae</i> | 1 | - | - | 1 | 2.27 | 33.33 |
| 11 | <i>Adalia bipunctata</i> | 1 | - | - | 1 | 2.27 | 33.33 |
| 12 | <i>Coccinella septempunctata</i> | 3 | - | - | 3 | 6.82 | 33.33 |
| 13 | <i>Coccinella duodecimpunctata</i> | - | - | 1 | 1 | 2.27 | 33.33 |
| 14 | <i>Adonia variegata</i> | 1 | - | - | 1 | 2.27 | 33.33 |
| 15 | <i>Propylaea quatuordecimpustulata</i> | 1 | - | - | 1 | 2.27 | 33.33 |
| 16 | <i>Braconidae</i> | - | - | 2 | 2 | 4.54 | 33.33 |
| | Total | 18 | 9 | 17 | 44 | | |

By the abundance values, we estimated the dominance of arthropod groups in the food of the toads, and hence in the trophic structure of the biocenosis they lived in.

As number, during the three months, the ants (*Myrmicidae*, with 616 specimens and *Formicidae*, with 519), followed by *Coleoptera* with 262 specimens (especially *Carabidae* species, by *Harpalus*), were dominant.

As gravimetric abundance, the species of *Gryllotalpa*, *Amphimallon*, *Abax*, *Poecilus*, *Zabrus* and *Glomeris* are outstanding, because of their large size.

According to the frequency values we established the constancy of the different groups in the food of toads. As species, coleopterans (especially *Harpalus*, *Amara*, *Poecilus*), *Forficula auricularia*, *Gryllotalpa gryllotalpa*, *Glomeris*, spiders, were constantly found, representing most of the permanent food of *Bufo viridis viridis* adults.

From the anthropocentric point of view, *Bufo viridis viridis* adults are an important factor in biological control of different arthropod pests. In their food, only *Poecilus*, *Abax*, *Staphylinidae*, *Coccinellidae*, *Geophilus* and spiders are useful, predaceous species, all the rest being specific for different crops or polyphagous pests.

CONCLUSIONS

Qualitative and quantitative analyses on the stomach content of 55 specimens of *Bufo viridis viridis* adults, collected in June, July and September have brought valuable information on food composition in these toads:

- *Bufo viridis viridis* from the anthropic ecosystem in Bucharest consumes a variety of prey types, composed especially of arthropods (*Insecta*, *Aranea*, *Chilopoda*, *Diplopoda*), but also of a few *Gastropoda*,
- Among the groups found in the toads' food, insects were dominant both as species and specimens number,
- From the insects, hymenopterans *Formicidae*, *Myrmicidae* and coleopterans, especially *Carabidae*, characteristic groups for ground level fauna, were dominant,
- As trophic structure, the identified groups belong to primary and secondary consumers, and less to coprophagous (*Aphodius*), necrophagous (*Dermestes*) and detritophagous (*Glomeris*) species. The phytophagous were dominant as species and specimens number, whereas zoophagous, represented mostly by predaceous, were much less numerous,
- In the dynamics of the prey consumed, a decrease of the species, and especially of the specimens number occurs by the approach of the autumn,
- *Bufo viridis viridis* is not selective in the choice of prey, consuming alive, mobile preys,
- Because many of prey species are pests to the human economy, toads deserve a special protection.

REFERENCES

- Bragg, An., 1957, *Some factors in the feedings of toads*, Herpetologica, 13, 3, 189-191.
- Gutowski, J. M., Krzysztofiak, L., 1988, *Materials for the investigation of food composition of anurous amphibians in north-eastern Poland*, Przeglad Zoologiczny, 32, 2, 225-235.
- Medvedev, S. I., 1974, *Data on the study of amphibians food in the region of the middle flow of the Severtsky Donets River*, Vest. Zool., 1, 50-59.
- Sin, G., Lăcătușu, Matilda, Teodorescu, Irina, 1975, *Hrana la broasca de lac Rana ridibunda ridibunda Pall*, St. cerc. Biol., ser. Biol. anim., 27, 4, 331-343.
- Turner, F. B., 1959, *An analysis of the feeding habits of Rana pretiosa in Yellowstone Park Wyoming*, Ann., Med., Natur., 61, 403-413.

- Vancea, Șt., Mândru, C., Simionescu, V., 1964, *Contribuții la cunoașterea hranei la Rana ridibunda ridibunda Pall. din împrejurimile orașului Iași*, St. cerc. St. Biol. și agric., Acad. R.P.R., Iași, **12**, 1.
- Zimka, J., R., 1974, *Predation of frog Rana arvalis Nilss in different forest and conditions*, Ekol., **22**, 1, 31-63.
- Zakrewski, M., Kepa, E., 1981, *Composition of natural food of the spotted salamander, Salamandra salamandra L., from western Beskid*, Acta Biol. Cracov, **23**, 77-86.

Received December 14, 1998

*Bucharest University, Faculty of Biology,
Splaiul Independenței 91-95, 76201-Bucharest, Romania

COMPARATIVE STUDIES ON *IN VITRO* FIBRILLOGENESIS OF COLLAGEN FROM FISH AND PIG CORNEA

LUCIA MOLDOVAN¹, OTILIA ZĂRNESCU², MARINELA BUNEA¹,
OANA CRĂCIUNESCU¹, LIDIA CONSTANTINESCU¹

The process of collagen self-assembly *in vitro* was investigated using type I collagen extracted and purified from fish (*Carassius auratus gibelio*) and pig cornea. The structural features of fish type I collagen were similar to those of pig, with differences in Hyp content and average molecular weight (3.8×10^6 in fish and 3.2×10^6 in pig). Fibril formation was evidenced by turbidimetric and electron microscopic methods. The self-assembly curve of fish collagen had a shorter nucleation phase and a longer growth phase than that of pig collagen. Our turbidimetric and electron microscopic studies demonstrated also that type I collagen from fish cornea assembled slower than collagen from pig cornea and formed thinner fibrils. In both cases, the collagen fibrils produced were native banded, with 65 nm periodicity and abnormal fibrils were not observed. However, the average diameter of the fibrils was about 85 nm in fish and 130 nm in pig.

The characteristics of various extracellular matrices are mostly determined by the synthesis and assembly of collagen molecules and their organization into unique macromolecular structures.

The synthesis of collagen molecules and their association in order to form fibrils require a great number of post-translational events, common to all fibrillar collagens (1). These include intracellular processes such as hydroxylation and glycosylation and other extracellular processes such as procollagen processing and cross-linking (2),(3). Fibril assembly can be altered by association of different fibrillar collagens in order to form heterotypical fibrils (4),(5), proteoglycan addition to form collagen-proteoglycan heteropolymers (6) or by addition of fibril-associated collagens to fibrils (1). Tissue-specific variations in all these events contribute to the diversity of collagen structures, noticed in different extracellular matrices. The cornea, for example, has fibrils of uniform and small diameter, organized into orthogonal lamellae; these characteristics determine the integrity and transparency of the tissue (7),(8).

Fibrillogenesis is a multistep process and there are numerous phases where fibril characteristics, such diameter, may be regulated. Among these, propeptide processing is very important. The COOH-propeptides of procollagen molecules are cleaved in the extracellular matrix before incorporation of collagen monomers into fibrils and also, COOH-propeptidase activity provides a limitation of fibril

formation (9), (10). Studies of immunoelectron microscopy indicate that corneal collagen fibril diameter depends on co-assembly of collagen types I and V (11) and also on composition and concentration of proteoglycans in extracellular space (12), (13). *In vitro* studies on the assembly of corneal collagen molecules into fibrils used mainly type I, known by its ability to form fibrils (14), (15). However, the objective of these studies is limited to terrestrial animal collagen, and there is nothing known about the assembly behaviour of fish collagen.

The aim of this work was to study *in vitro* fibrillogenesis of type I collagen from an aquatic vertebrate cornea (*Carassius auratus gibelio*) comparative to that of the pig.

MATERIAL AND METHODS

Biological material. Fish eyes (*Carassius auratus gibelio*) were provided from Fisheries Research Farm - Nucet and pig eyes from the Slaughter House - Bucharest.

Preparation and characterization of type I collagen. Type I collagen was prepared and purified from pig and fish cornea, as in our previous paper (16). The following investigations were performed:

- content of collagen by colorimetric determination of hydroxyproline according to Woessner's modified method (17);
- denaturing temperature (T_D) and average molecular weight according to the viscosimetric method (18);
- electrophoresis for collagen according to Laemmli's modified method (19).

Collagen fibril reconstruction. Type I collagen from fish and pig cornea was dissolved in 0.5 M acetic acid at 1 mg/ml concentration, was centrifuged at 10.000 rpm, for 30 minutes and dialysed against phosphate buffer pH 7.4, at 4°C. Collagen solutions were warmed at 30°C, for 6 h. The collagen self-assembly process was monitored by the absorbance at 315 nm, using a UV-spectrometer (CECIL 1020).

Electron microscopy. The collagen fibrils were examined and photographed using a Philips transmission electron microscope, after negative staining with 1% phosphotungstic acid, pH 7.0.

Immunoelectron microscopy. The nickel grids were floated only on collagen solutions, 10 min., and then rinsed in TBS (Tris-buffered saline), 30 min., at 4°C. After fixation in 4% paraformaldehyde in TBS, 15 min., the grids were successively treated with TBS containing 0.1 M glycine (15 min.), and 2% BSA (2 h) to minimize nonspecific binding of the antibodies. The grids were floated on collagen type I and, respectively, type II polyclonal antibody, diluted 1:50 with TBS containing 2% BSA, overnight. All incubations were performed at 4°C. After five 1-min. washings with TBS, each grid was incubated with the secondary antibody protein A-10 nm colloidal gold labelled (Sigma), diluted 1:10 with TBS, 1 h, at

room temperature. The grids were rinsed five times in TBS and fixed with 2.5% glutaraldehyde in TBS for 2 min. After a final wash in distilled water, the grids were dried and stained with 1% phosphotungstic acid, pH 7.0.

RESULTS

Structural features of corneal collagen. For comparative study on collagen fibrillogenesis from fish and pig cornea, we used type I collagen. Isolation of this collagen from both sources was performed by an enzymic method and the purification was carried out by successive precipitations with NaCl. The solution of type I collagen obtained from fish cornea had a denaturing temperature and a Hyp content lower than those of collagen from pig cornea (Table 1). Average molecular weight of fish collagen was about 380.000 compared to 320.000 of pig collagen. These differences suggest the presence of a molecular dispersion in fish collagen.

Table 1

Analytical determinations for type I collagen from pig and fish corneas

| Collagen source | Hyp (%) | Denaturing temperature (°C) | Average molecular weight |
|-----------------|---------|-----------------------------|--------------------------|
| Pig cornea | 10.1 | 37 | 320.000 |
| Fish cornea | 8.2 | 30 | 380.000 |

The purity of collagens obtained from fish and pig cornea was determined by SDS - polyacrylamide gel electrophoresis (fig. 1). Electrophoretic mobilities of the constituting chains are similar for collagens from aquatic and terrestrial vertebrate cornea.

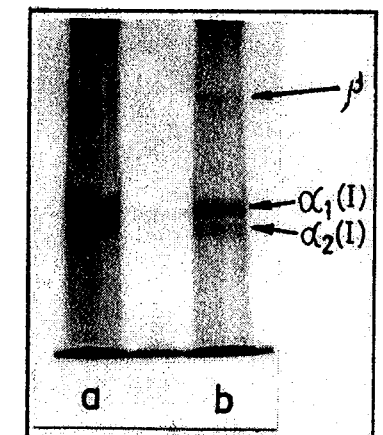


Fig. 1. - SDS -polyacrylamide gel electrophoresis of type I collagen from pig (a) and fish (b) cornea. Alpha monomers and beta dimers are clearly resolved from each other.

The process of collagen self-assembly. The self-assembly process of type I collagen from fish and pig cornea was studied by two methods: turbidimetry and

electron microscopy. Fibril formation was initiated by collagen solutions' dialysis against a saline solvent at neutral pH, and then the samples were incubated at 30 °C.

The kinetics of formation of type I collagen fibrils, during incubation, was turbidimetrically observed by measuring the absorbance at 315 nm. The precipitation curves (fig. 2) are constituted of three clearly defined regions. The first domain is a lag phase without absorbance variation and it corresponds to collagen fibril nucleation. The second domain is the phase of fibril growth with a rapid absorbance increase. The third domain is a maturity phase with a constant value of absorbance and includes the formation of three-dimensional networks of fibrils.

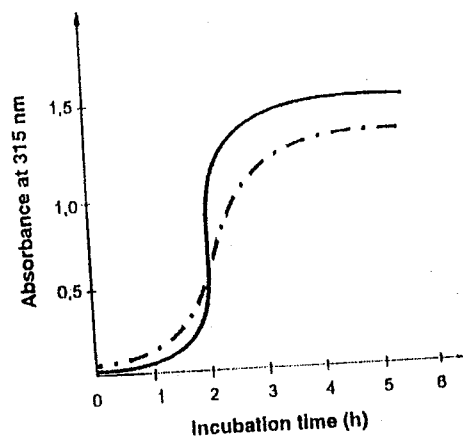


Fig. 2. – Kinetics of type I collagen fibril assembly from fish (---) and pig (—) cornea.

The self-assembly curve of fish collagen had a shorter lag phase and a longer growth phase than that of pig collagen. Final absorbance of reconstituted crucian carp collagen at the maturity phase was lower than that of pig collagen, suggesting that in fish, the obtained fibrils were thinner.

The fibrils formed from fish and pig collagen were examined by transmission electron microscopy. In both cases, the collagen fibrils produced were native banded with 65 nm periodicity and abnormal fibrils were not observed (fig. 3). The fibrils incubated at 30 °C had an average diameter of about 130 nm in pig and of 85 nm in fish.

In order to demonstrate the occurrence of type I collagen in fish cornea fibrils by immunoelectron microscopy we used collagen types I and II polyclonal antibodies. Fibrils reacted positively with the antibodies against type I collagen (fig. 4A), but had no reactivity with antibodies against type II collagen (fig. 4B).

DISCUSSION

To study the process of corneal collagen self-assembly we used type I collagen extracted and purified from fish and pig corneal tissues. Type I collagen solutions were redissolved and reprecipitated under physiological conditions.

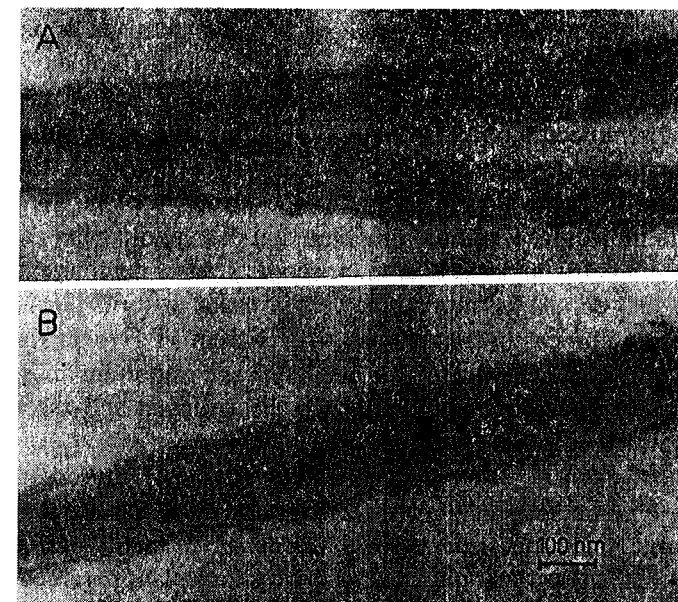


Fig. 3. – Morphology of type I collagen fibrils formed *in vitro*; fish collagen (A) and pig collagen (B). All preparations were negatively stained with 1% phosphotungstic acid, pH 7.0.

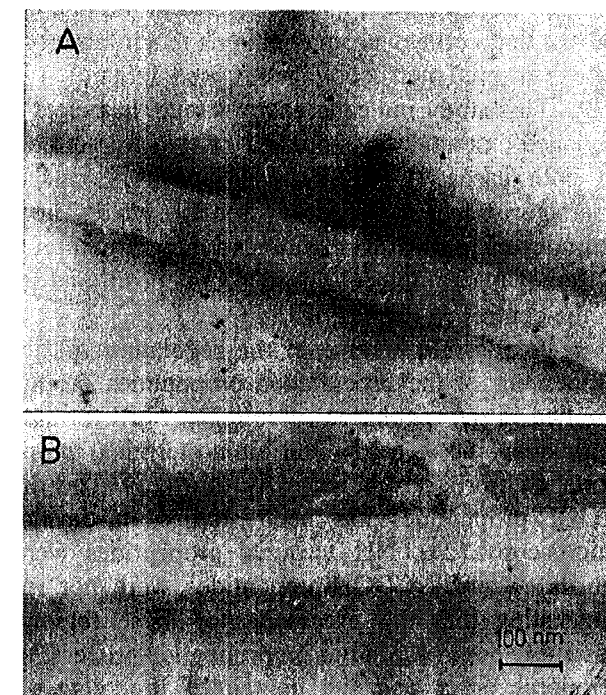


Fig. 4. – Immunolabelling of type I collagen fibrils from fish cornea, formed *in vitro*. Collagen fibrils reacted positively with type I collagen antibodies (A) and had no reactivity with antibodies against type II collagen (B).

Comparing the self-assembly curve of collagen from an aquatic vertebrate cornea (fish) with that obtained from pig cornea, some differences were noticed, particularly regarding nucleation and maturation phases. These differences may be due to collagen molecule microstructure including the distribution of surface charge, hydrophobic groups, and Hyp content. We consider that the shorter nucleation phase of fish collagen is due to the presence of monomers and their aggregates with molecular weight higher than that of pig collagen (Table 1).

Both turbidimetric and electron microscopic studies demonstrated that type I collagen from fish cornea assembled slower, in order to form fibrils thinner than collagen from pig cornea. In this respect, the content of Hyp in fish collagen is lower than in pig collagen. Since Pro and Hyp are important in stabilizing the collagen helix, the difference may influence the collagen self-assembly and the properties of formed collagen fibrils (19).

Like most dense stromal connective tissues, the cornea contains predominantly type I collagen. Nevertheless, unlike other tissues containing type I collagen in large quantities, the corneal fibrils have small, uniform diameters (about 25 nm). Collagen fibril diameter is a very important parameter for corneal tissue function, being influenced by the following aspects: primary structure of molecules, molar ratios and topography of various collagen types, content and spatial distribution of noncollagenous macromolecules associated to fibrils, processing of the propeptides and the assembly conditions. This unique morphology of cornea may be related to the fact that in several species, it has been shown that corneal stroma contains much more type V collagen than other tissues whose stromal matrix collagen is predominantly type I (20), (21), (22).

This study indicates that average diameters of fibrils reconstituted of type I collagen extracted from corneas of the two vertebrates are different. Nevertheless, in both cases, the fibrils had diameters much larger than those of 25 nm, characteristic of the corneal stroma *in vivo*. The difference is due to the role of keratocytes in fibril formation and their structure. Cellular control of the mixing of different macromolecules and post-depositional processing has an important role in the control of fibril formation.

A possible control in the regulation of fibril structure may reside in the processing of the procollagen propeptides during fibrillogenesis. This has been implied in the regulation of collagen fibril formation both *in vivo* and *in vitro*. In dermatoparactic cattle, the amino-terminal propeptide is not removed and the collagen fibrils are abnormally thin (23). The different processing of NH₂- and COOH-propeptides has been studied in developing skin by immunoelectron microscopy (24). NH₂-terminal propeptides were only associated with thinner fibrils, whereas COOH-propeptides were not regularly associated with fibrils, suggesting that the processing of these regions may be important for fibril assembly control. Studies on propeptide processing *in vitro* have indicated that the temporal order and the degree of procollagen processing may be important

determinants of fibril structure, especially for initial determination of fibril diameter (25). When COOH-terminal propeptide was removed prior to the removal of the NH₂-terminal peptide, thin fibrils formed. However, if the order of propeptide processing was reversed, thick fibrils formed.

REFERENCES

1. T.F. Linsenmayer, 1991, *Cell Biology of the Extracellular Matrix*, Plenum Press, New York, 7.
2. J.K. Marchant, R.A. Hahn, T.F. Linsenmayer, D.E. Birk, 1996, *J. Cell Biol.*, **135**, 1415.
3. M. Yamauchi, G.S. Chandler, H. Tanzawa, E.P. Katz, 1996, *Biochem. Biophys. Res. Commun.*, **219**, 311.
4. D.R. Keene, L.Y. Sakai, H.P. Bachinger, R.E. Burgeson, 1987, *J. Cell Biol.*, **105**, 2393.
5. T.F. Linsenmayer, E. Gibney, F. Igoe, M.K. Gordon, J.M. Fitch, D.E. Birk, 1993, *J. Cell Biol.*, **121**, 1181.
6. K.G. Vogel, 1994, *Extracellular Matrix Assembly and Structure*, Academic Press, New York, 243.
7. E.R. Berman, 1991, *Biochemistry of the eye*, Academic Press, New York, 1989.
8. L. Moldovan, O. Zărnescu, A. Oancea, D. Turcu, 1993, *Rev. Roum. Biol.*, **38**, 2, 163.
9. K.E. Kadler, D.J.S. Hulmes, Y. Hojima, D.J. Prockop, 1990, *Ann. N.Y. Acad. Sci.*, **580**, 214.
10. J.D. Prockop, K.I. Kivirikko, 1995, *Annu. Rev. Biochem.*, **64**, 403.
11. D.E. Birk, M.A. Lande, 1981, *Biochim. Biophys. Acta.*, **670**, 362.
12. J.A. Rada, P.K. Cornuet, J.R. Hassell, 1993, *Exp. Eye Res.*, **56**, 635.
13. D.E. Birk, T.F. Linsenmayer, 1994, *Extracellular Matrix Assembly and Structure*, Academic Press, New York, 91.
14. P. Sini, A. Denti, E. Tira, C. Balduini, 1997, *Glycoconjugate J.*, **14**, 871.
15. L. Moldovan, A. Oancea, D. Turcu, O. Zărnescu, 1994, *Rev. Roum. Biol.*, **39**, 1, 65.
16. G. Negroiu, L. Moldovan, M. Caloianu, N. Mirancea, D. Mirancea, 1988, *Rev. Roum. Biochim.*, **25**, 2, 143.
17. L. Roden, J. R. Baker, J. Cifonelli, M. B. Mathews, 1972, *Meth. Enzymol.*, **XXVIII**, Part B, 131.
18. E.J. Miller, R.K. Rhodes, 1982, *Meth. Enzymol.*, **82**, Part A, 61.
19. Y. Nomura, M. Yamano, C. Hayakawa, Y. Ishii, K. Shirai, 1997, *Biosci. Biotech. Biochem.*, **61**, 1919.
20. C. Welsh, S. Gay, R. K. Rhodes, R. Pfister, E. J. Miller, 1980, *Biochim. Biophys. Acta.*, **625**, 78.
21. C. Cintron, H. I. Covington, C. S. Kublin, 1980, *Current Eye Res.*, **1**, 1.
22. L. Moldovan, M. Caloianu, O. Zărnescu, O. Crăciunescu, 1997, *Stud. Cerc. Biol.*, **49**, 2, 139.
23. A. Lenaers, M. Ansay, B.V. Nusgens, C.M. Lapiere, 1971, *Eur. J. Biochem.*, **23**, 535.
24. R. Fleischmayer, J. S. Perlish, R. E. Burgeson, R. Timpl, 1990, *Ann. N. Y. Acad. Sci.*, **580**, 161.
25. M. Miyahara, K. Hayashi, J. Berger, F.K. Tanzawa, R.L. Trelstad, D.J. Prockop, 1984, *J. Biol. Chem.*, **259**, 9891.

Received January 13, 1999

¹ National Institute of Biological Sciences Research
Bucharest, Spl. Independenței 296

² Faculty of Biology, Bucharest
Spl. Independenței, 91-95

THE GENITAL SYSTEM IN *Lamyctes anderis* (HENICOPIDAE, LITHOBIOMORPHA, CHILOPODA)

C-C.PRUNESCU, PAULA PRUNESCU

The male genital system comprises a single flagelliform testis, two seminal vesicles, two ejaculatory ducts, a pair of accessory dorsal glands and a pair of accessory ventral glands. The female genital system comprises a tubular ovary and two oviducts, two seminal receptacles and two pairs of accessory glands. The anatomy of the genital system in *Lamyctes anderis* is similar with that one of *Esastigmatobius* and so both seem to be characteristic for the tribe Henicopini. The male genital system in Henicopini is similar with the male genital system of the Family Lithobiidae and is essential different from the male genital system of the tribe Anopsobiini.

The family Henicopidae is formed of the tribe Anopsobiini and the tribe Henicopini.

The genital system of the representatives of the tribe Anopsobiini (4, 5) is formed by two testes: a testis with the distal extremity named macrotestis, which continues with an elongated and flexuous deferent duct called microtestis because of the presence in this organ of a series of small-size germinative cells which come to maturity till the formation of numerous spermatozoa; the other testis is small and includes only spermatogonies.

The functional testis of the Anopsobiini is formed exactly like in Scutigermorpha (3, 6, 7) a fact which demonstrates the close relationship between the Chilopoda Notostigmophora and Pleurostigmophora.

The genital system of *Esastigmatobius longitarsis* (tribe Henicopini) (8) has a simple testis, similar to the single testis of the Lithobiidae (1). Given the radical differences between the male genital system of the Anopsobiini and Henicopini, we considered necessary to continue research into the genital system of the tribe Henicopini, with the species *Lamyctes anderis*.

MATERIAL AND METHODS

An immature male individual and two female individuals of *L. anderis* were given to us for study by Senckenberg Museum - Frankfurt (Germany). The preservation and fixation of the material was made in ethyl alcohol. After the inclusion in paraffin, 8 μ m thick sections were stained with hemalum - eosine (H.-E.).

RESULTS

The Male Genital System. The testis is a single tubular organ that winds in the dorsal zone, close to the posterior half of the midgut. The germinative cells - spermatogonia and spermatocytes in course of maturation are grouped in follicles close to the testis wall. The big-sized spermatocytes and the spermatides in various stages of spermiogenesis occupy the lumen of the testis (Fig. 1). At the posterior extremity, the testis continues with a single deferent canal. The testis is accompanied by two seminal vesicles. These are tubular organs with thick wall, formed of a glandular epithelium (Fig. 2). The seminal vesicles get closer to each other and unite through their posterior extremities. The deferent canal opens in the medio-dorsal region of the zone where the seminal vesicles unite. Two ejaculatory ducts depart from this zone. They surround the posterior intestine, get closer to each other and open separately in the atrium (Fig. 3).



Fig. 1. - Transversal section through the testis in spermatogenesis (80 ×).



Fig. 2. - Seminal vesicles (vs), deferent canal (cd) and dorsal accessory glands (gd) (100 ×).

The accessory glands - a pair of dorsal glands and a pair of ventral glands - are tubulo-acinous glands. The canals of the dorsal accessory glands unite and open in the central zone of the genital atrium. The canals of the ventral accessory glands unite in a short canal, which opens in the ventral wall of the genital atrium (Fig. 4).

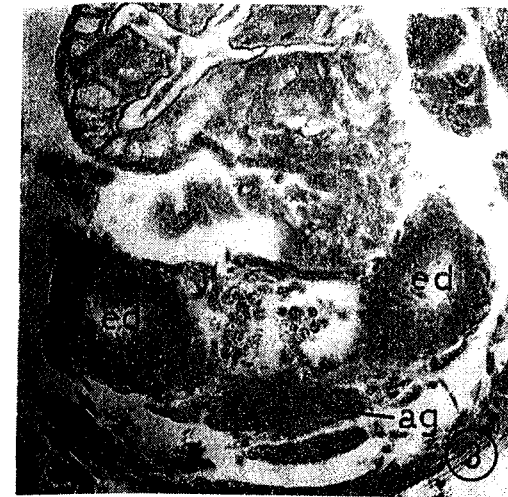


Fig. 3. - Ejaculatory ducts (ed) situated ventrally near the anterior extremity of the genital atrium (ag) (120 ×).

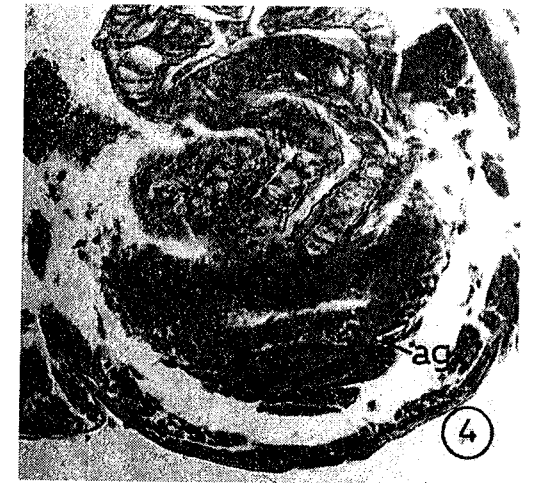


Fig. 4. - Transversal section through the genital atrium (ag) (80 ×).

The Female Genital System is composed of a single elongated ovary that continues caudally with two oviducts. The oviducts descend under the posterior intestine (Fig. 5) and open separately in the lateral parts of the genital atrium. The genital atrium has a dorsal diverticulum (Fig. 6) and a parietal glandular structure

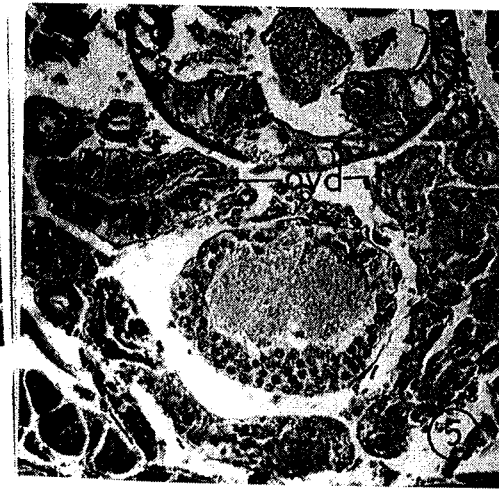


Fig. 5. - The oviduct (ovd) descends ventrally the posterior intestine, the canals of the seminal receptacles (crs) (110 ×).

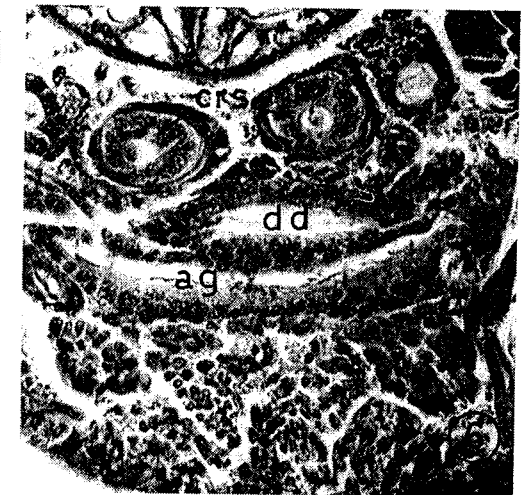


Fig. 6. - Transversal section through anterior zone of the female genital atrium (ag) and the dorsal diverticulum (dd); the canals of the seminal receptacles (crs) (110 ×).

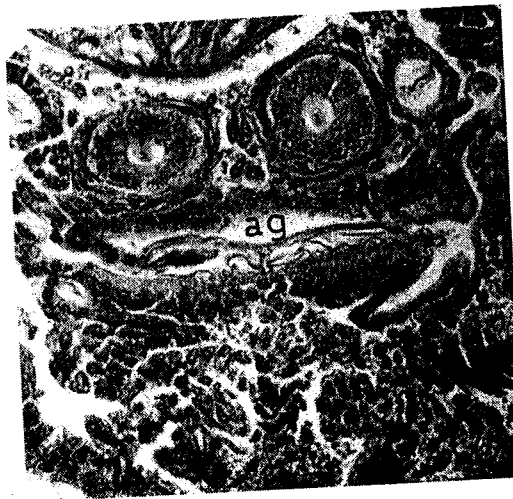


Fig. 7. – Transversal section through female genital atrium (ag). Note the openings of the dorsal and ventral accessory glands in the atrium (110 ×).



Fig. 8. – Section through the caudal extremity of the female genital atrium; the canal opening of the seminal receptacles (crs) (110 ×).

located in the ventral zone of the atrium (Fig. 6). The two ovoid seminal receptacles continue with the flexuous canals which open cavitarily in the dorsal diverticulum (Figs. 7, 8). The two accessory dorsal glands open in the lateral extremities of the dorsal wall of the atrium. The accessory ventral glands open symmetrically, in the lateral ventral wall of the atrium (Figs. 6, 7).

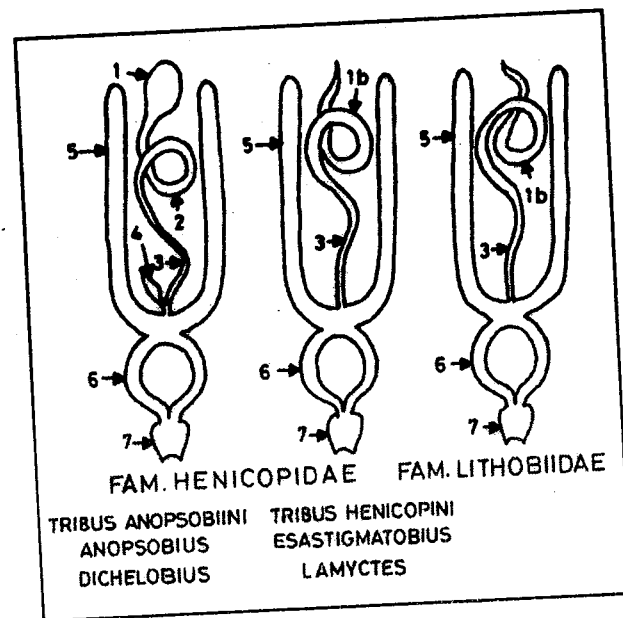


Fig. 9. – Male genital system in order Lithobiomorpha (Scheme). 1=Macrotestis (Macrospermatogenesis); 1b=single testis (Macrospermatogenesis); 2=microtestis (microspermatogenesis); 3=deferent canal; 4=immature testis (spermatogonia); 5=seminal vesicles; 6=ejaculatory duct; 7=genital atrium.

DISCUSSION

The genital system of *Lamyctes anderis* is similar to the genital system described in *Esastigmatobius longitarsis* (8) and resembles that of the fam. Lithobiidae (1, 2).

The important anatomical and histological differences between the representatives of the tribe Anopsobiini and that one of Henicopini are also valid in *Lamyctes anderis* (Fig. 9).

The male genital system in the tribe Henicopini is essentially different from the male genital system of the tribe Anopsobiini.

REFERENCES

1. PRUNESCU C.-C., 1964, *Rev. roum. Biol. (Zool)*, **9** (2): 101-107.
2. PRUNESCU C.-C., 1965, *Rev. roum. Biol. (Zool)*, **10** (1), 11-16
3. PRUNESCU C.-C., 1969, *Rev. roum. Biol. (Zool)*, **14** (3), 185-190.
4. PRUNESCU C.-C., JOHNS P.M. 1969 *Rev. roum. Biol. (Zool)*, **14** (6), 407-409.
5. PRUNESCU C.-C., 1992 a, *Ber. nat-med. Verein Innsbruck*, suppl. **10**, 87-91.
6. PRUNESCU C.-C., 1992 b, *Ber. nat-med. Verein Innsbruck*, Suppl. **10**, 93-97.
7. PRUNESCU C.-C., DESCAMPS M., FABRE MARIE-CHANTAL, SERRA A., 1995, *Zygote*, **3**, 171-176.
8. PRUNESCU C.-C., MESIBOV R., SHINOHARA K. 1996, "Preliminary data on the anatomy of the genital system ..." in: *Acta Myriapodologica*, J.-J. Jeoffroy, J.-P. Mauries, M. Nguyen - Duy eds., *Mem. Mus. natl. Hist. nat.*, **169**, 341-346, Paris.

*Institute of Biology, 296 Spl. Independenței,
RO-79651, Bucharest, Romania*

MORPHOLOGIC ASPECTS AND DIFFERENTIATION OF SOME DIGESTIVE TRACT SEGMENTS DURING ONTOGENESIS

N. MIRANCEA, DORINA MIRANCEA

In this paper we present some ultrastructural aspects which characterize the ontogenesis of some segments of the digestive tract during golden hamster (*Mesocricetus auratus*) development. We focused our interest on the epithelium differentiation as well as on the epithelial-mesenchymal junctional zone. Ultrastructural analysis of the esophagus epithelium reveals that at the stage of 15 mm cranio-caudal axis fetus length epithelial cells are yet undifferentiated and an amorphous material basement membrane-like separates epithelial cells from the adjacent mesenchyme. No hemidesmosomal junctions can be detected. By contrast, adult animal esophagus exhibits a multilayered epithelium with cornified uppermost cell layers. Basement membrane is well developed and hemidesmosomes are numerous with outer plaque and inner plaque which strongly connects cytoskeletal filaments. Concerning epithelial cell differentiation of the small intestine epithelium we describe a gradual transition from less differentiated epithelial cells to specialised cell status.

INTRODUCTION

Development and maturation of the intestinal mucosa is essential for absorption of water and nutrients. This process of gut development includes morphogenesis of intestinal mucosa from a simple tube into a tube lined with villi and the differentiation of immature epithelium into four major epithelial cell types. The gastro-intestinal tract ontogeny of *Mesocricetus auratus* has received little attention, the available information being mainly limited for the rodents to the mice. Here we focus our interest on the ultrastructural aspects of the epithelial cell differentiation of some digestive tract segments as well as on the intestinal mucosa-mesenchymal junction zone.

MATERIALS AND METHODS

The development of fetus in same litter is not synchronous so that to appreciate the stage of development we considered cranial-caudal axis lengths of fetuses. Small fragments which belong to different segments of the digestive tract (esophagus, intestine) during hamster development (5mm, 10mm and 15 mm fetuses, new-born and adult) were fixed in 2.5% glutaraldehyde and postfixed in 2% osmium tetroxide in sodium cacodylate buffer. Semithin sections were stained

with 0.1 toluidine blue for light microscopical examination. Ultrathin sections (70-90nm) were counterstained with uranyl acetate and lead citrate and investigated by means of an electronmicroscope operated at 60 kV.

RESULTS AND DISCUSSIONS

Virtually, all organs in Vertebrates are formed through an interaction between epithelial and mesenchymal cells, that is between ectoderm-mesoderm and endoderm-mesoderm, respectively (Gurdon J.B., 1992). That is the case of digestive tube: at the buccal cavity, esophagus and recto-anal digestive segments, mucosal epithelium is of ectodermal origin and for the rest of digestive tube, epithelium is originated from endoderm but everywhere along the digestive tube, the epithelium interacts with the mesoderm.

Differentiation of the digestive endodermal cells, *in vivo*, during embryonic and fetal development and in the post-natal life (Haffen et al., 1989, Yasugi, 1993, cited by Beaulieu J.F., 1997) as well as *in vitro* (Kedinger, 1987, Yasugi, 1993, cited by Beaulieu J. F., 1997) requires a mesenchymal support.

Another important element in this epithelial-mesenchymal interface is the basement membrane which is located at the epithelial-mesenchymal interface.

Here we focus our interest on epithelial cell differentiation and basement membrane ontogenesis the following digestive tract segments: esophagus (fetal and adult animals), primitive gut and small intestine of new-born animals.

Esophagus

Esophagus of 15mm of cranio-caudal axis fetus length

At this stage, an undifferentiated epithelium, apparently 2-3 cell layers, with large nuclei separated by a thick basement membrane-like structure can be seen (Fig. 1). The virtual lumen of the esophagus seems to be filled with some amorphous material, including few nucleated cells. No hemidesmosomal junction can be detected.

Esophagus of adult animal

Adult esophagian epithelium is multilayered epidermal-like. This is separated by subjacent mesenchyme by a well developed basement membrane (Fig. 2). Hemidesmosomes exhibit hemidesmosomal outer plaque as well as hemidesmosomal inner plaque.

Cytoskeletal filaments are inserted into hemidesmosomal inner plaque. Subbasal dense plaque can be detected. In suprabasal cell, round, small and reduced as number keratohyaline granules can be seen. No typically lamellar bodies or intercellular deliverance can be detected but transitional keratinocyte exhibits a cornified envelope (Fig. 4). The uppermost cell layers are cornified (Fig. 3).

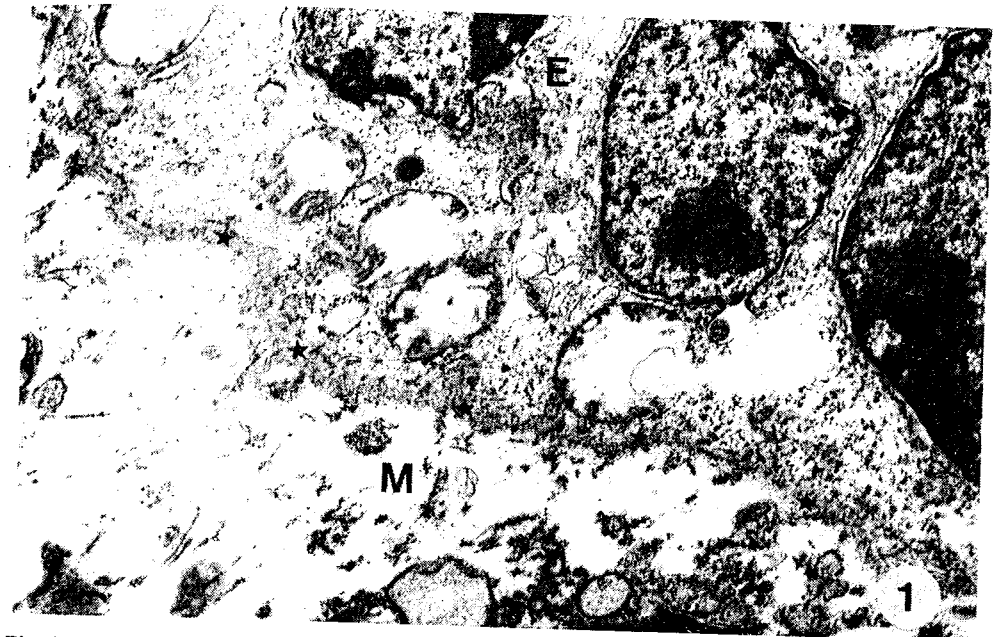


Fig. 1. - At the epithelial (E) -mesenchymal (M) junction a thick basement membrane-like structure (asterisks) can be seen. (esophagus, fetus 15 mm) ($\times 13,000$).

Fig. 2. - Hemidesmosomal junctions strongly connect epithelial cells (E) to the subjacent mesenchyme (M). Mature hemidesmosomes exhibit outer hemidesmosomal plaque (HDop) as well as inner hemidesmosomal plaque (HDip) which connect cytoskeletal filaments (cf). Subbasal dense plaque is distinct (arrows) (esophagus adult) ($\times 22,000$).

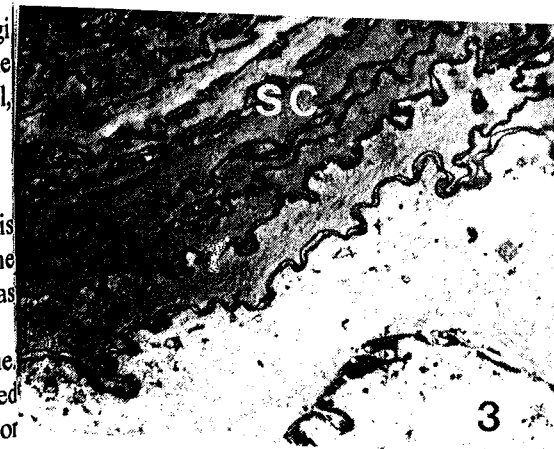
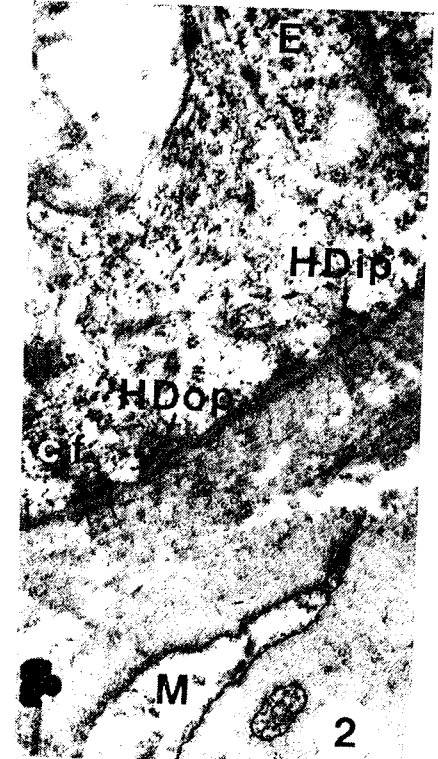


Fig. 3. - The uppermost cell layers of adult esophagus are keratinized (SC) ($\times 6,400$).

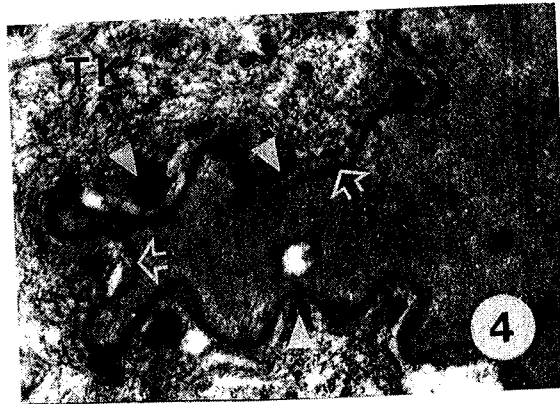


Fig. 4. - A transitional keratinocyte (TK) exhibits desmosomal remnants (white triangles); (open arrows mark cornified envelope), (adult esophagus), ($\times 22,500$).

Primitive small intestine (gut)

Cranio-caudal axis fetus length is 5-7 mm

The epithelial cells are not columnar but cuboidal or polymorphic. No Goblet cells can be detected. Towards primitive lumen of the gut, epithelial cells exhibit some cell projections heterogeneous as morphology and dimensions.



Fig. 5. - Desmosomes (white triangles) connect apical pole of the intestinal epithelial cells (E). The cytoplasm of the epithelial cells is prevalently filled with ribosomes. No microvilli can be seen. L marks primitive lumen of the primitive gut. (fetus of 5-7 mm) ($\times 14,000$).

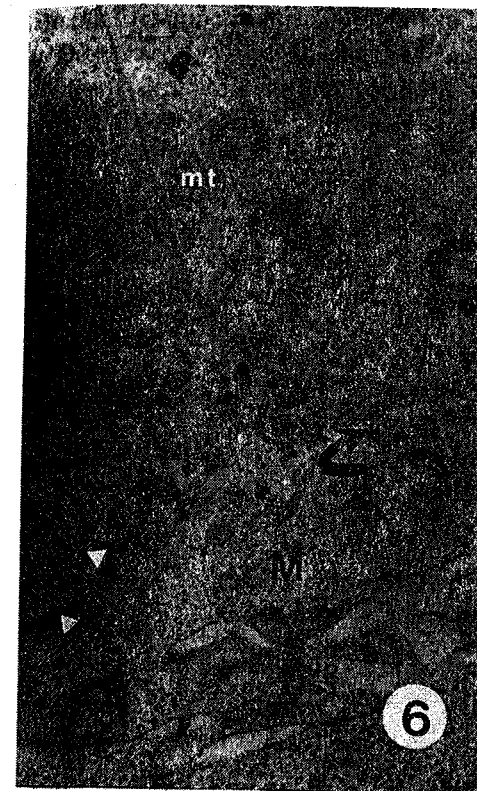


Fig. 6. - General view at the epithelial (E) - mesenchymal (M) zone. Numerous ribosomes, polymorphic mitochondria (m) and long profile of microtubules (mt) can be seen in the basal pole of epithelial cell. An amorphous material like a basement membrane (head arrows) is often in direct contact with numerous fibrils (curved arrows) which seem to be produced by mesenchymal cells (white triangles), (small intestine) (fetus 5-7 mm).

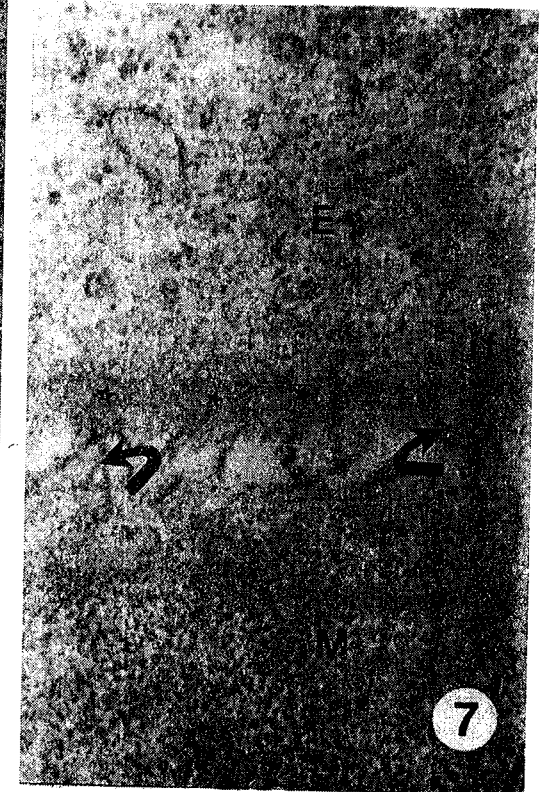


Fig. 7. - Ultrastructural detail of the basement membrane (asterisk). Numerous intermedium filaments (if) connect basement membrane. No hemidesmosomal junctions can be detected. Curved arrows mark fibrils which strongly connect basement membrane to the mesenchymal components. (small intestine) (fetus 5-7 mm), ($\times 51,000$).

They are "blebsus-like" or "microvilli-like" but no brush-border can be observed. Nuclei are large, ovoidal and euchromatine is predominant.

Often, at the apical pole, small or large vesicles tend to be separated of the rest of the epithelial cell. It seems that by this process of shedding vesicles a veritable lumen is formed (primitive lumen of the gut), (Fig. 5). Frequently, desmosomal junctions strongly connect apical-lateral domains of plasmamembrane of adjacent epithelial cells.

Ultrastructural analysis of the epithelial-mesenchymal junction zone reveals a thick amorphous material like a basement membrane (Figs. 6 and 7). No

hemidesmosomal junctions can be detected but numerous intermedium filaments are directed to the basal pole of the epithelial cells which seem to be strongly connected to the basement membrane. In turn, the basement membrane is strongly connected by numerous fibrils which seems to be a fibrillar collagen produced by the neighbouring mesenchymal cells (Figs. 6 and 7).

With respect to the basement membrane origin, it was demonstrated that the basement membrane components at the interface between the epithelium and the mesenchyme is of a dual origin (Beaulieu J.F., 1997).

The epithelium is monolayered. Epithelial cells are prismatic, with the basal pole faced by a basement membrane (Fig. 8).



Fig. 8. – Epithelial cells (E) of the intestinal mucosa are prismatic and become in direct contact by basal pole with basement membrane (small arrows) adjacent to subjacent mesenchyme (M). Short and thin collagen fibres associated to basement membrane can be seen. Black triangle marks a dark cell. (small intestine) (fetus 5-7 mm) ($\times 6,400$).

Except for some dark-cells (Fig. 8), the rest of epithelial cells seem to be undifferentiated. Only scanty heterochromatin can be seen inside of the large epithelial nuclei.

Apparently three zones of different cell density can be distinguished.

Monolayer adventiceal cells overlap the periphery of the digestive tract (Fig. 9). A well-developed basement membrane separates cuboidal adventiceal cells from mesenchymal cells. Desmosomal junctions connect adjacent adventiceal cells.

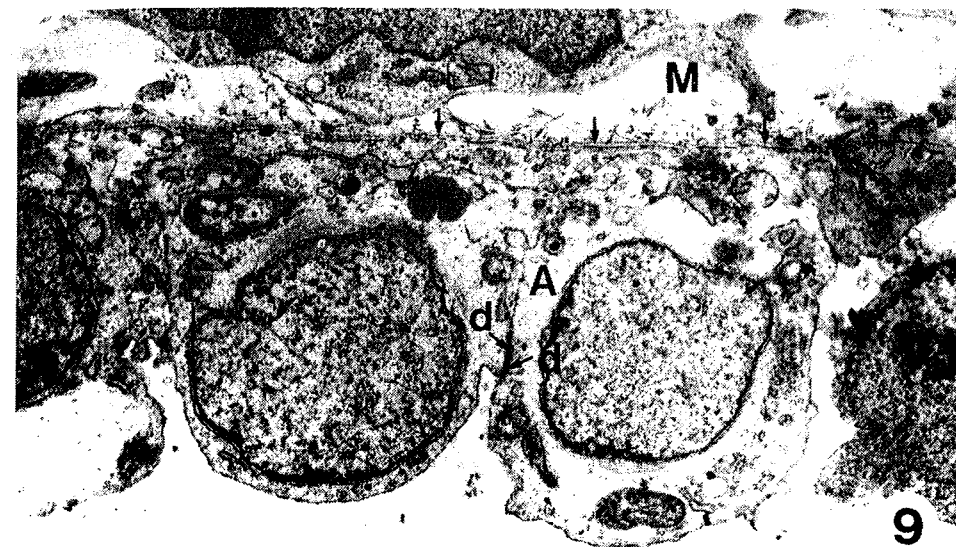


Fig. 9. – At the periphery of small intestine adventiceal cells (A) are unilayered. Adventiceal cells are polarized: basal pole contact a continuous basement membrane (arrows), d = desmosomes, M = mesenchyme. (small intestine) (fetus 5-7 mm), ($\times 8,000$).

Small intestine (fetus of 10 mm)

At this stage, monolayered epithelial cells are columnar-cylindric (Fig. 11). Zonula occludens and desmosomes strongly connect apical-lateral plasmamembranes of epithelial cells (Fig. 10). Moreover, numerous interdigitating folds improve the strength of the cell-to-cell adherence, preparing the mucous epithelium for the mechanic stress during adult life.

The free luminal cavity of the small intestine is relatively large. At this stage, monolayered intestinal epithelium is projected towards luminal cavity as villi each one being centered by a mesenchymal bud which originates from the circularly oriented mesenchymal cells. Inside of the mesenchymal tissue, sanguine cells can be seen: lymphoid cells as well as erythroblasts, reticulocytes-like and adult hematia.

The apical pole of epithelial cells exhibits a lot of microvilli which are projected inside of the gut lumen (Fig. 11). At this time, numerous epithelial cells are engaged in different stages of mitotic division (Fig. 12).

The basement membrane is well developed with distinct lamina lucida and continuous lamina densa (Fig. 13) and numerous fibrils connect basement membrane and consequently the intestinal epithelium to the adjacent mesenchyme.

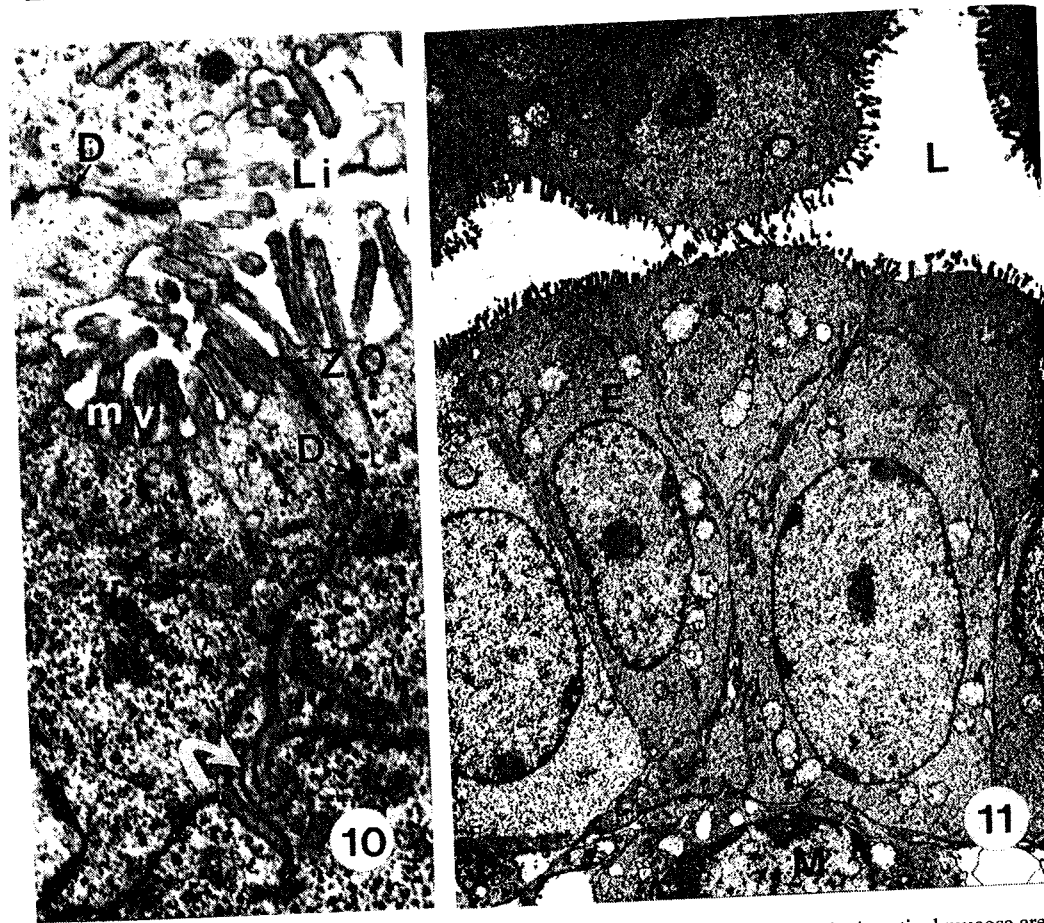


Fig. 10. - Detail of the apical pole of intestinal mucosa. Junctional complexes (zonula occludens = Z.O. and desmosomes = D) connect lateral-apical plasmamembranes of the adjacent epithelial cells. Curved arrow marks interdigitating fold. Apical microvilli (mv) are projected inside of the intestinal lumen (L i). (fetus 10mm) ($\times 20,000$).

Fig. 11. - Epithelial cells of the intestinal mucosa are prismatic unilayered and undifferentiated. Numerous microvilli are oriented towards intestinal lumen (L). Basal pole of the epithelial cells rest on the basement membrane (for detail see Fig. 13). M = mesenchymal cell. (fetus 10mm), ($\times 6,500$).

Jejunal segment of the small intestine (new-born animal)

At this stage of the gut ontogenesis, at least two types of differentiated epithelial cells of intestinal mucosa can be counted: absorptive columnar cells with a dense brush border and rare mucus-producing Goblet cells (Fig. 14). Goblet cells have a plethora of polymorphic mucous droplets.

Whereas the general pattern of digestive tract development is similar in most mammals, temporal differences exist among species. Epithelial cellular differentiation

and maturation, gut villus, formation in humans, sheep and pig, with comparatively longer gestational periods, occur early in gestation.

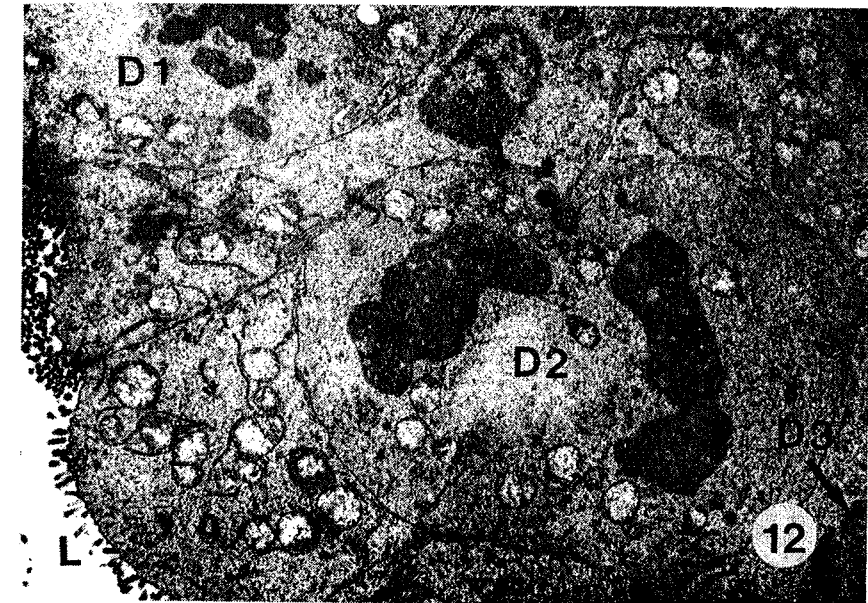


Fig. 12. - Three epithelial cells during different phases of cell division = (D1-D3). L = lumen. (fetus 10 mm). ($\times 6,500$).



Fig. 13. - Ultrastructural detail of the basement membrane (open arrows) and fibrillar material (small arrows) which connect epithelium of intestinal mucosa to the subjacent mesenchyme. (fetus 10 mm) ($\times 26,000$).



Fig. 14. – Differentiated epithelial cells of intestinal mucosa can be seen: an absorptive columnar cell (A) and Goblet cell (G). Absorptive cell exhibits brush border (mv). V = large fused vacuoles; only few small microvilli (small arrows) can be seen at the apical pole of the Goblet cell. (jejunum of a new born animal). ($\times 12,500$).

In contrast, mucosal morphogenesis and cellular differentiation of epithelium in rodents take place late in gestation (during the last few days of gestation and may continue short time after parturition (Dekaney Ch. et al., 1997). Indeed, concerning cell differentiation of the epithelium during digestive tract ontogenesis of *Mesocricetus auratus*, our results show that the gradual transition from less to more differentiated cells is a slow process. Specialized cell phenotypes appear around the parturition time.

REFERENCES

1. BEAULIEU J.F., Extracellular matrix components and integrins in relationship to human intestinal epithelial cell differentiation, *Progress in Histochemistry and Cytochemistry*, **31**(4), p.1-87, 1997.
2. CALVERT R., MALKA D., MENARD D., Establishment of regional differences in brush border enzymatic activities during the development of fetal mouse small intestine, *Cell Tissue Res.*, **214**:97-106, 1981.
3. DEKANEY C., BAZZER F.W., JAGER L.A., Mucosal morphogenesis and cytodifferentiation in fetal porcine small intestine, *Anat. Rec.*, **249**: 517-523, 1997.
4. GURDON J.B., The generation of diversity and pattern in animal development, *Cell*, **68**(2), 185-199, 1992.
5. ROTH K.A., HERMISTON M.L., GORDON J.I., Use of transgenic mice to infer the biological properties of small intestinal stem cells and to examine the lineage relationship of their descendants, *Proc. Natl. Acad. Sci. U. S.A.*, **88**: 9407 -9411, 1991.
6. SQUIER C.A., KAMMEYER G.A., The role of connective tissue in the maintenance of epithelial differentiation in the adult, *Cell Tissue Res.*, **230**: 615-630, 1982.

Received January 20, 1999

Institute of Biology
Splaiul Independenței 296,
Bucharest

CHROMOSOMAL ALTERATIONS IN RUBINSTEIN-TAYBI SYNDROME

ZORICA-ILEANA HERTZOG*, F.MIXICH*, R.HERTZOG**

This paper presents the results of a genetic examination in two cases of Rubinstein - Taybi syndrome. The cytogenetic analysis of the first case reveals a chromosome instability expressed by chromosome breaks on chromosomes 4,5,10,11,12,14 and X (12.7%), terminal deletions in chromosome 17 (9.6%), dicentric chromosome (16;9) (6.45%), pericentric inversions on chromosome 9 (2.5%) and a microdeletion on 16p. In the second case we reported a microdeletion at 16p13. The pedigree analysis suggests an autosomal dominant inheritance and the examination of dermatoglyphics shows the prevalence of loops, the absence of triradius *c* and thenar drawings in one case.

Keywords: broad thumb and hallux, chromosome 16, microdeletion, chromosome instability.

INTRODUCTION

The Rubinstein - Taybi syndrome (RTS) was described for the first time in 1963 by Rubinstein and Taybi, although the first paper about this syndrome named broad thumb and hallux syndrome, was presented by Michail and coworkers in 1957.

RTS has low incidence. Till now, about 600 cases were reported all around the world (5,7). This is a syndrome with many congenital anomalies such as: reduced physical growth, mental retardation, broad thumb and hallux, downward-slanting palpebral fissures, hypertelorism, strabismus, coloboma, cataract, glaucoma, highly-arched palate, microcephaly, respiratory malformations (laryngomalacia), cardiovascular (coarctation of the aorta) and genitourinary malformations (nephrosis, incomplete descent of the testes, hypospadias, small angulate penis), cutaneous manifestations (hirsutism) (7, 12).

The molecular analysis of this syndrome revealed a microdeletion on 16p13.3 (5, 10) and a translocation t (8;16).

This paper shows the results provided by the genetic examination of two young male patients (14 years and 5 years old, respectively). The first subject has Rubinstein-Taybi diagnosis and the second was suspected of Down syndrome

MATERIALS AND METHODS

A. Clinical Description

The first subject, 14 years old, presented the following clinical symptoms: discrete microcephaly, mongoloid palpebral fissures, aquiline nose, irregular teeth

implantation, jaw prognathism, low implanted ears, broad thumb and hallux, pale tegument, IQ=78.

The second patient, 5 years old, presented microcephaly, broad thumb and hallux, incomplete syndactyly between the II-nd and the III-rd fingers of both legs, muscular hypotonicity, IQ=71.

B. Karyotype analysis

In order to study the karyotype we made cultures of lymphocytes raised for 72h in MEM culture medium supplemented with 10% calf serum and stimulated to divide with PHA -M (3). The mitosis was stopped in metaphase with colcemid (2µg/ml culture medium). KCl solution (0.075M) was used to give the hypotonicity and a methanol/acetic acid mixture (3:1) as fixing solution. We used Benn and Pearl's technique (as cited by Rooney and Czepulkowski) to make the Giemsa banding of the mounts (6). For each case, 40 metaphases were tested.

C. Pedigree

We made the three-generation pedigree for each case using the PSTF recommended symbols (Pedigree Standardization Task Force) (1).

D. Dermatoglyphics

The fingerprints and the palmar prints have been analyzed.

RESULTS AND DISCUSSIONS

In the first case, the analysis of mitotic chromosomes revealed chromosome instability expressed by chromosome breaks in 4,5,10,11,12,14 and X(12.7%), terminal deletions in 17p (9.6%), dic (16;9q) (6.45%) (fig.1). We also observed pericentric inversions in one of chromosomes 9 (2.50%). Otherwise these inversions represent a heterochromatic variant (3). In 2.5% of examined metaphases, we observed a high quantity of heterochromatin in the long arm of chromosome 11 (11qh+) (fig.2). This variant is very rare and can be associated with a phenotype effect. In 5% of metaphases we noted abnormally banded regions (abr) in 5q and 12q (fig.3). These regions could be a gene amplification event.

In the second case, we noted microdeletions in 16p13 for 51% of examined metaphases (fig.4). The figures 5 and 6 represent the pedigree for these cases. The analysis of pedigree leads to the conclusion that broad thumb and hallux is an autosomal dominant syndrome. The lack of the character (broad thumb and hallux) in the ascendancy of the second case can be explained through a "de novo" mutation. This presumes a gene mutation, which could be a macrolesion observed

in prometaphasic chromosomes, as it has been reported by molecular techniques (4,5,8,9,11,12). The associated malformations are due either to diversity of chromosome alterations or to the pleiotropic effect of the mutation.

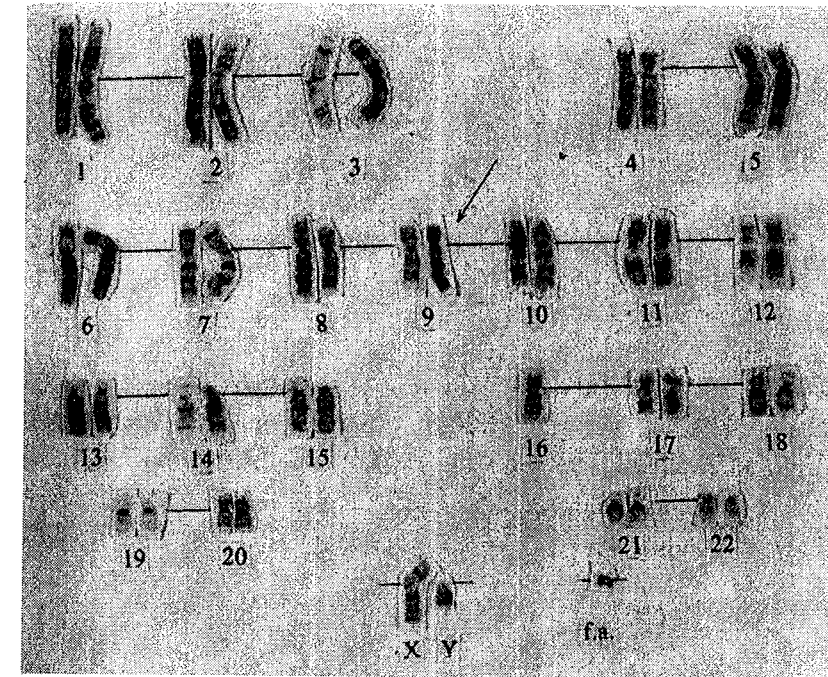


Fig. 1. - Karyotype 45, XY, dic (9;16) + acentric fragment.

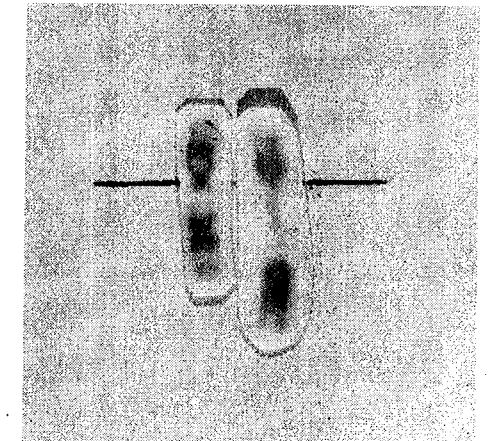


Fig. 2. - Pair of chromosomes 11 with one of homologues 11qh+.

The analysis of dermatoglyphics for the first case reveals loops and whirls, the absence of triradius *c* at both hands, the proximal position of triradius *t*. The

second case presents only loops, the absence of triradius *c*, the proximal position of triradius *t* and a whirl in thenar area.



Fig. 3. – Abnormally banded regions in 12q and 5q.

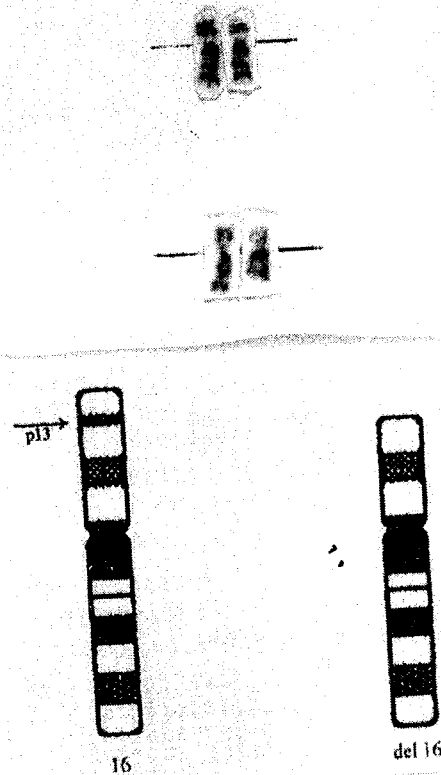


Fig. 4. – Diagram and partial karyotype of microdeletion 16p.

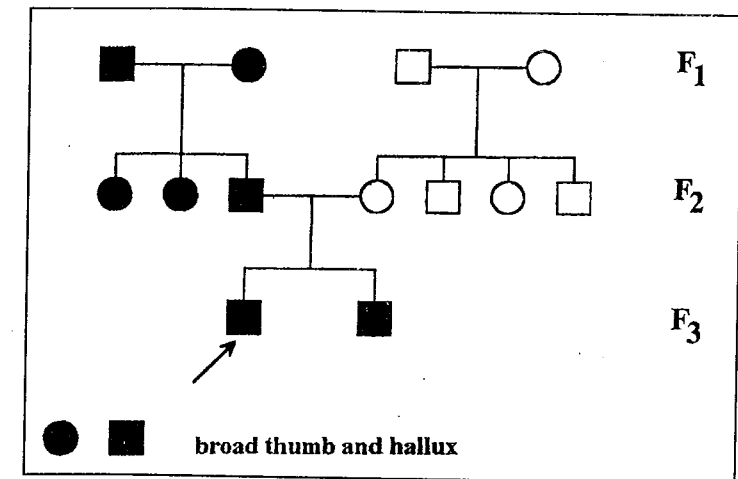


Fig. 5. – Pedigree of the first case.

After the hybridization with RT1 cosmid there was observed a microdeletion in 16p13.3 at 7 patients from 64 subjects with obvious clinical symptoms (5).

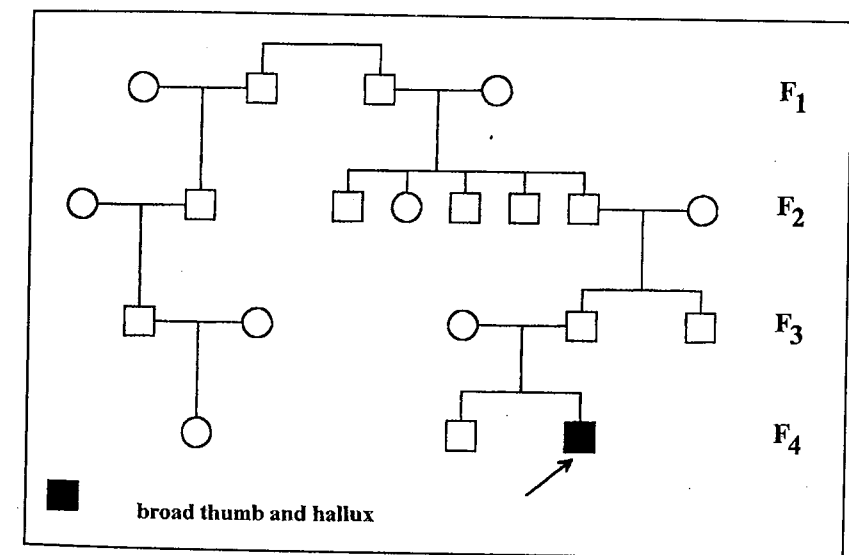


Fig. 6. – Pedigree of the second case.

Tanaka and his research team suggest that the RTS involves several mutations in *Cbp* gene. This gene codes a transcription coactivator, the morphogenetic protein, required by many transcription factors for transactivation. The same team reports that *Cbp* mutations in heterozygous mice (*C57B2/6-CBA* x *BALB/c*) lead to skeletal anomalies (9).

Taki et al. reported a translocation t(11;16)(q23;p13) in two cases of myelodysplastic syndrome. The MLL gene from 11q23 fused to Cbp gene from 16p13. In this fusion, a part of the gene coding the methyltransferase fuses to one part of Cbp. This observation and the discovery of MOZ-Cbp fusion in t(8;16)-AML suggest that Cbp gene could be associated with leukemogenesis through translocations (8).

Giles R.H. and coworkers cloned and analyzed the gene involved in two different diseases: Rubinstein-Taybi syndrome and acute myeloid leukemia both associated with t(8;16)(p11;p13.3). They reported that Cbp gene acts as an integrator of different regulatory multiprotein complexes (4).

Verloes et al. include RTS among type 2 Biemond syndrome (SB2), an autosomal recessive condition involving mental retardation, coloboma, obesity, polydactyly, hypogonadism, hydrocephalus, and facial dysostosis (11).

The 16p13 locus contains the genes coding the hydroxyacyl-glutathione hydrolase, phosphoglycolate-phosphatase, polycystic kidney disease, adult type 1 (2). The molecular analysis of 16p13.3 using DNA probes (D16S22 - D16S85) could bring more useful informations to clarify the genetic cause of this syndrome.

REFERENCES

1. BENNETT R.L., STEINHAUS K.A., UHRICH S.B., O'SULLIVAN C.K., 1995, *Recommendation for Human Standardized Pedigree Nomenclature*, Am.J.Hum.Genet., **56**:745-752.
2. FRÉZAL J., BAULE MARIE-SOPHIE, FOUGEROLLE THÉRÈSE, KAPLAN JOSSELINE, MERRER M., *Genatlas*, INSERM, pp 333.
3. HERTZOG ZORICA-ILEANA, 1998, *Human genetics - Principles and Methods*, Edit.Sitech, pp 57-58, 161-169.
4. GILES R.H., PETRIJ F., DAUWERSE H.G., DEN HOLLANDER AL., LUSHNIKOVA T., VAN OMMEN G.J., GOODMAN R.H., DEAVEN L.L., DOGGETT N.A., PETERS D.J., BREUNING M.H., 1997, *Construction of a 1.2- Mb Contig surrounding and molecular analysis of the human CREB - binding protein (CBP/CREBBP) gene on chromosome 16p13.3*, Genomics, **42**(1): 96-114.
5. MCGAUGHRAN J.M., GAUNT L., DORE J., PETRIJ F., DAUWERSE H.G., DONNAI D., 1996, *Rubinstein-Taybi syndrome with deletions of FISH probe RT1 at 16p13.3 two UK patients*, J.Med.Genet., **33**(1): 82-83.
6. ROONEY D.E. AND CZEPULKOWSKI B.H., 1992, *Human Cytogenetics - A Practical Approach*, Oxford University Press, pp 95-96.
7. ROSIANU-WALTER ANNELIESE, GEORMANEANU M., 1986, *Hereditary Diseases in Pediatrics*, Edit. Medicală București, pp 104-107.
8. TAKI T., SAKO M., TSUCHIDA M., HAYASHI Y., 1997, *The t(11;16)(q23;p13) translocation in myelodysplastic syndrome fuses the MLL gene to the CBP gene*, Blood, **89**(11): 3945-3950.
9. TANAKA Y., NARUSE I., MAEKAWA T., MASUYA H., SHIROISHI T., ISHII S., 1997, *Abnormal skeletal patterning in embryos lacking a single Cbp a partial similarity with Rubinstein-Taybi syndrome*, Proc.Natl.Acad.Sci USA, **94**(19): 10215 - 10220.

10. TUDOSE OLIMPIA, 1998, *Submicroscopic Chromosome Anomalies*, The 1st National Conference of Medical Genetics, Iași, pp 15-20.
11. VERLOES A., TEMPLE I.K., BONNET S., BOTTANI A., 1997, *Coloboma, mental retardation, hypogonadism and obesity: critical review of the so-called Biemond syndrome type 2, updated nosology, and delineation of three "new" syndromes*, Am.J.Med.Genet., **69**(4): 370-379.
12. WALLERSTEIN R., ANDERSON C.E., HAY B., GUPTA P., GIBAS L., ANSARI K., COWCHOCK F.S., WEINBLATT V., REID C., LEVITAS A., JACKSON L., 1997, *Submicroscopic deletions at 16p13.3 in Rubinstein-Taybi syndrome: frequency and clinical manifestations in North American populations*, Am.J.Med.Genet., **34**(3): 203-206.

* University of Medicine and Pharmacy, Faculty of Stomatology,
4 P.Rares St, 1100 Craiova, Romania
** Military Hospital of Craiova,
132 Caracal, 1100 Craiova, Romania

THE STRUCTURE OF THE BENTHIC OLIGOCHAETA COMMUNITIES IN THE AQUATIC ECOSYSTEMS OF THE DANUBE DELTA

GETA RÎȘNOVEANU, A. VĂDINEANU, GH. IGNAT

Four species of Naididae, ten of Tubificidae and one species of Lumbricidae were identified during 1991-1994 within the benthic oligochaeta communities. The constancy and dominance criteria were satisfied only by *P. hammoniensis*, *Limnodrilus sp.* and in Isacova lake, also by *P. barbatus* populations. The other oligochaeta species were sporadic having very low densities, being around the critical level of species persistence.

During the last decade, as a consequence of the trophic state evolution of the aquatic ecosystems, a change of the communities structure has taken place. This consists in replacing a relative complex structure dominated by *L. hoffmeisteri*, *Tubifex tubifex* and *Spirosperma ferox* by a simplified one in which *P. hammoniensis* is obviously dominating.

INTRODUCTION

The evolution of the Danube Delta aquatic ecosystems during the last 10 - 15 years has been led by the eutrophication process, which is the main drive variable that has modified the ecological succession of these ecosystems (9). The research works that have been done during this interval of time have concluded that the main part of the primary production has been transferred - as particulate organic carbon - to the sediments, thus inducing major changes at the benthic fauna level (1, 2). As a consequence of the transition from mesotrophy towards hypertrophy, the structure of the benthic community became simplified, the dominance and constancy criteria being fulfilled only by *Chironomids* and *Oligochaeta* (1,5).

The aim of this paper is to assess the structural dynamics of the benthic oligochaeta communities in eight representative lakes of the Danube Delta during September 1991 - July 1994. Taking into consideration their dominance in the eutrophic ecosystems, as well as their specific responses to substrate changes which made them to be important bioindicators (4, 6), this paper is trying to assess and discuss the trends and the amplitude of the community structure changes during the last decades. For this reason, the structural status of the studied communities during 1991 - 1994 is compared with those existing during 1976 - 1982 interval.

MATERIALS AND METHODS

The sampling program included 16 collecting times, between September 1991 - July 1994. Nine to fifteen sample units from 3 to 5 stations in each lake (chosen to provide a good coverage of the biotope heterogeneity) were taken (5). The samples were collected with a 50 cm² corer, sieved through a net of 250µ mesh size and preserved in 4% formalin.

The identification of the taxa and the measurements were made using a phase contrast microscope. Data processing included the following parameters: the frequency of occurrence (F), numerical (D₁) and biomass (D₂) densities, numerical (A₁) and biomass (A₂) percentage. Obtained data were discussed in comparison with those from the reference period 1976-1982.

RESULTS AND DISCUSSIONS

Four species of Naididae (*Stilaria lacustris* Linnaeus, *Vejdovskyella comata* Vejdovsky, *Dero sp.* Muller, *Ophidonais serpentina* Muller), ten species of Tubificidae (*Potamothrix hammoniensis* Michaelsen, *Psammoryctides barbatus* Grube, *Psammoryctides albicola* Michaelsen, *Limnodrilus hoffmeisteri* Claparede, *Limnodrilus claparedeianus* Ratzel, *Limnodrilus udekemianus* Claparede, *Limnodrilus profundicola* Verrill, *Branchiura sowerbyi* Beddard, *Spirosperma ferox* Eisen, and *Tubifex ignotus* Stolc), and one species of Lumbricidae (*Eiseniella tetraedra* Savigny) were identified within the benthic oligochaete community structure. Within each lake, at every sampling time, the oligochaete community consisted in one to six species, but more frequently only in two or three species (Fig. 1A-1D).

The constancy (occurrence frequency over 50%) and dominance (numerical abundance -A₁- more than or equal to 10% and/or biomass percentage -A₂- more than or equal to 5%) criteria were fulfilled by the following species (Fig. 2A-2D):

- *P. hammoniensis*, in all studied lakes (frequencies of 90-100%, excepting Merhei lake with only 50%; A₁ between 13 and 100% and A₂, excepting August 1992 in Bogdaproste lake and June 1993 in Băclăneşti lake, over 5%);
- *L. hoffmeisteri*, in Bogdaproste, Băclăneşti and Roşu lakes, (frequencies of 100%, 80% and 64% respectively; large fluctuations of density and biomass percentage between the low limit of dominance and 100%);
- *Limnodrilus sp.*, a species complex including the *L. hoffmeisteri* and *L. claparedeianus* populations from Babina (F=100%), Puiu (F=92%) and excepting 1993, from Isacova (F=75%) lakes;
- *P. barbatus*, only in Isacova lake where the population occurred with frequencies of 93.3%, at low densities but accomplishing the biomass dominance criterion.

P. barbatus and *B. sowerbyi* were accessories in Puiu lake (F=41.6%) and also *S. ferox* in Isacova lake (F=26.6%). All the other species were sporadic (frequencies less than 20%), the size of their populations being constantly kept around the critical level of species persistence (Fig. 1).

During the studied period there were not significant changes in terms of species richness and their annual numerical share of representativity (A₁), excepting a slow increase of the share of representativity for *Limnodrilus sp.* (Fig. 3A-3D). Although in 1992 and 1993 new component species were present within the structure of studied communities (Băclăneşti, Babina, Puiu, Matîţa, Bogdaproste), they were not constant, their densities were near the critical level of persistence and their presence might be caused by cyclic fluctuations characterised by a permanent tendency to reinstall some populations and than to eliminate them as a consequence of unfavourable conditions at the sediment/water interface.

The comparison of the benthic oligochaeta communities structure during 1991-1994 interval with that of 1975-1985 period of time (1, 8) reveals that during the last decade a change of the community structure took place as a consequence of the trophic state transition of the Danube Delta aquatic ecosystems towards eutrophy (2, 3, 7, 9). The change consisted mainly in replacing of a relative complex structure (dominated mainly by *L. hoffmeisteri*, *Tubifex tubifex* and *Spirosperma ferox*) by a simplified one (dominated by *P. hammoniensis*). Similar trends in the structural dynamics of the studied communities and their main drive forces were recorded in all studied lakes. The differences in their geographical position, morphometry and flooding regime have affected only the amplitude of the processes.

No clitellate specimens of *T. tubifex* were identified during 1992-1994.

CONCLUSIONS

The comparative analyses of the benthic oligochaeta communities structure within 1991-1994 interval and the assessment of their dynamics during the last decades revealed that:

- the species richness was limited to two or three species in each lake at every sampling time;
- the communities structure was dominated by the *P. hammoniensis* population;
- excepting a slow increase of the share of representativity for *Limnodrilus sp.*, not significant changes in terms of species richness and their share of representativity took place during the study interval;
- during the last decade, as a consequence of the trophic state transition towards eutrophication, the relative complex structure dominated by *L. hoffmeisteri*, *T. tubifex* and *S. ferox* species was replaced by a simplified one, dominated by *P. hammoniensis*;

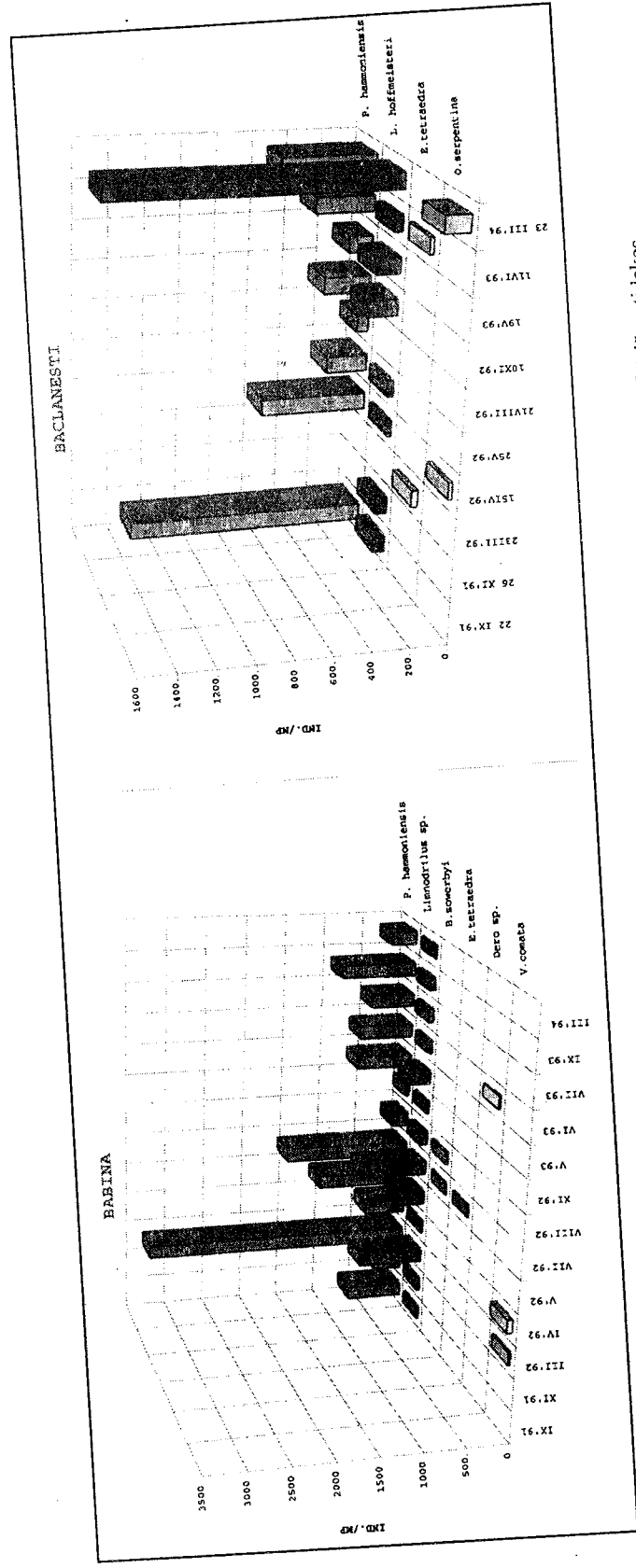


Fig. 1 A – Dynamics of monthly numerical densities (ind/m³) of oligochaeta species in Babina and Băclănești lakes.

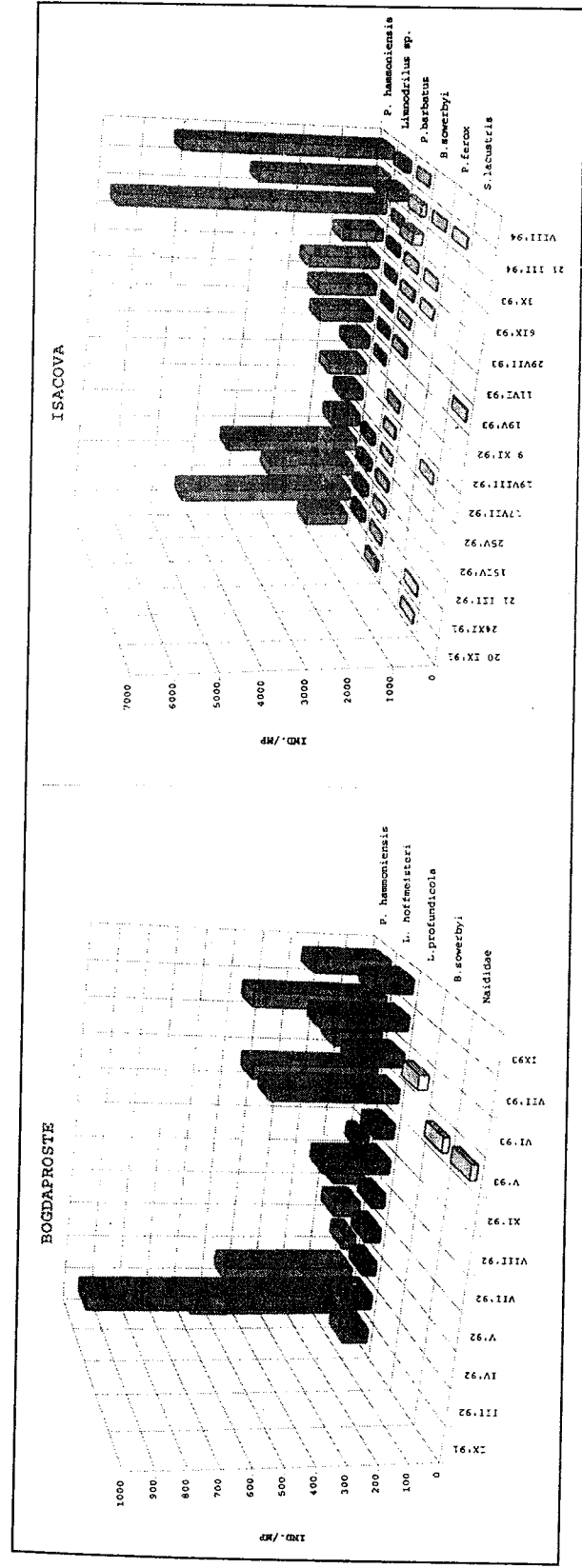


Fig. 1 B – Dynamics of monthly numerical densities (ind/m³) of oligochaeta species in Bogdaproste and Isacova lakes.

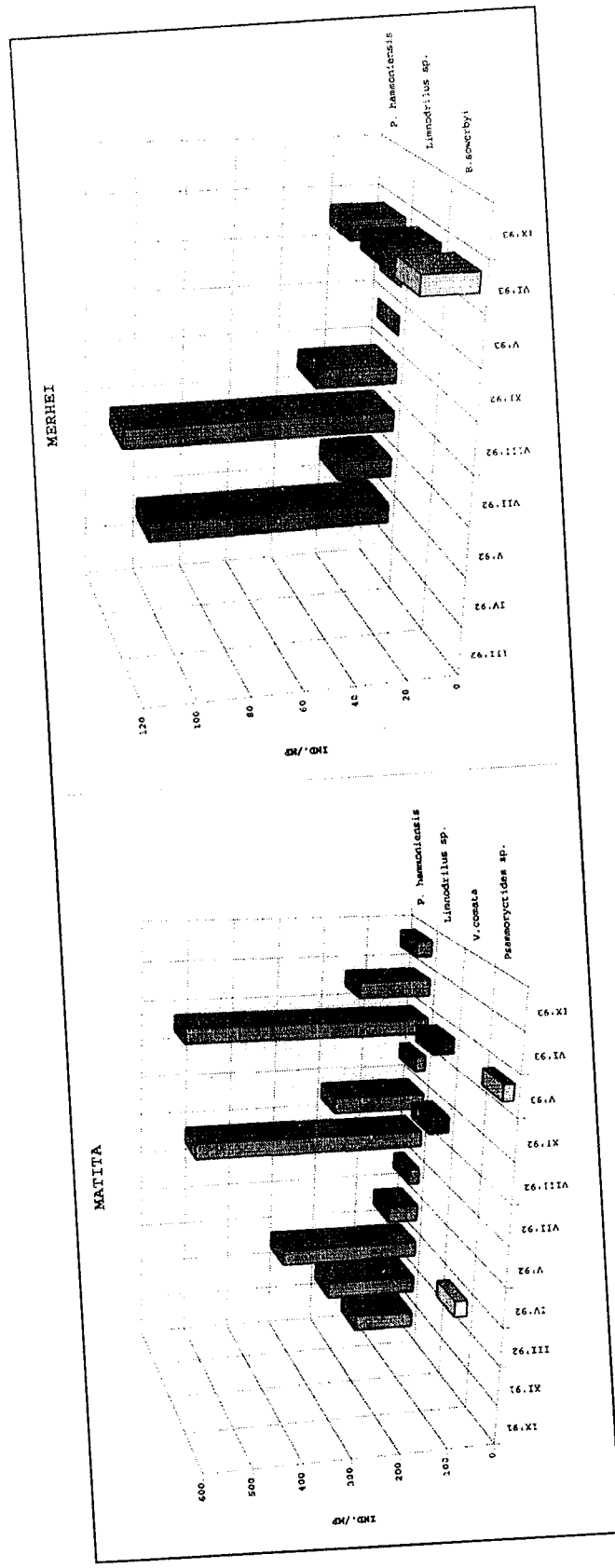


Fig. 1C – Dynamics of monthly numerical densities (ind/m³) of oligochaeta species in Matita and Merhei lakes.

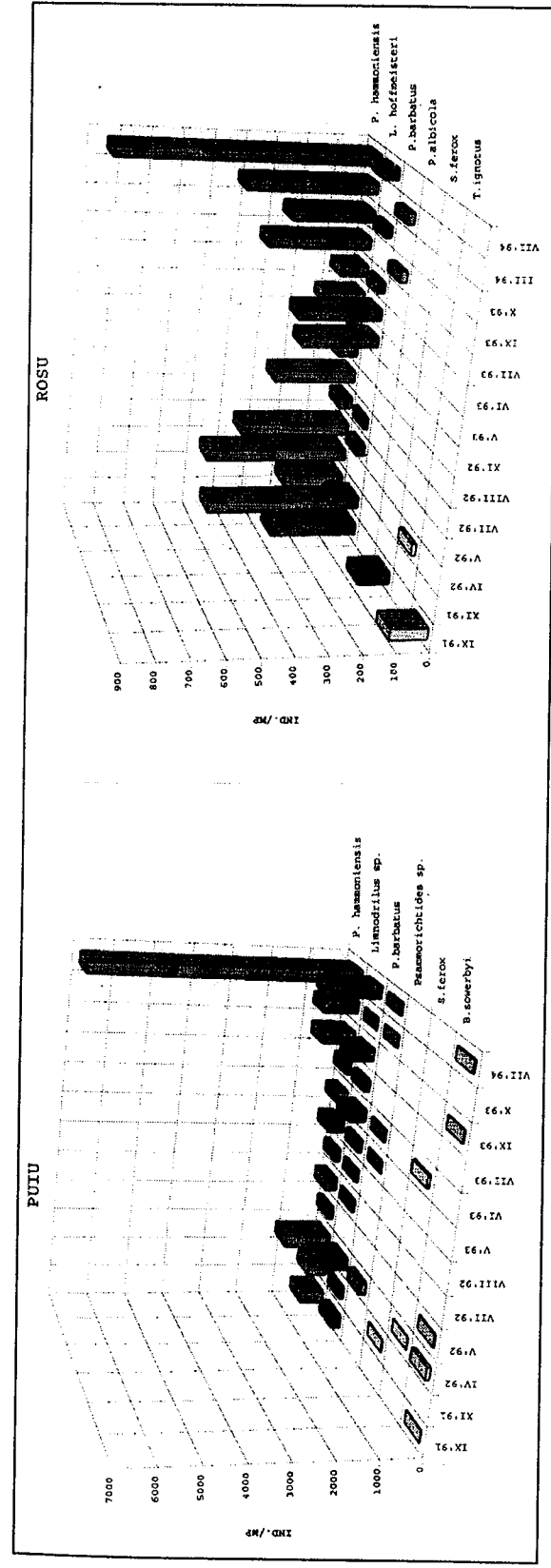


Fig. 1D – Dynamics of monthly numerical densities (ind/m³) of oligochaeta species in Puiu and Rosu lakes.

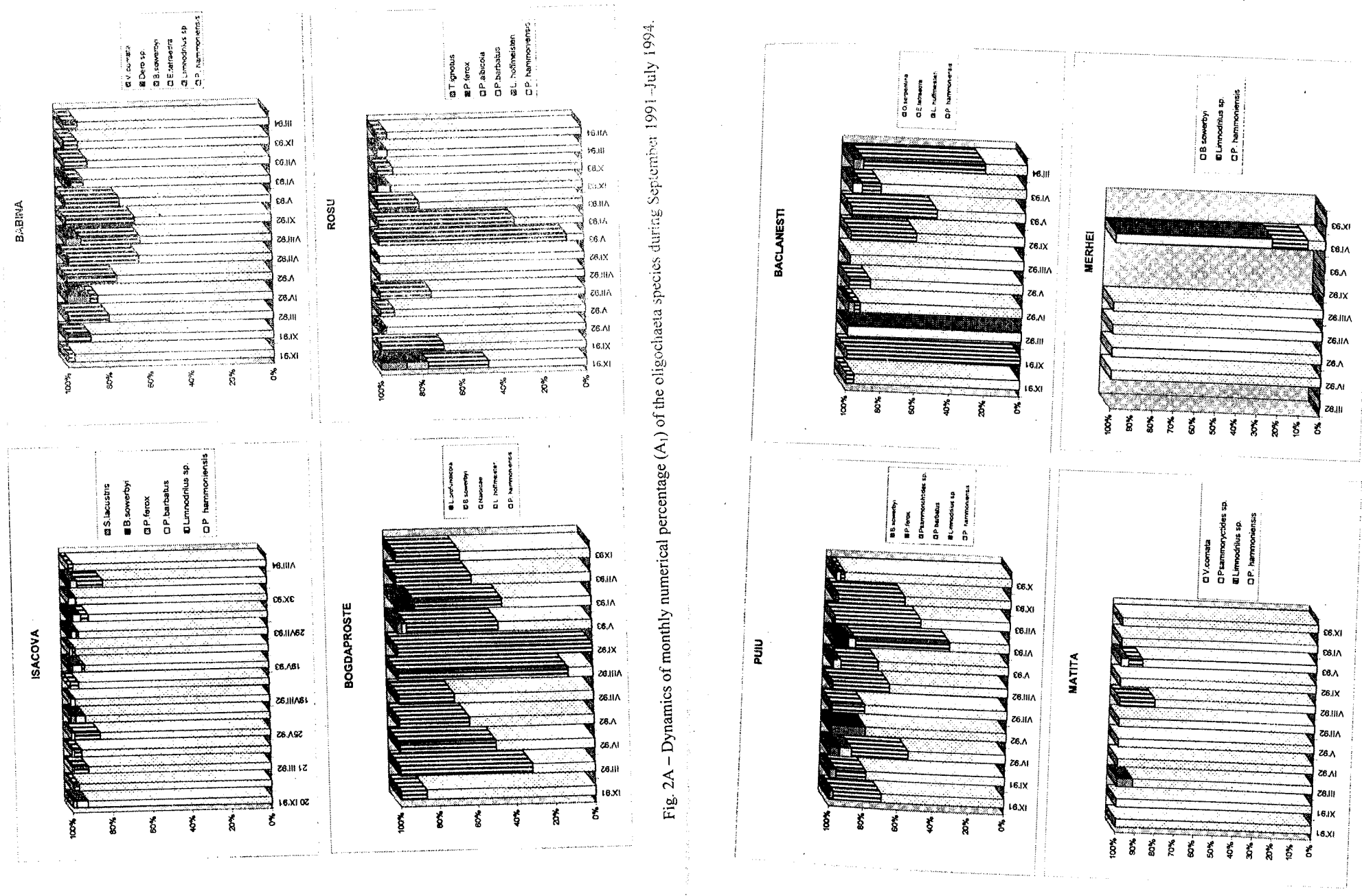


Fig. 2A – Dynamics of monthly numerical percentage (A_i) of the oligochaeta species during September 1991–July 1994.

Fig. 2 B – Dynamics of monthly numerical percentage (A_i) of the oligochaeta species during September 1991–July 1994.

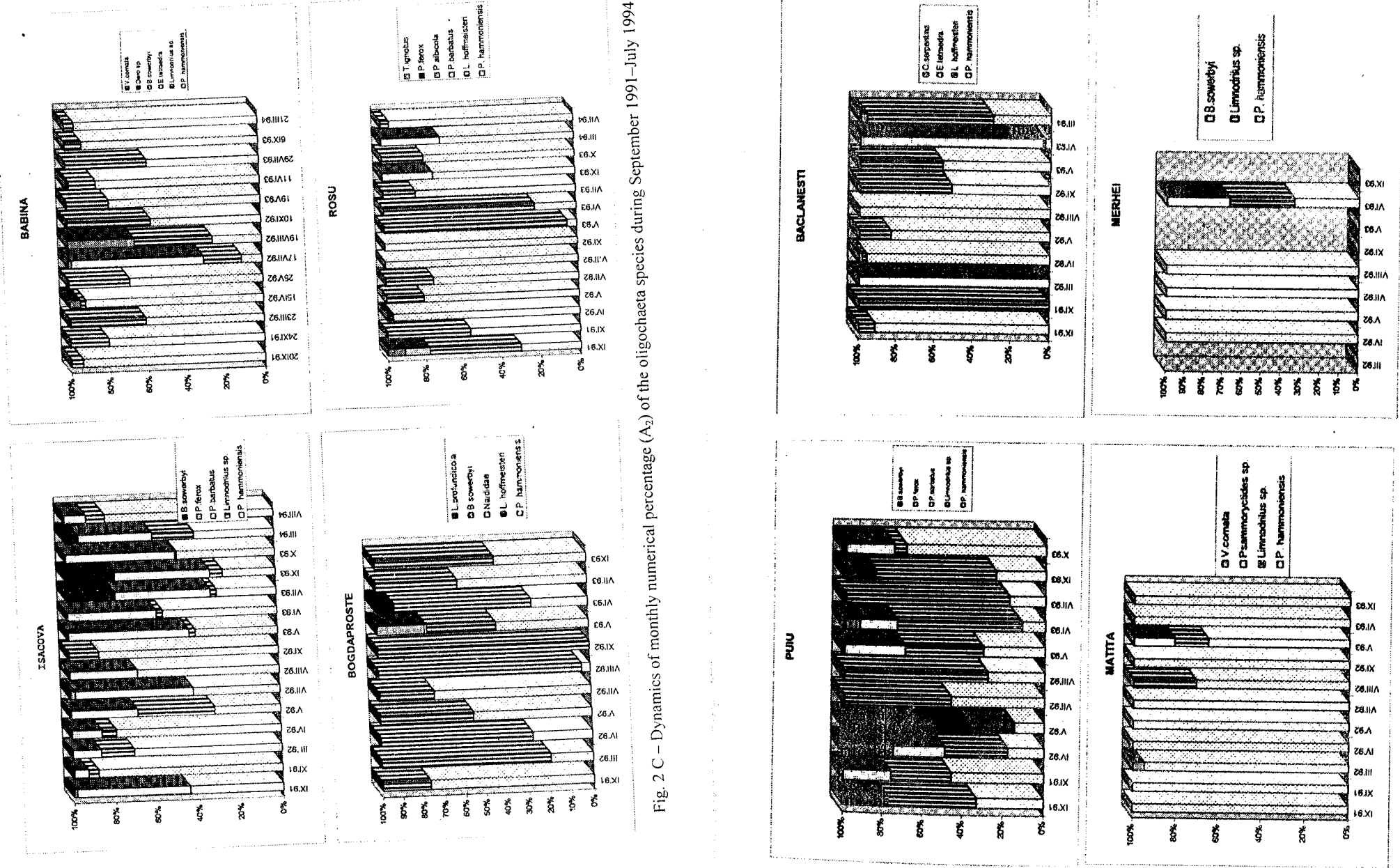


Fig. 2 C - Dynamics of monthly numerical percentage (A_2) of the oligochaeta species during September 1991-July 1994.

Fig. 2 D - Dynamics of monthly numerical percentage (A_2) of the oligochaeta species during September 1991-July 1994.

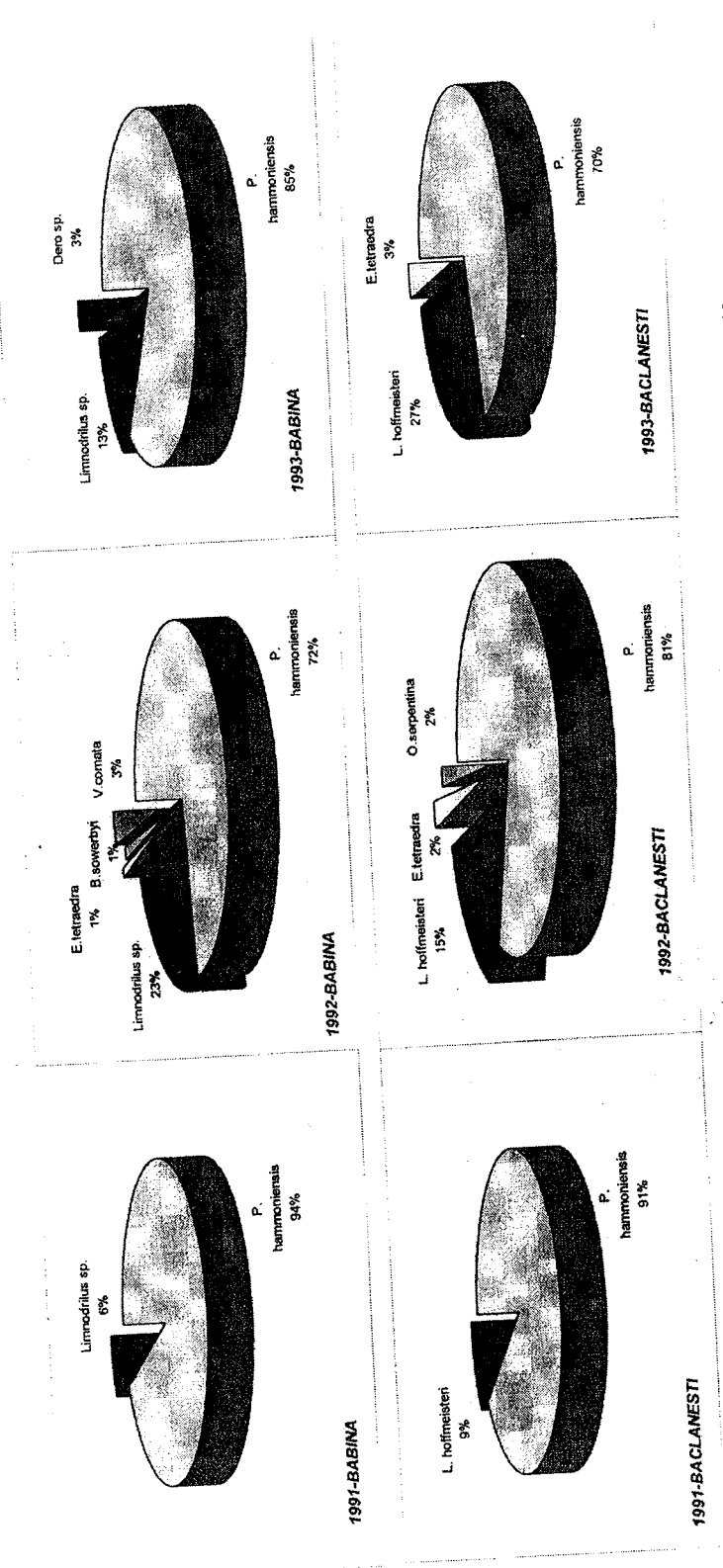


Fig. 3A – The annual dynamics of the benthic oligochaeta communities structure during 1991–1993.

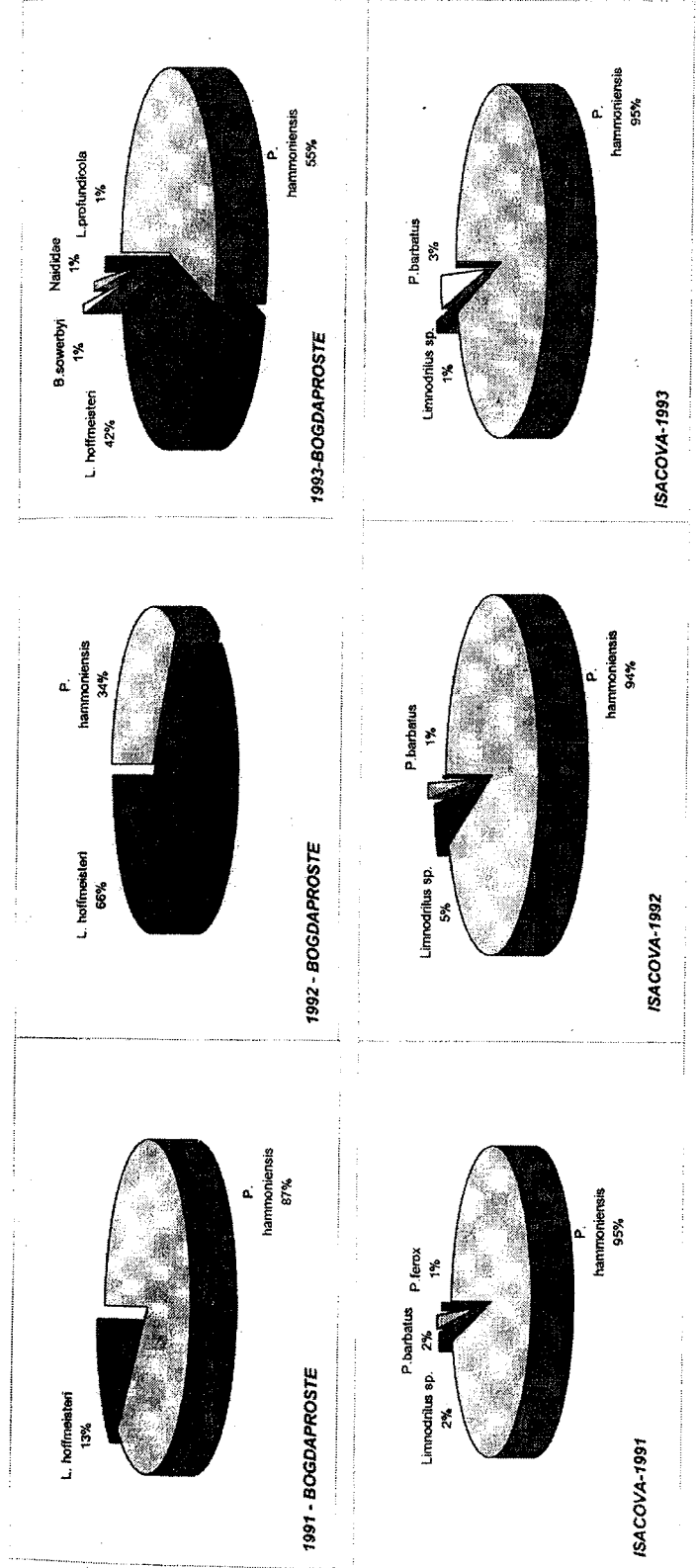


Fig. 3B – The annual dynamics of the benthic oligochaeta communities structure during 1991–1993.

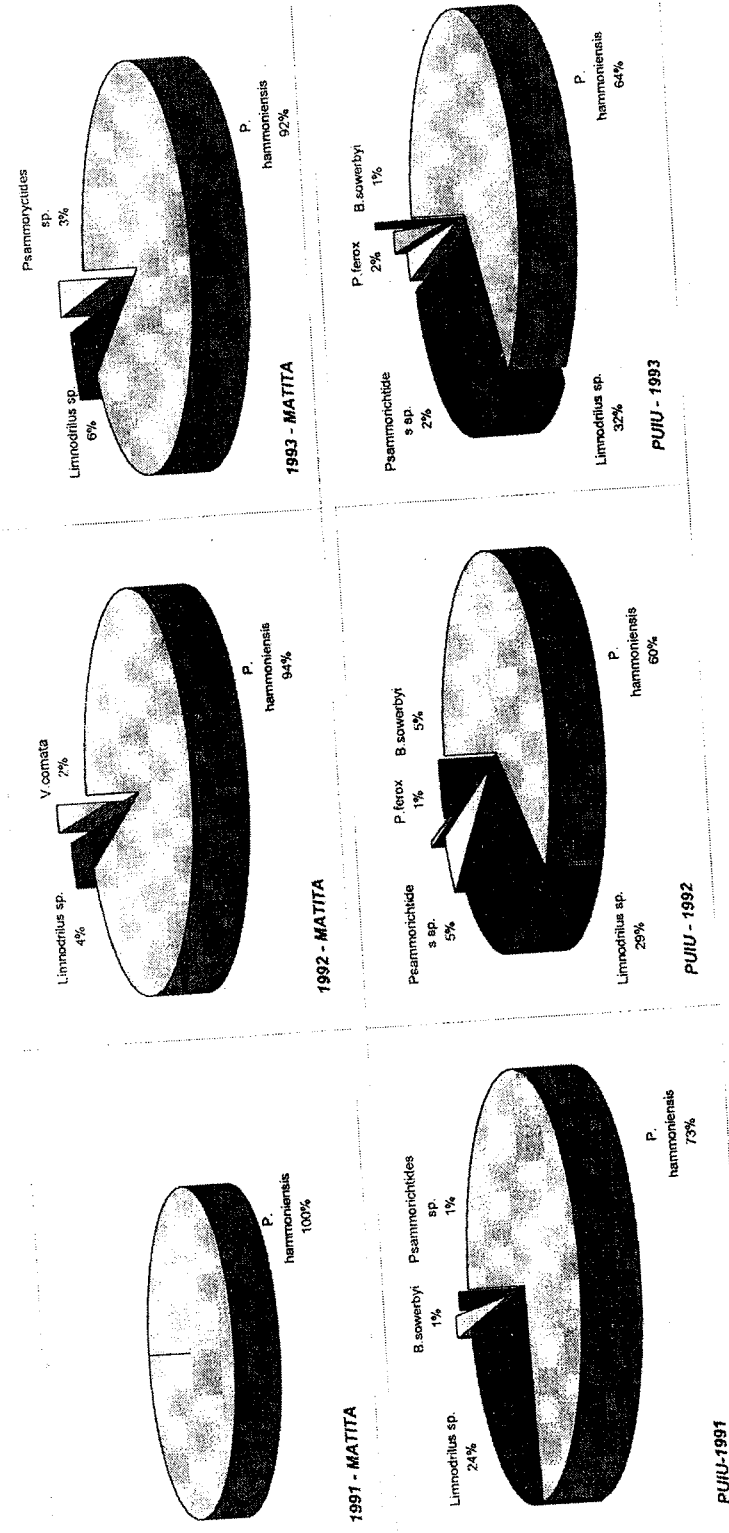


Fig. 3C – The annual dynamics of the benthic oligochaeta communities structure during 1991–1993.

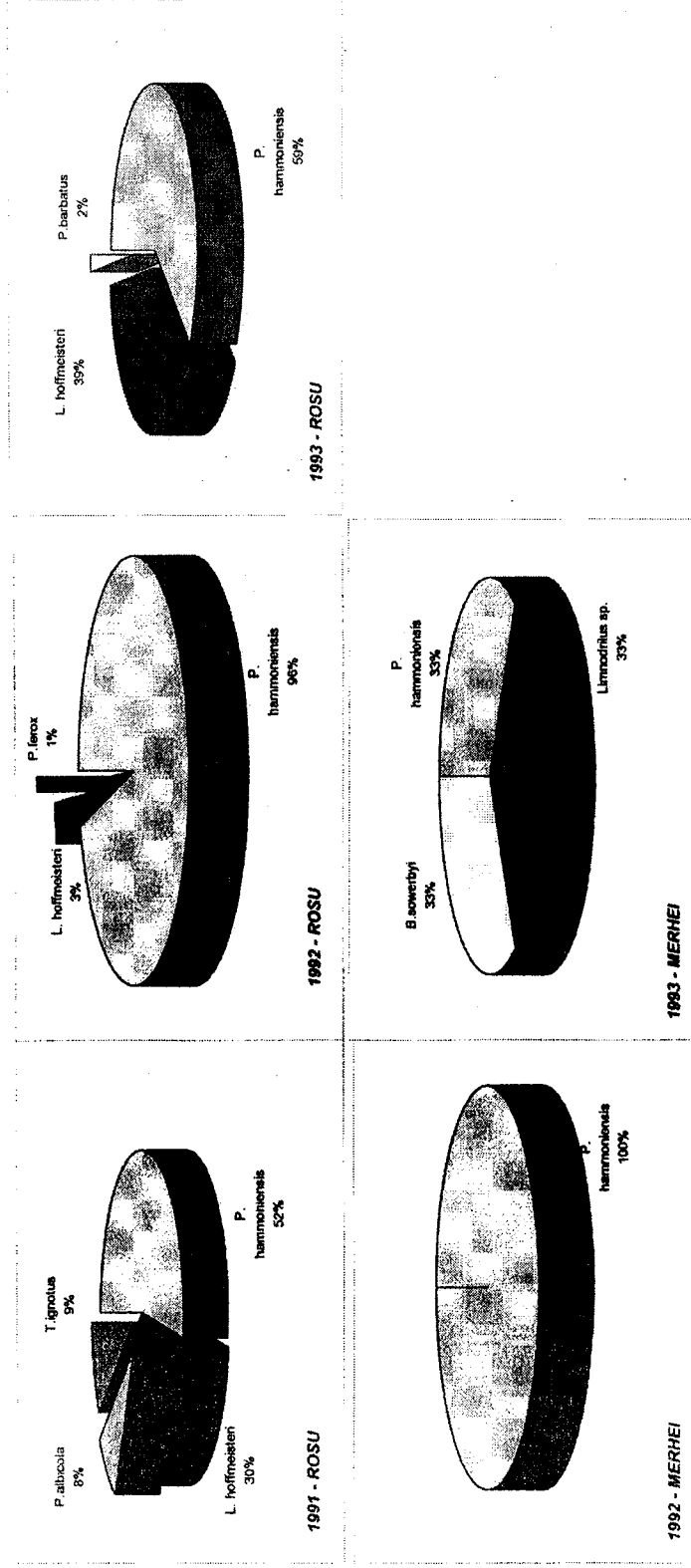


Fig. 3D – The annual dynamics of the benthic oligochaeta communities structure during 1991–1993.

- similar trends in the structural dynamics of the studied communities and their main drive forces were recorded in all studied lakes. Differences are related only with the amplitude of the processes.

Acknowledgements. We express our thanks to Dr. Patrick Martin for confirmation of the identified species.

REFERENCES

- BOTNARIUC N., GH. IGNAT, I. DIACONU, A. VĂDINEANU, 1987, Rev. Roum. Biol. Anim., 32, 2, p. 121-127.
- CRISTOFOR S., A. VĂDINEANU, G. IGNAT, 1993, Hydrobiologia, 251: 143-148.
- DIACONU I., 1986, Doctorate thesis University of Bucharest.
- HARE L., 1992, Critical Rev. In Tox., 22 (5/6): 327-369.
- RÎŞNOVEANU GETA, GH. IGNAT, G. NAFORNIŢĂ, C. CIUBUC, A. VĂDINEANU, 1995, The 7th European Ecological Congress, Budapest, 20-25 August.
- SCHLOESSER D.W., T.B.REYNOLDSON & B.A.MANNY, 1995, J.Great Lakes Res., 21(3): 294-306.
- TIMM T., K. KANGUR, H. TIMM & V. TIMM, 1994, Proc. Estonian Acad. Sci. Ecol., 4(1): 21-32.
- TUDORANCEA CL., GH. IGNAT, I. DIACONU, 1976, Ocrotirea Naturii Dobroge, Acad. RSR, p.90-112.
- VĂDINEANU A., N. BOTNARIUC, S. CRISTOFOR, GH. IGNAT, C. DOROBANŢU, 1989, Ocrot. Nat. Med. Inconj., 33(1), p.27-34.

Received October 15, 1997

Faculty of Biology
Bucharest
Spl. Independenței 91-95

THE ROLE OF BENTHIC BIVALVE MOLLUSC POPULATIONS IN THE NITROGEN AND PHOSPHOROUS CYCLES

PRELIMINARY RESULTS

GALINA NĂFORNIŢĂ, CARMEN POSTOLACHE, A. VĂDINEANU

The present paper presents the preliminary results of the study concerning the elucidation of the benthic mussels role in the cycle of two principal nutrients. The initial part of this study was based on the measurement of the nitrogen (N) and phosphorus (P) in the tissues, and the analysis of the distribution of P and N in three dominant species of the community (*Anodonta piscinalis*, *Unio pictorum*, *Unio tumidus*) from the following aquatic systems of the Danube Delta: Băclăneşti, Babina, Bogdaproste, Isac, Matia, Puiu, Roşu, Uzlina. We have tried to determine the existing relationship between the nutrient contents of the molluscs tissues and the concentration of the nutrients in the water as well as between the N, P -contents in the molluscs tissue and their age. We have evaluated the stock of nutrients biodeposited by the molluscs in the examined ecosystems.

INTRODUCTION

Nutrient cycling describes the passage of an element from dissolved inorganic nutrient through its incorporation into the living tissue to its possible remineralization by excretion or decomposition (J. D. Allan, 1993).

Nutrients are inorganic materials necessary for life, the supply of which is potentially limiting to biological activity within aquatic ecosystems. Their uptake, transformation and release are influenced by a number of abiotic and biotic processes. Important metabolic processes likely to affect and to be affected by the supply of nutrients include primary production and the microbial decomposition of organic matter.

The bivalves, together with the larvae of chironomidae and gasteropoda, use the freshdetritus, labile stored at the sediment-water interface. These macrofauna species are apt to intercept the fresh detritus precipitated on the sediments surface and to use it directly with an efficiency as great as 40% (Mann, 1988).

MATERIAL AND METHOD

The molluscs were collected by dredging in the period May 1993 - May 1995. The nutrient content was analysed for three species of benthic bivalves:

REV. ROUM. BIOL. -BIOL. ANIM., TOME 44, P. 77-83, BUCAREST, 1999

A. piscinalis, *U. pictorum*, *U. tumidus* from the following benthic aquatic ecosystems of the Danube Delta: Băclănești, Babina, Bogdaproste, Isac, Matița, Puiu, Roșu, Uzlina.

The nutrient content of the molluscs bodies was determined on a total number of 220 individuals captured at different moments of sampling, from which 106 individuals were *A. piscinalis*, 82 *U. pictorum* and 32 *U. tumidus*.

In order to carry out the analysis of nutrients, the mollusc samples were dried up to a constant weight, at 65-70°C. The next stage consisted of mineralising the tissues with oxidising agents (concentrated sulphuric acid) and hydrogen peroxide. The mineralisation was carried out in a special outfit, TECATOR. The sulphuric acid and the hydrogen peroxide are oxidising agents which realise the oxidation of organic material and the transformation of organic nitrogen and phosphorus in the form of ammoniacal nitrogen and phosphate respectively.

N and P were determined in the solution obtained after mineralisation, by specific spectrophotometric methods. As reference, mussels standards were used.

The values of the nutrient contents of mollusc tissues were expressed in mg N, P/g dry tissue and in water in $\mu\text{g N}$, P/l. In order to be comparable with those in existing literature, data were presented in percentage of the dry substance.

The nitrogen assay

The solution obtained after mineralisation contains the initial organic and inorganic ammoniacal nitrogen from the analysed sample in the form of ammonium sulphate. Determination was performed by the Nessler method, after the neutralisation of the solution. The absorption determined at 410 nm was interpolated on the calibration curve obtained in the range 0,4 $\mu\text{g N/ml}$ - 2 $\mu\text{g N/ml}$, thus determining the concentrations of the solutions (mg/l) after the mineralisation in $\mu\text{g N/ml}$ (mg/l). Taking into account the quantity of substance taken for analysis, the nitrogen content of the samples in mg N/g dry tissue was calculated.

The phosphorus assay

The analysis method used consists of forming a phosphomolybdic complex of blue colour by treating the mineralised sample that contains phosphate with ammonium molybdate, using ascorbic acid as a reductive agent. The calibration curve was drawn up in the range 2,5 $\mu\text{g P/ml}$ - 12,5 $\mu\text{g P/ml}$ and the absorption values obtained for the analysed solution, were interpolated, thus obtaining the corresponding concentration which was later expressed in mg P/g dry tissue.

Determination of nutrients in the water

In order to determine the dissolved inorganic nitrogen (DIN) in water, the ammoniacal nitrogen and the nitrate contained in the water samples were

measured. The ammoniacal nitrogen was determined by Nessler method. The assay of nitrate consists of obtaining a complex with the phenoldisulphonic acid, which presents a yellow colour in a basic solution. Its concentration was finally determined spectrophotometrically by reading the absorption at 410 nm followed by its interpolation on the calibration curve.

Calculation of the inorganic nitrogen dissolved was carried out by summing the content of ammoniacal nitrogen and nitrate nitrogen of water.

The analysis of the total reactive phosphorus (TRP) was performed using the method with ammonium molybdate and stannous chloride as reducing agents.

The statistical processing of data obtained was carried out using the test ANOVA (variance analysis).

RESULTS AND DISCUSSIONS

For the populations of *A. piscinalis* the values obtained for nitrogen were between: 55 mg N/g (Isac, September 1993) and 99 mg N/g (Roșu, March 1994) (Fig. 1). DIN values of the water in the same periods varied in a much larger range: 50 $\mu\text{g/l}$ and 1600 $\mu\text{g/l}$. The total P content varied for *A. piscinalis* between 12 mg P/g (Matița, May 1995) and 30 mg P/g (Uzlina, August, 1994). In comparison with DIN, the TRP varied in a much smaller interval (3-87 $\mu\text{g/l}$) (Fig. 1).

For *U. pictorum* the smallest value of total N was 48 mg N/g (Babina, July 1994) and the largest - 93 mg N/g (Șontea, September 1993). The total P content in the tissues was, for this population, between 13 mg P/g (Bogdaproste, July 1994) and 24 mg P/g (Isac, July 1994, Băclănești, May 1995). In the ecosystems in which *U. pictorum* was investigated for nutrients, DIN in water varied between 62 $\mu\text{g/l}$ (Isac, July 1993) and 1602 $\mu\text{g/l}$ (Băclănești, July 1994), while TRP had the minimal value of 7 $\mu\text{g/l}$ (Babina, May 1995) and maximum of 87 $\mu\text{g/l}$ (Băclănești, July 1993, July 1994) (Fig. 2).

The total content of N for the *U. tumidus* populations investigated is included in the range: 50 mg N/g (Babina, July 1994) and 78 mg N/g (Uzlina, May 1995), but the total P was between 13 mg P/g (Bogdaproste, May 1993, Babina, July 1994) and 29 mg P/g (Băclănești, July 1994). DIN in water varied between 79 $\mu\text{g/l}$ (Uzlina, May 1995) and 525 $\mu\text{g/l}$ (Bogdaproste, May 1995) (Fig. 3).

The variation of the nutrient content immobilised by the benthic bivalves of the ecosystems Babina, Băclănești, Bogdaproste, Isac, Matița, Puiu, Roșu, Uzlina in the period of research is in a limited range. The mean value of the total N content in the tissues was approximately 70 mg/g of tissue, which represents 7.0% of the dry substance, and the total P was of 20 mg/g tissue (2.0% of the dry substance). Data for the content of P (%) are in accordance with those obtained by Nalepa and collab. (1988) who reported a percentage of 2.7% for the dry tissue of the *Unionidae* molluscs in the lake St. Clair.

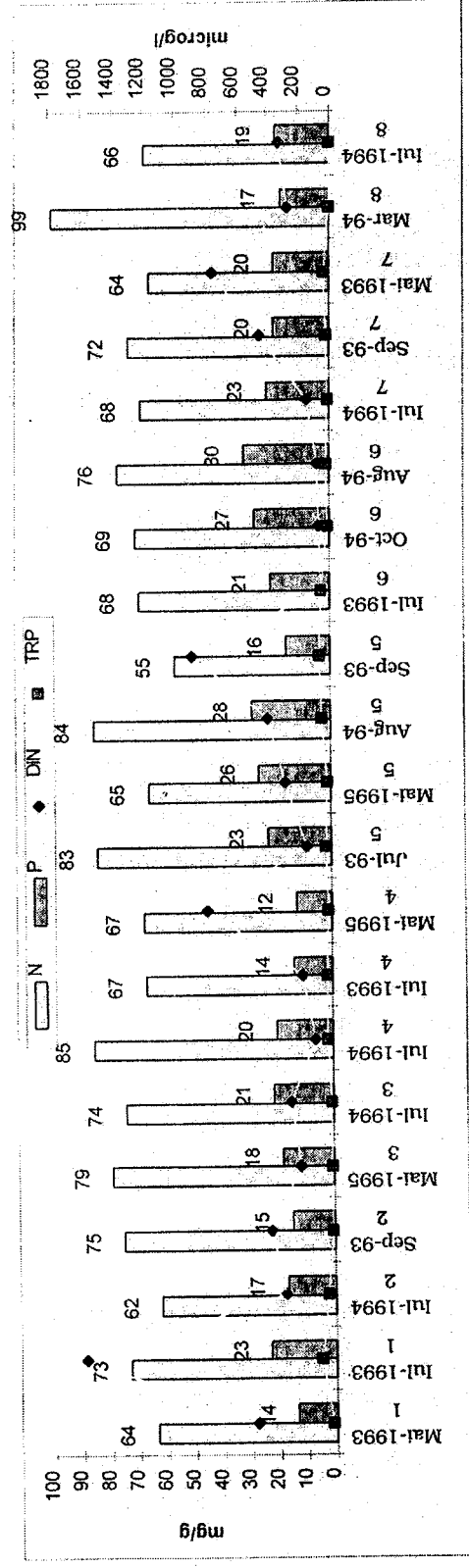


Fig. 1 – Comparative dynamics of the nutrients content in tissues at *A. piscinalis* and DIN and TRP in water, in the aquatic ecosystems of the Danube Delta: Băclănești (1), Bogdaproste (2), Babina (3), Matia (4), Isac (5), Uzlina (6), Puiu (7), Roșu (8).

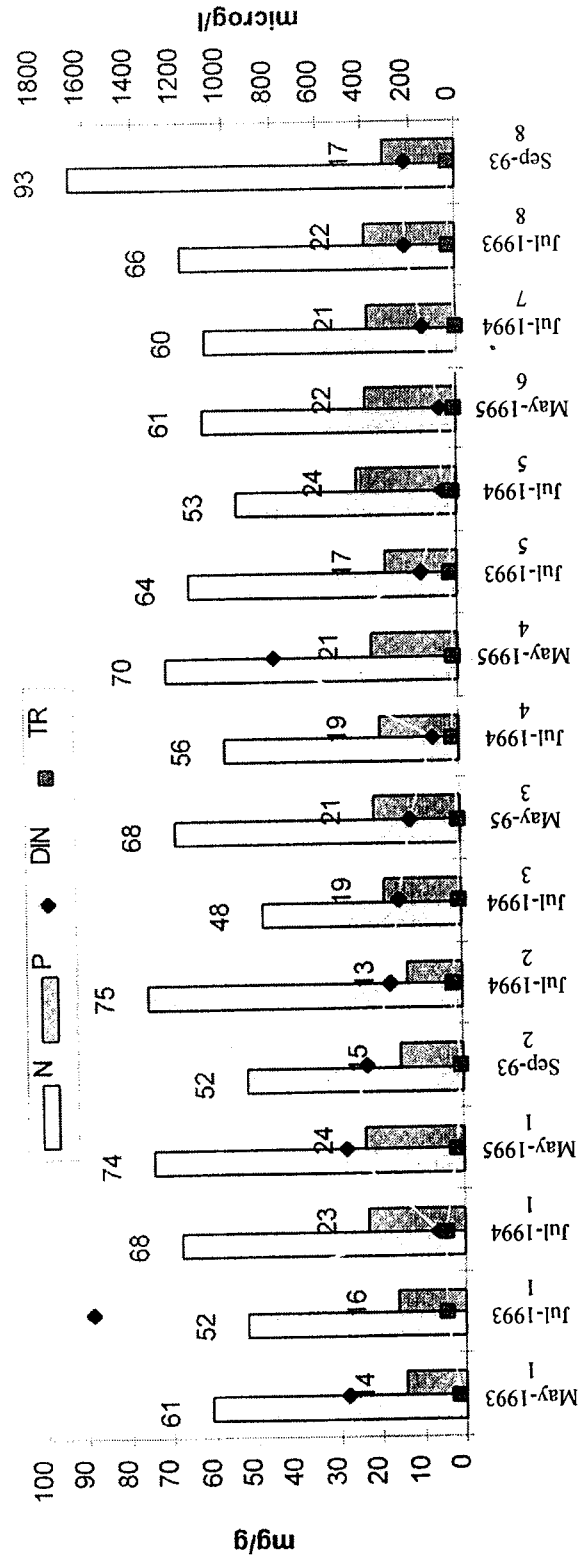


Fig. 2 – Comparative dynamics of the nutrients content in tissues at *U. pictorum* and DIN and TRP in water, in the aquatic ecosystems of the Danube Delta: Băclănești (1), Bogdaproste (2), Babina (3), Matia (4), Isac (5), Uzlina (6), Puiu (7), Șonțea (8).

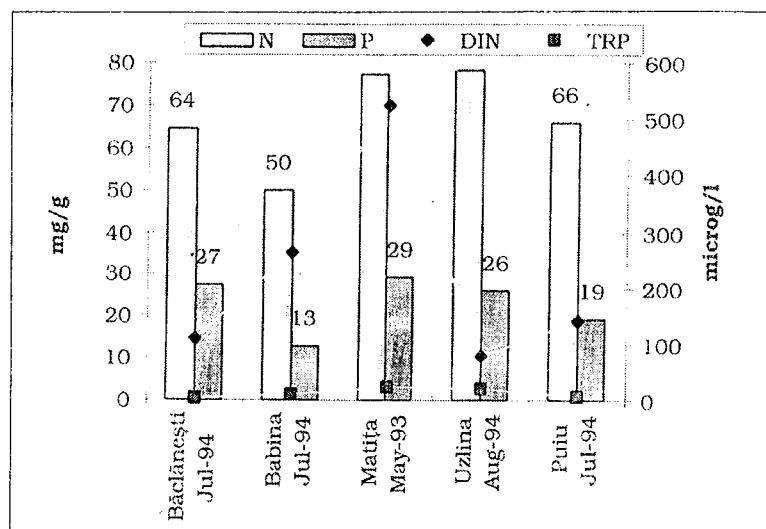


Fig. 3 – Comparative dynamics of the nutrients content in tissues at *U. tumidus* and DIN and TRP in the water, in the aquatic ecosystems of the Danube Delta.

The comparative dynamics of nutrient content in the molluscs tissue does not show any correlation with the momentary load of nutrients in water. The trophic state of the ecosystem does not influence the storing of nutrients in the molluscs bodies.

The attempt to realise a correlation between the content of nutrients in the tissues and the age, has not given positive results for any of the species.

Table 1

The amount (tons) of nutrients biodeposited in the tissue of *A. piscinalis*, *U. pictorum* and *U. tumidus* and the stock of nitrogen and phosphorus of the ecosystems water which they populate

| Species/Ecosystems | N (t) | P (t) | DIN (t) | TRP (t) |
|----------------------|-------|-------|---------|---------|
| <i>A. piscinalis</i> | | | | |
| Băclănești | 7.39 | 2.14 | 3.56 | 0.19 |
| Babina | 10.01 | 2.63 | 1.97 | 0.08 |
| Bogdaproste | 18.58 | 3.69 | 2.36 | 0.18 |
| Isac | 40.81 | 12.93 | 9.11 | 0.88 |
| Matia | 6.19 | 1.35 | 5.27 | 0.43 |
| Puiu | 12.83 | 3.90 | 10.11 | 0.42 |
| Roșu | 48.25 | 11.36 | 11.20 | 0.13 |
| Uzlina | 11.84 | 4.45 | 0.75 | 0.30 |
| <i>U. pictorum</i> | | | | |
| Băclănești | 5.01 | 1.53 | 2.30 | 0.19 |
| Bogdaproste | 1.49 | 0.37 | 2.36 | 0.17 |
| Babina | 12.26 | 4.47 | 1.97 | 0.08 |
| Isac | 15.39 | 5.62 | 2.60 | 0.58 |

| | | | | |
|-------------------|-------|------|------|------|
| Matia | 10.05 | 3.16 | 7.09 | 0.41 |
| Puiu | 6.03 | 2.14 | 3.17 | 0.11 |
| Uzlina | 17.15 | 6.12 | 0.78 | 0.06 |
| <i>U. tumidus</i> | | | | |
| Băclănești | 5.66 | 2.42 | 0.39 | 0.02 |
| Bogdaproste | 2.54 | 0.47 | 3.26 | 0.14 |
| Babina | 0.61 | 0.08 | 2.16 | 0.09 |
| Puiu | 6.37 | 3.68 | 3.21 | 0.18 |
| Uzlina | 6.60 | 2.00 | 0.84 | 0.22 |

Data of Table 1 present the values of nutrient amounts stocked by the benthic bivalves, which were calculated taking into account the gravimetric density of the investigated populations, the surface of the ecosystems, and the nutrient stocks in water. According to this data, the quantity of N, P (nutrients) stocked by the benthic bivalves is several times greater than the stock of nutrients in water. The great quantities of N and P biodeposited by the molluscs become, after the death of the animals, an important source of nutrients for other biotic components of the lakes (detritophagous invertebrates, macrophytes etc.)

CONCLUSIONS

- The nutrient content of benthic bivalve molluscs has no seasonal dynamics and does not depend on the momentary charge of nutrients in the water.
- The nutrient content of tissues does not depend on the age of the individuals.
- The benthic bivalve populations represent an important compartment for N and P biodeposition.

The biodeposition or stock N and P by molluscs is an important source of nutrients for other biotic components of the lake.

REFERENCES

- Nalepa, T. F., Gardner, W. S., Malczyk, J. M., 1991. Phosphorus cycling by mussels in lake St. Clair. *Env. Asses. Hab. Eval. Upper Great Lakes Connect. Chan.*, **219**, 229-250.
- Sakamoto M., Hayashi H., Otsuki K., Watanabe Y., Hanazato T., Yasuno M., 1989. Role of bottom sediments in sustaining plankton production in lake ecosystem - Experimental demonstration using enclosed water bodies in a shallow lake. *Ecol. Res.*, **4**, 1-16.
- Sautschi P., Hohener P., Benoit G., Buchholtz-ten B., 1990. Chemical processes at the sediment-water interface. *Marine Chemistry*, **30**, 269-315.
- David Allan J. 1992. *Stream ecology. Structure and function of running waters.* School of Natural Resources and Environment, University of Michigan, USA.

Received October 15, 1999

Faculty of Biology
Bucharest
Splaiul Independenței nr. 91-95

ARTHROPOD DIVERSITY ALONG AN ENVIRONMENTAL GRADIENT ON THE SACALIN ISLAND, THE DANUBE DELTA

IRINA TEODORESCU*, DAN COGĂLNICEANU*, CLEOPATRA STERGHIU **

The diversity of terrestrial arthropods was investigated on the Sacalin Island in July and October, 1994. Pit-fall traps were used along three transects across the island. The island is situated at the limit of the Danube Delta and the Black Sea and salinity decreases in a linear way from the sea-shore. A high diversity of arthropod species was found; thus, in July out of 355 arthropods captured in traps, a number of 45 species were identified. Despite the recent origin of the island, the vicinity of the Sărățuri sand bank and its position at the mouth of the Sf. Gheorghe arm facilitated colonisation. The changes in the vegetation cover along the environmental gradient provide a high diversity of non-overlapping habitats and allow the co-existence of a large number of species with narrow distribution ranges.

INTRODUCTION

The Island of Sacalin has been recently formed and is a highly dynamic ecological system located at the border of the Danube Delta and the Black Sea. According to Rudescu et al. (1965) the island raised above the sea-level after the severe floods of the Danube in 1897 that had a high sediment load, part of which was deposited on the already existing submerged sand banks. In 1918 the island was already 5 km long and in 1924 it reached 10 km. The island is moving westwards under the pressure of waves and currents that have a dominant action on the NE - SW direction. During the last 60 years it moved approximately 750 m giving an average speed of 12 m/year. Presently, the island is about 14 km long and is between 70-400 m wide.

Because it is positioned between the Black Sea and the Danube, there is a strong variation in salinity, creating a steep, linear environmental gradient. The distribution and diversity of vegetation along this gradient were recently described (Dinu et al., 1997). Information on arthropods is scarce, fragmented, and does not reflect their distribution and diversity along this gradient.

MATERIALS AND METHODS

The present data were gathered at the same moments with the vegetation survey and physico-chemical measurements previously reported (Dinu et al.,

1997). Arthropods were captured with pit-fall traps during two sampling periods, in July and October 1994. Three transects were done on both occasions, each consisting of a different number of sampling sites due to the heterogeneity of the environment. Seventeen sampling sites were done in July and only nine in October, when the rise in water level reduced the width of the island, so only three sites were sampled for each transect. The detailed description of the transects, of the physico-chemical parameters, and of the vegetation cover are presented in Dinu et al. (1997).

Traps were filled with ethylenglycol, emptied after 24 hours and arthropods were preserved in 70% alcohol. Terrestrial arthropods were then determined to species level and counted.

Various diversity measures were computed. Two α -diversity indexes were used: the Shannon-Wiener (H) and Simpson (D).

$$H = -\sum p_i \ln p_i$$

$$D = 1 / \sum (p_i)^2$$

where p_i is the proportional abundance of the i th species = (n_i/N).

To ascertain the degree of turnover in species composition along the environmental gradient two β -diversity measures were computed: Whittaker's measure (β_w) and Cody's index (β_c).

$$\beta_w = (S/\alpha) - 1$$

where S = the total number of species recorded in the system and α = the mean species richness; and

$$\beta_c = (g-l)/2$$

where g = the number of species gained along the transect and l = the number of species lost. All diversity measures were computed according to Magurran (1988).

For each sampling moment, based only on the presence/absence data, the similarity between pairs of sites was compared using the Jaccard measure. A dendrogram was afterwards computed from the similarity matrix using the clustering method UPGMA (unweighed pair-group method based on arithmetic averages).

RESULTS

A total number of 1107 specimens were captured in traps, 355 in July and 752 in October. Since we were interested only in ground-dwelling arthropods, only the following taxa were analysed: Crustacea, Arachnida (Aranea, Acarina), and Insecta (Dermaptera, Orthoptera, Homoptera, Hymenoptera, Coleoptera, Collembola).

Table 1 presents a list of the species identified in one or both of the two sampling moments. The total number of individuals was positively correlated with

species richness in July ($R=0.76$, $p<0.001$, $n=17$), but not in October. The dynamics along the transects of the total number of arthropods captured and species richness is presented in Figure 1. In July, insects and spiders were dominant, each taxon with a proportion of 35%. In October, insects were dominant, representing 93%, mainly due to the large number of collembolans captured that represented 85%.

Table 1

The list of species identified and the number of specimens captured in July and October

| Taxa | Species | July | October |
|--------------------------------|---------------------------------|------|---------|
| Crustacea, Isopoda, Oniscoidea | <i>Oniscus asellus</i> | 6 | 17 |
| Crustacea, Isopoda | <i>Pontogammarus moeticus</i> | 75 | 11 |
| Aranea, Lycosidae | <i>Arctosa leopardus</i> | 22 | 8 |
| Aranea, Lycosidae | <i>Arctosa cinerea</i> | 18 | 2 |
| Aranea, Lycosidae | <i>Arctosa neaculata</i> | 5 | 0 |
| Aranea, Lycosidae | <i>Pardosa luctinosa</i> | 21 | 8 |
| Aranea, Lycosidae | <i>Pardosa cribrata</i> | 4 | 0 |
| Aranea, Lycosidae | <i>Pardosa agrestis</i> | 1 | 0 |
| Aranea, Lycosidae | <i>Xerolycosa miniata</i> | 3 | 0 |
| Aranea, Lycosidae | <i>Trochosa spinipalpis</i> | 1 | 0 |
| Aranea, Lycosidae | <i>Trochosa robusta</i> | 32 | 0 |
| Aranea, Lycosidae | <i>Pirata piraticus</i> | 4 | 1 |
| Aranea, Tetragnathidae | <i>Pachygnatha degeeri</i> | 1 | 0 |
| Aranea, Micriphanthidae | <i>Oedothorax apicatus</i> | 1 | 0 |
| Aranea, Thomisidae | <i>Oxyptila brevipes</i> | 1 | 0 |
| Aranea, Gnaphosidae | <i>Berlandina cinerea</i> | 1 | 0 |
| Aranea, Gnaphosidae | <i>Zelotes villicus</i> | 2 | 0 |
| Aranea, Gnaphosidae | <i>Gnaphosa muscorum</i> | 1 | 0 |
| Dermaptera, Labiduridae | <i>Labidura riparia</i> | 33 | 1 |
| Orthoptera, Gryllidae | <i>Gryllulus frontalis</i> | 2 | 0 |
| Orthoptera, Gryllidae | <i>Gryllotalpa gryllotalpa</i> | 5 | 0 |
| Orthoptera, Tetrigidae | <i>Tetrix vittata</i> | 1 | 0 |
| Homoptera, Aphididae | <i>Therioaphis ononidis</i> | 0 | 6 |
| Coleoptera, Anthicidae | <i>Notoxus brachyuros</i> | 1 | 0 |
| Coleoptera, Anthicidae | <i>Anthicus humilis</i> | 0 | 1 |
| Coleoptera, Cicindelidae | <i>Cicindela litterata</i> | 4 | 0 |
| Coleoptera, Carabidae | <i>Scarites laevigatus</i> | 2 | 0 |
| Coleoptera, Carabidae | <i>Acupalpus elegans</i> | 6 | 0 |
| Coleoptera, Carabidae | <i>Pterostichus nigrita</i> | 1 | 1 |
| Coleoptera, Carabidae | <i>Poecilus cupreus</i> | 1 | 0 |
| Coleoptera, Carabidae | <i>Harpalus distinguendus</i> | 6 | 0 |
| Coleoptera, Carabidae | <i>Harpalus aeneus</i> | 2 | 0 |
| Coleoptera, Carabidae | <i>Anisodactylus binotatus</i> | 1 | 0 |
| Coleoptera, Carabidae | <i>Chlaenius vestitus</i> | 1 | 0 |
| Coleoptera, Carabidae | <i>Chlaenius sulcicollis</i> | 8 | 0 |
| Coleoptera, Carabidae | <i>Agonum viridicupreum</i> | 5 | 0 |
| Coleoptera, Carabidae | <i>Dyschirius politus</i> | 4 | 0 |
| Coleoptera, Carabidae | <i>Omophron limbatus</i> | 2 | 0 |
| Coleoptera, Carabidae | <i>Dichirotrichus obsoletus</i> | 1 | 7 |
| Coleoptera, Carabidae | <i>Bembidion varium</i> | 1 | 0 |

| | | | |
|----------------------------|----------------------------------|---|----|
| Coleoptera, Carabidae | <i>Brosicus cephalotes</i> | 0 | 2 |
| Coleoptera, Chrysomellidae | <i>Phyllotreta atra</i> | 1 | 0 |
| Coleoptera, Chrysomellidae | <i>Aphthona euphorbiae</i> | 0 | 1 |
| Coleoptera, Coccinellidae | <i>Adonia variegata</i> | 1 | 1 |
| Coleoptera, Coccinellidae | <i>Coccinella septempunctata</i> | 0 | 1 |
| Coleoptera, Curculionidae | <i>Sphenophorus abbreviatus</i> | 1 | 0 |
| Coleoptera, Histeridae | <i>Saprinus semistriatus</i> | 1 | 0 |
| Coleoptera, Hydrophilidae | <i>Hydrous picaeus (larva)</i> | 1 | 0 |
| Coleoptera, Scarabeidae | <i>Aphodius erraticus</i> | 0 | 1 |
| Coleoptera, Staphylinidae | <i>Sphenophorus abbreviatus</i> | 1 | 3 |
| Coleoptera, Staphylinidae | <i>Aleochara bipustulata</i> | 0 | 21 |
| Coleoptera, Staphylinidae | <i>Microglossa gentilis</i> | 0 | 3 |
| Coleoptera, Tenebrionidae | <i>Opatium sabulosum</i> | 1 | 0 |

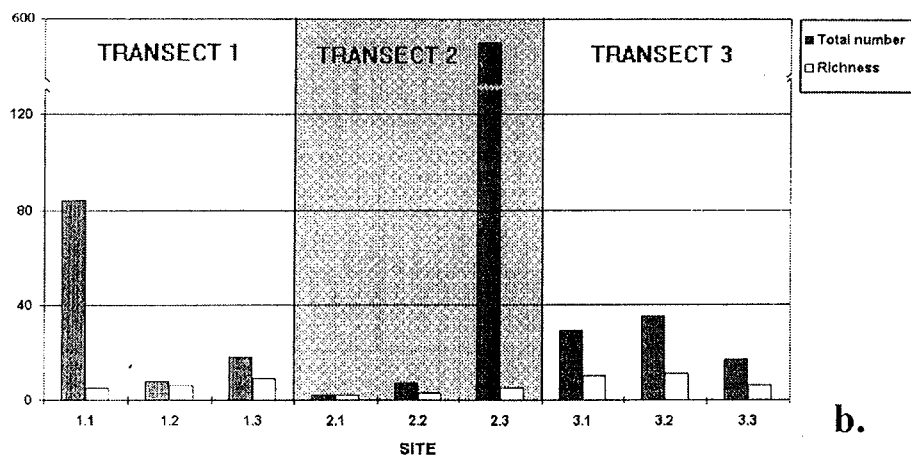
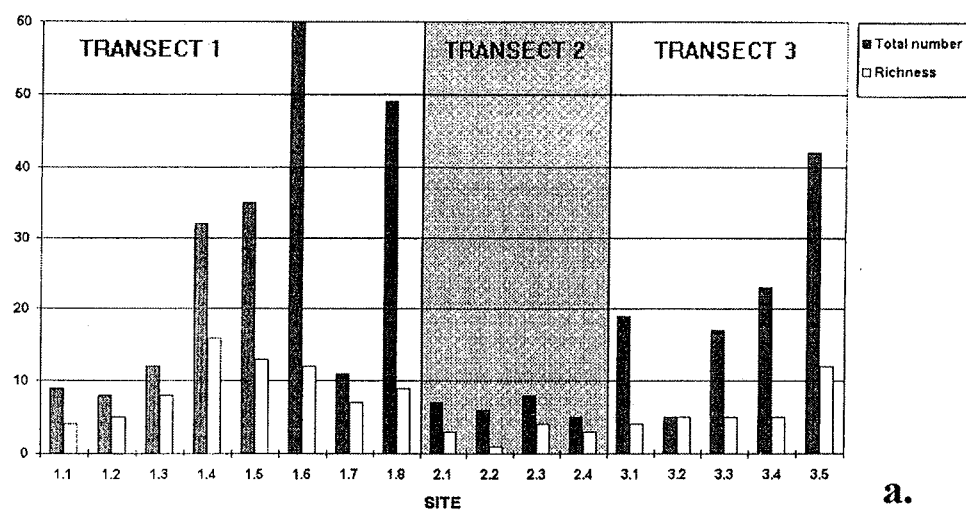


Fig. 1. – The dynamics of the total number of arthropods captured and species richness in July (a) and October (b).

The variation in species diversity along the transects sampled is shown in Figure 2.

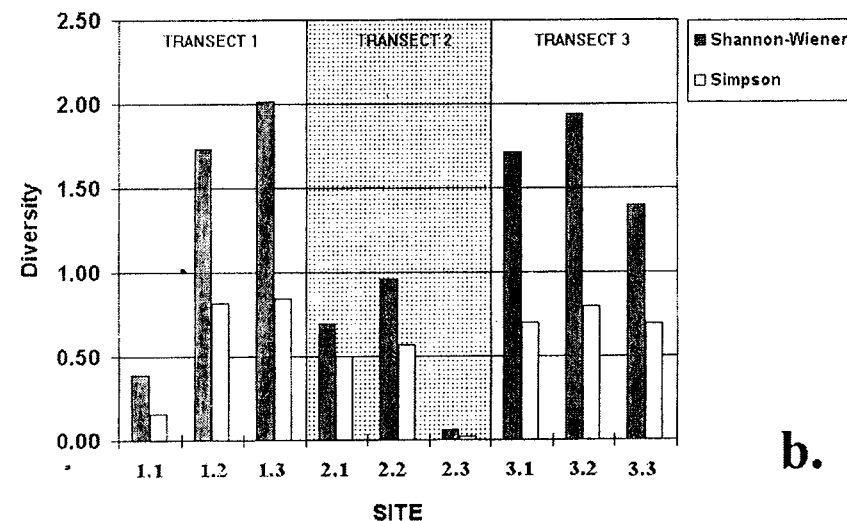
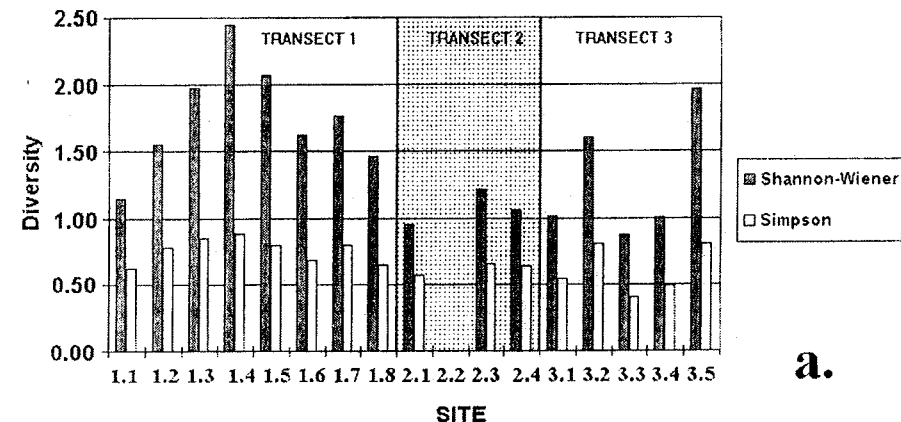


Fig. 2. – Variation in α -diversity along the transects sampled in July (a) and October (b).

A high number of flying insects were accidentally captured in October. The following taxa were identified: Diptera Nematocera (Chironomidae, Culicidae, Tipulidae), and Brachycera (Drosophilidae, Pipunculidae, Sciaridae, Tephritidae, Calliphoridae), Hymenoptera (Chalcidoidea, Cynipidae, Serphidae, Diapriidae, Scelionidae), Neuroptera (Chrysopidae) and Lepidoptera (Noctuidae). They were not used in the analysis of diversity.

The β -diversity measures are presented in Table 2.

Table 2

The β -diversity values for the three transects sampled in July and October

| | Month Tr. | VII | | | X | | |
|-----------|--------------|-----|-----|-----|-----|-----|-----|
| | | 1 | 2 | 3 | 1 | 2 | 3 |
| β_w | | 3.7 | 1.5 | 2.2 | 1.5 | 1.5 | 1 |
| β_c | | 16 | 4 | 10 | 5.5 | 3 | 4.5 |

DISCUSSIONS

The entire lower Danube Delta suffered severe changes during the Quaternary, due to the dynamic changes of the hydrology of the Danube and the shifting sea-level (Ghenea and Mihăilescu, 1991). Despite its recent origin, the Sacalin Island has a high diversity of arthropod species. This can be explained by the vicinity of the Sărățuri sand bank, a pre-deltaic island, and its position at the mouth of the Danube's Sf. Gheorghe arm that has certainly facilitated colonisation by both pioneer and more competitive species. The diversity of the vegetation and the existing environmental gradient provides non-overlapping habitats and allows the co-existence of a large number of species, with narrow distribution ranges.

The β -diversity values (Table 2) indicate large differences among the investigated transects. This reflects the dynamics of the vegetation cover, that indicates the changes in salinity and in the chemistry of the substrate.

When comparing the dendrograms constructed using the similarity between sampling sites and compare them with vegetation types (Dinu et al., 1997), it is possible to associate clusters with a specific vegetation type - halophyte or xerophyte - (Figure 3).

During the animal species inventories carried on during 1991-1995 in the Danube Delta, 2256 species of insects, 166 of spiders, 138 of mites, 8 of millipedes, and 194 crustaceans were identified (Oțel, 1997). Of these, 53 terrestrial (representing 2%), soil-dwelling arthropods were identified on Sacalin Island. A large number of recent publications offering distribution records for the Danube Delta Biosphere Reserve were consulted for comparison (Bulimar, 1992; Chiriac, 1994; Crișan, 1993, 1994, 1995; Kis, 1994; Moglan, 1993; Nițu, 1992; Ostaficiuc, 1994; Popovici, 1992; Teodor, 1993; Tomescu, 1992). Based on the species cited in these publications we can conclude that of the identified species several are described for the first time in the Danube Delta and the large majority are new for the Sacalin Island.

Acknowledgements. We acknowledge the help of our colleagues Sergiu Cristofor and Anca Șerban in collecting the samples.

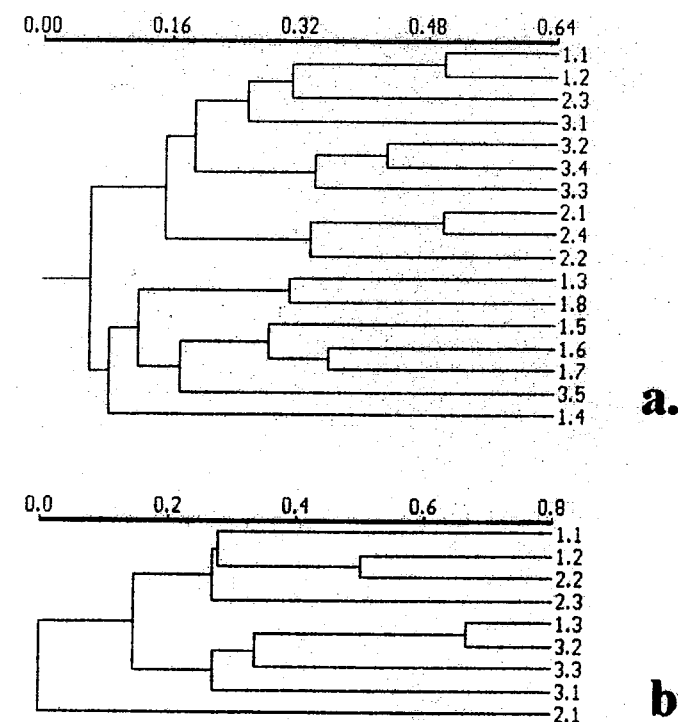


Fig. 3. - Dendrograms based on Jaccard's similarity measure between sampled sites computed using the UPGMA clustering method, for July (a) and October (b).

BIBLIOGRAPHY

- Bulimar, F., 1992, Compoziția faunistică și structura comunităților de colembole (Collembola: Insecta) în ecosistemele stuficole din Delta Dunării. Anal. Șt.Inst.Delta Dunării, 1:95-99.
- Chiriac, I., 1994, Fauna insectelor parazite (Hymenoptera, Aphidiidae) și a afidelor (Homoptera, Aphidoidea) din Rezervația Biosferei Delta Dunării. Anal. Șt.Inst.Delta Dunării, 3:81-82.
- Crișan, A., 1993, Date asupra familiei Chrysomelidae (Coleoptera) în partea sudică a Deltei Dunării. Anal. Șt.Inst.Delta Dunării, 2:67-74.
- Crișan, A., 1994, Noi date asupra familiei Chrysomelidae (Coleoptera) în Rezervația Biosferei Delta Dunării. Anal. Șt.Inst.Delta Dunării, 3:159-165.
- Crișan, A., 1995, Cercetări faunistice asupra familiei Chrysomelidae (Coleoptera) în zona maritimă a Rezervației Biosferei Delta Dunării. Anal. Șt.Inst.Delta Dunării, 4:161-168.
- Dinu, C. et al., 1997, Răspunsuri ale vegetației din Insula Sacalin la regimul hidrologic și hidrochimic. Anal. Șt.Inst.Delta Dunării, 5(1):357-380.
- Ghenea, C., Mihăilescu, N., 1991, *Paleogeography of the Lower Danube Valley and the Danube Delta during the last 15 000 years*. Chap.15, In: *Temperate paleohydrology*. Starkel, L., Gregory, K.J., Thornes, J.B. Editors, John Wiley and Sons.
- Kis, B., 1994, Dermapterele din Rezervația Biosferei Delta Dunării. Anal. Șt.Inst.Delta Dunării, 3:41-45.
- Magurran, A.E., 1988, *Ecological diversity and its measurement*. Croom Helm, London.

- Moglan, V., Coccinelide utile (Coleoptera, Coccinellidae) din câteva zone umede ale României. Anal. Șt.Inst.Delta Dunării, 2:129-133.
- Nițu, E., Specii de Carabidae noi pentru fauna Dobrogei și a Deltei Dunării. Anal.Șt.Inst.Delta Dunării, 1:119-120.
- Ostaficiuc, V., 1994, Fauna stafflinidelor (Coleoptera, Stafflinidae) și Elateridelor (Coleoptera, Elateridae) Rezervației Biosferei Delta Dunării. Anal. Șt.Inst.Delta Dunării, 3:85-86.
- Oțel, V., 1997, The strategy of the wild species assessment in the Danube Delta Biosphere Reserve. The first results. Anal. Șt. Inst. Delta Dunării, 5(1):3-12 (in Romanian).
- Popovici, L.R., 1992, Varietatea specifică a Carabidelor din Delta Dunării - Rezervația Biosferei. Anal. Șt.Inst.Delta Dunării, 1:111-118.
- Rudescu, L., Niculescu, C., Chivu, I. (Editors), 1965, *Monografia stufului*. Editura Academiei RSR.
- Teodor, L., Contribuții la cunoașterea Curculionidelor (Coleoptera) din Delta Dunării. Anal. Șt.Inst.Delta Dunării, 2:193-196.
- Tomescu, N., Isopode terestre (Crustacea: Isopoda) din Delta Dunării - Caraorman și Maliuc. Anal. Șt.Inst.Delta Dunării, 1:89-90.

Received December 14, 1998

* Bucharest University, Faculty of Biology,
Splaiul Independenței 91-95,
76201-Bucharest, Romania
**Institute of Biology,
Splaiul Independenței 296,
Bucharest, Romania

NUMERICAL STRUCTURE OF EARTHWORM POPULATIONS IN DIFFERENT FORESTRY SOIL ECOSYSTEMS

MARIN FALCĂ

Earthworm numerical densities were studied in the forestry soil ecosystems of beech, spruce fire, spruce fire upper limit and juniperus, located in different parts of the country. The identified values were influenced by pH, humidity and C/N ratio of the soils. The soils of beech forests showed a dominance of *Aporrectodea rosea rosea* - *Octolasion lacteum* sinuzia, while spruce fire, spruce fire upper limit and juniperus soils showed a dominance of *Dendrobaena alpina alpina*-*Dendrobaena octaedra* sinuzia. Earthworm spatial distribution showed a grouped distribution of individuals, according to binomial negative theoretical model, with $P < 0.95$. Multiple correlation coefficients between earthworm numerical densities and soil pH and humidity showed a significant positive correlation during the spring time.

Numerical structure parameters of earthworm populations from different types of forestry soils are well known. Spatial distribution of earthworms, multiple correlations between earthworm species and different abiotic factors as well as regression of earthworm density, as a result of the influence of pH, humidity and C/N of soils were less or not done by now for the Romanian forestry ecosystems. Objectives were to: 1. describe taxonomic composition; 2. establish numerical density; 3. establish the type of spatial distribution of earthworms; 4. assess the influence of pH, humidity and C/N ratio of soils on earthworm densities.

MATERIAL AND METHODS

This study was conducted in the following types of forestry ecosystems: beech forests (different types), spruce fire, spruce fire upper limit and juniperus. For quantitative sampling, earthworms were randomly sampled, two times in a year (May and August) by a metal frame of 25/25 sq cm). Soil samples were divided as follows: litter (different depths), 10 cm and 20 cm. Extraction of individuals was performed by hand in the field. According to the type of spatial distribution of earthworm species, the necessary number of samples was 20, with an estimated error of 20 %.

RESULTS AND DISCUSSIONS

The short characterization of those ecosystems is as follows: 1. Beech forest with *Carpinus* and *Carex pilosa* (Cocorasti) is located in the South part of the country, in the Subcarpathians area, 320 m altitude, North exposition, with a slope of 20°. Precipitations were around 687 mm per year. The soil is brown-reddish-sandy clayish to clayish, with pH=5.4 at first 10 cm deep (moderate acid), C/N=16, and relative humidity=21.43. 2. Hill beech forest with mull flora (Lespezi) is located in the South part of the country, at the bottom level of the Bucegi Mountains, 830 m altitude. Soil pH=5.3 in the first 20 cm of soil, with relative humidity=40.14, and C/N=30.1. 3. Mountain beech forest with *Oxalis-Dentaria-Asperula* (Galbenul) is located in the South part of the country, Parâng Mountains, 740 m altitude, with East-South-East exposition. Precipitations were around 863 mm per year. The soil is acid brown, sandy-clayish, with pH=4.7 (strongly acid), relative humidity=18.58, and C/N=17. 4. Mountain beech forest with *Festuca drymeia* (Galbenul) is located in the South part of the country, Parâng Mountains, 770 m altitude, South-West exposition, with a slope of 5-10°. Precipitations were around 730 mm per year. The soil is acid brown, sandy-clayish; pH=4.7 (strongly acid), with relative humidity=13.2, and C/N=17. 5. Mountain beech forest with *Luzula* (Galbenul) is located in the South part of the country, 745 m altitude. Soil pH=3.8 (very strongly acid), with relative humidity=23.27, and C/N=17. 6. Hill beech forest with mull flora (Furnicosi) is located in the South part of the country, Argeş District, 580 m altitude. Soil pH=4.8 (strong acid), with relative humidity=33.5, and C/N=40.6. 7. Mountain beech forest with *Oxalis-Dentaria-Asperula* (Piscu Cîinelui) is located in the South part of the country, Gârbova Mountains, South-West exposition, with a slope of 35°. Precipitations were around 808 mm per year. The soil acid brown, clayish-sandy-clayish, with pH=5.3 (moderate acid), relative humidity=29.94, and C/N=14. 8. Hill beech forest with *Luzula luzuloides* (Govora) is located in the South part of the country, North-West exposition, with a slope of 30°, 350 m altitude. Precipitations were around 770 mm per year. The soil is acid brown, sandy-clayish, with pH=4.4 (strong acid), relative humidity=36.33, and C/N=17. 9. Hill beech forest with mull flora (Govora) is located in the South part of the country, 420 m altitude. Soil pH=5.4 (moderate acid), soil relative humidity=34.67, and C/N=16. 10. Hill beech forest with *Asperula-Asarum-Stellaria* (Hemeius) is located in the East part of the country, North exposition, with a slope of 5°. Precipitations were around 560 mm per year. The soil is brown, sandy-clayish, with pH=5.04 (moderate acid), relative humidity=18.83, and C/N=20. 11. Hill beech forest with *Asperula-Asarum-Stellaria* (Dolhasca) is located in the East part of the country, 350 m altitude, North-East exposition, with a slope of 14°. Precipitations were around 635 mm per year. Soil is brown, sandy, sandy-clayish, with pH=5.28 (moderate acid), relative humidity=19.2, and C/N=14. 12. Hill

beech forest with acid flora (Cucuieti) is located in the East part of the country, 450 m altitude. Soil is brown, with pH=4.8 (strongly acid), relative humidity=14.33, and C/N=18. 13. Hill beech forest with *Carpinus* and *Carex pilosa* (Sighisoara) is located in the center part of the country, on Tirnava Plateau, Soil is brown, sandy-clayish, with pH=4 (very strong acid), relative humidity=23.45, and C/N=13. 14. Mountain beech forest with *Festuca drymeia* (Lemnia) is located in the center part of the country, 940 m altitude, South exposition, with a slope of 30°. Precipitations were around 680 mm per year. Soil is sandy, sandy-clayish, with pH=4.65. relative humidity=24.41, and C/N=29. 15. Hill beech forest with *Festuca drymeia* (Poiana Sarata) is located in the East part of the country, 590 m altitude, South-East exposition, with a slope of 20°. Precipitations were around 635 mm per year. Soil is sandy-clayish, with pH=5.32 (moderate acid), relative humidity=26.6, and C/N=16.

16. Mountain beech forest with *Vaccinium* (Gutin) is located in the North part of the country, Gutii Mountains, 880 m altitude, South-West exposition, with a slope of 20°. Precipitations were around 976 mm per year. Soil is sandy-clayish, with pH=4.4 (strongly acid), relative humidity=64.95, and C/N=16. 17. Mountain beech forest with *Oxalis-Dentaria-Asperula* (Butin) is located in the North part of the country, Gutii Mountains, 670 m altitude, South exposition, with a slope of 20°. Precipitations were 976 mm per year. Soil is acid brown, sandy-clayish, with pH=4.22 (strongly acid), relative humidity=35.2, and C/N=17.

18. Mountain beech forest with *Festuca drymeia* (Huedin) is located in the North part of the country, Vladeasa Mountains, 900 m altitude, West exposition, with a slope of 30°. Precipitations were 768 mm per year. Soil is brown, sandy-clayish, with pH=4.45 (strongly acid), relative humidity=35.89, and C/N=19. 19. Mountain spruce fire forest (Sinaia) is located in the Bucegi Mountains, 1650-1700 m altitude, North-West exposition, with a slope of 30°. Soil is brown, with pH=3.55 (very strongly acid), relative humidity=37.41, and C/N=22.6. 20. Spruce fire upper limit forest (Peștera) is located in the Bucegi Mountains, 1770-1810 m altitude, North-West exposition, with a slope of 30°. Soil is strongly acid, with pH=4.73, relative humidity=31.73, and C/N=20.2.

21. Juniperus ecosystem (Peștera) is located in the Bucegi Mountains, 1850-1870 m altitude, North - North-West exposition, with a slope of 20°. Soil is typically brown, with pH=4.15 (strongly acid), relative humidity=19.8, and C/N=16.9.

Taxonomic features. 17 earthworm species were identified in all 21 forestry soils, as follows: 1. *Allolobophora leoni*; 2. *Allolobophora dacica*; 3. *Aporrectodea caliginosa caliginosa*; 4. *Aporrectodea georgii*; 5. *Aporrectodea rosea rosea*; 6. *Octodrilus complanatus*; 7. *Octodrilus lissaensis*; 8. *Octodrilus transpadanus*; 9. *Octolasion lacteum*; 10. *Eisenia lucens*; 11. *Lumbricus terrestris*; 12. *Lumbricus rubellus*; 13. *Dendrobaena alpina alpina*; 14. *Dendrobaena byblica*; 15. *Dendrobaena clujensis*; 16. *Dendrobaena octaedra*;

17. *Dendrodrilus rubidus rubidus*. From all 21 biotopes, *Aporrectodea rosea rosea* was identified in 17 biotopes, being the most common species; *Octodrilus complanatus* was the most rare species, being identified only in one biotope. Earthworm species were clearly divided in 2 categories (sinuzia): 1. *Aporrectodea rosea rosea* - *Octolasion lacteum*, including all species of this genus and 3 other species of *Lumbricus* and *Eisenia lucens*, for beech forests, and 2. *Dendrobaena alpina alpina* - *Dendrobaena octaedra*, including all species of this genus, for spruce fire, spruce fire upper limit and juniperus ecosystems (Fig. 1).

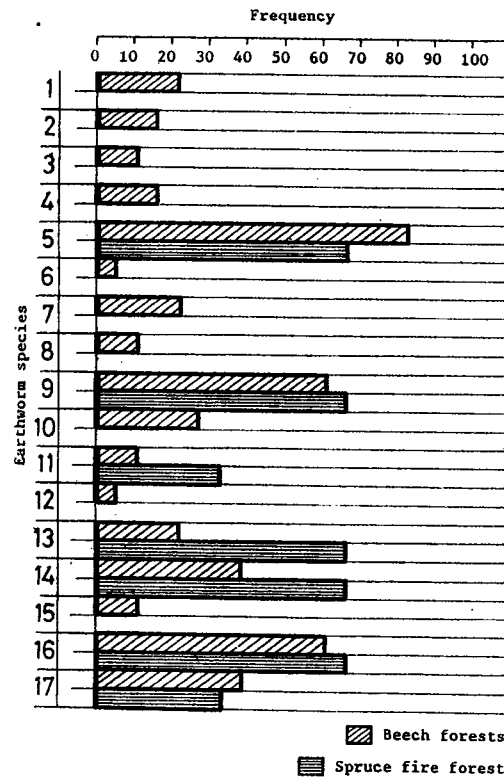


Fig. 1. - Two characteristic species groups: 1) *Aporrectodea rosea rosea* (5) - *Octolasion lacteum* (9) for beech forests; 2) *Dendrobaena alpina alpina* (13) - *Dendrobaena octaedra* (16) for spruce fire forests.

From all 9 species of *Allolobophora*, *Octodrilus* and *Octolasion*, characteristic for beech forests, only 2 - *Allolobophora rosea rosea* and *Octolasion lacteum*-, which are species with a large ecological spectrum, were identified in spruce fire forests. *Dendrobaena* species, on the other hand, characteristic for spruce fire, spruce fire upper limit and juniperus forests, were identified in both types of forests. The explanation of this situation consists in the raised acidity of studied beech forest soils, characteristic feature of spruce fire soils.

Earthworm densities, represented as mean numbers of individuals / m², are shown in Fig. 2. They ranged from < 10 to > 250, with 2 distinct features:

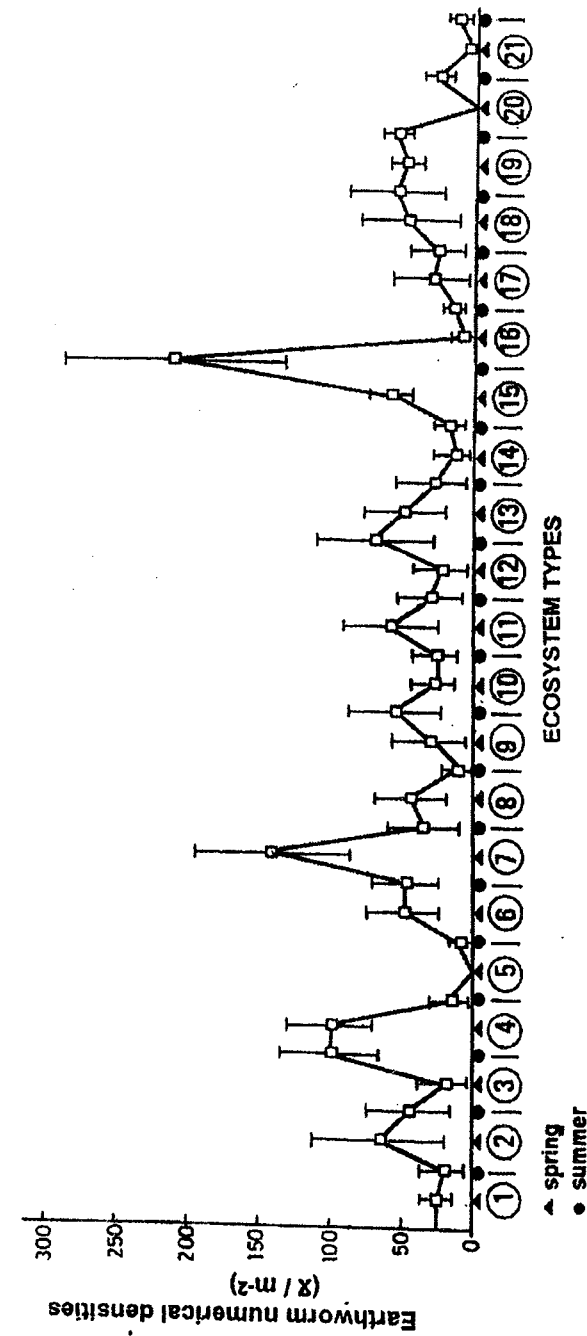


Fig. 2. - Earthworm species densities (mean numbers of individuals/m²).

1. showed differences between ecosystem types; 2. showed differences between seasons, with higher values in spring and lower ones in summer-autumn. This pattern has to be seen as a general feature, with more or less peculiarities, depending on the local conditions of each biotope. Ecosystem number 15 (Poiana Sarata) showed a very distinct exception from this pattern: the highest mean of individuals was in summer. 75% of total individuals identified in this biotope were *A.rosea rosea*, and one quarter of them were immature, which are known to become quiescent during extreme soil conditions (C.A.Edwards and J.R.Lofty, 1972). Since pH, humidity as well as C/N of soils were nearly the same like in the spring, the only explanation of this pattern could be the soil temperature during the summer time (13°C) which was lower than usual and, as a result, the quiescent did not take place.

Spatial distribution. In order to establish the type of spatial distribution of earthworm populations the ratio $\frac{S^2}{x}$ was used, which gives a first image of spatial distribution. Because of its value >1, it could be appreciated that earthworm individuals are distributed according to the grouped model, frequently met in animal species. Grouped distribution comprises many types of spatial distributions, so it is necessary to establish the theoretical type according to which earthworm individuals were distributed. In this sense was tested negative binomial distribution. According to the test, earthworm individuals were distributed corresponding to negative binomial distribution, with probability of 0.05 for observing χ^2 with 3 degrees of freedom smaller and greater in value than 1.175, for *Aporrectodea rosea rosea* in Cocorasti biotope (Table 1).

Table 1

Spatial distribution of *Aporrectodea rosea rosea* according to the theoretical model of negative binomial distribution

| Number of individuals identified in samples | Observed frequency | Expected frequency | $f_1 - f_2$ |
|---|--------------------|-----------------------|-------------|
| | f_1 | f_2 | f_1 |
| 0 | 1 | 2 | 3 |
| 0 | 13 | 11.62 | 0.106 |
| 1 | 3 | 4.06 | 0.353 |
| 2 | 2 | 3.08 | 0.540 |
| 3 | 6 | 5.06 | 0.176 |
| | | 0.352 < 1.175 < 7.815 | |
| | | 0.05 | 0.05 |

Influence of pH, humidity and C/N ratio of soils on earthworm densities.

pH and soil humidity represent the factors that have the greatest influence on earthworm densities. A multiple correlation between earthworm density, as dependent variable and pH and soil humidity, as independent variables, showed a significant

correlation (0.59) during the spring time. The correlation between earthworm densities and C/N is not significant, both during the spring and summer time.

CONCLUSIONS

The study of earthworm densities from different types of forestry ecosystems could be concluded as follows:

- *Aporrectodea rosea rosea* was identified in 17 biotopes, having the highest frequency percent (80%);
- *Octodrilus complanatus* was the most rare species, having the lowest frequency percent (4.8%);
- according to the type of soil and vegetation and soil acidity, two categories (sinuzies) of earthworm species were identified: *A. rosea rosea* - *O. lacteum*, for beech forests and *D. alpina alpina* - *D. octaedra*, for spruce fire, spruce fire upper limit and juniperus ecosystems;
- earthworm densities showed different values between ecosystem types and between seasons, with higher values in beech forests and during spring;
- earthworm individuals were grouped being distributed according to negative binomial distribution;
- pH and soil humidity proved to influence earthworm densities; the multiple correlation between those two independent variables and earthworm densities showed a significant correlation during the spring.

REFERENCES

1. Beldie Al., 1967, *Flora și vegetația Munților Bucegi*, Edit. Academiei R.S.R., 678 p.
2. Easton, E. G., 1983, *Earthworm ecology from Darwin to vermiculture*. 475 - 488 p., Chapman and Hall Ltd., London.
3. Edwards, C. A. and Lofty, J. R., 1972, *Biology of earthworms*. Chapman and Hall Ltd., London.
4. Falcă M., Liliana Oromulu, Viorica Honciuc, 1992, *St. cerc. biol. anim.*, **44**, 2, p. 101-110, București.
5. Falcă M. and Oltean M., 1994, *Mitt. hamb. zool. Mus. Inst.*, Band 89, Ergbd. 2, S. 83 - 87, Hamburg.
6. Paucă Comănescu Mihaela, C. Bândiu, N. Doniță, Tăcină Aurica, Falcă M., H. Almășan, Oromulu Liliana, Honciuc Viorica, Vasu Alexandrina, C. Arion, 1989, *Făgetele din România. Cercetări ecologice*, Edit. Academiei Române, 262 p.
7. Pop V., 1948, *Lumbricidile din România*, Edit. Academiei I, 9, 124 p.

Received February 12, 1999

Institute of Biology
Splaiul Independenței 296

LÉSIONS DU PÉRITOINE CHEZ LES RATS INTOXIQUÉS AVEC DU PLOMB

PAULA PRUNESCU, C.-C. PRUNESCU

Histological and ultrastructural observations on the rat peritoneum after intraperitoneal inoculations with a solution of lead acetate are presented. A typical inflammatory reaction with great accumulation of monocytes, macrophages and multinucleated giant cells developed in the peritoneum. The lead toxic effect consisted of granulomatous cells necrosis and apoptosis. The squamous mesothelial cells of the peritoneum were loaded with significant quantities of lead. The peritoneum inflammation was associated with a diffuse fibrosis.

À la différence de la péritonite chronique, bien décrite dans le saturnisme (1), la péritonite expérimentale provoquée par le plomb n'a pas été étudiée.

L'objet de cette note sera de décrire l'évolution aux niveaux histologique et ultrastructural de la réaction inflammatoire péritonéale chez les rats inoculés par voie intrapéritonéale (ip) avec des sels de plomb.

MATÉRIEL ET MÉTHODES

10 rats mâles jeunes à 70 ± 5 g ont reçu par voie ip. une solution 1% acétate de plomb, contenant 5 mg Pb pour chaque dose, jusqu'à l'occurrence de 50 mg/animal. Les rats ont été sacrifiés après la 6^e et la 10^e inoculation.

Les rats témoins ont reçu des injections avec du sérum physiologique.

Des pièces découpées du tissu péritonéal ont été fixées dans une solution 10% formol salin et incluses dans de la paraffine, d'après les techniques de routine. Les sections histologiques à 5 μ m ont été colorées à l'hémalun-éosine (H.E.) pour l'observation de la topographie générale, la méthode de Perls pour révéler le fer ferrique, le picro-Sirius red pour mettre en évidence la présence du collagène, la coloration Giemsa-colophane pour les cellules d'inflammation (3).

Pour les observations de microscopie électronique de petits fragments de tissu péritonéal ont été fixés dans une solution 2,5% glutaraldéhyde dans le tampon cacodylate pH 7,2 à 4°C, 12 h et postfixés dans une solution 1,33% tétraoxyde d'osmium, pendant 2 h. Le matériel a été inclus dans EPON 812. Les sections ultrafines ont été contrastés avec acétate d'uranyl et citrate de plomb et ont été ensuite étudiées en microscopie électronique par transmission (TEM).

RÉSULTATS

Le péritoine se présente épais, adhérent aux organes viscéraux et parsemé de petites zones inflammatoires de couleur blanchâtre.

Le processus inflammatoire débute par une congestion vasculaire et la présence des nombreuses cellules de petite taille de type lymphoïde et monocytaire.

Les granulomes situés dans les épaisses couches du péritoine se développent par accumulation des monocytes, macrophages, cellules épithélioïdes et cellules géantes multinucléaires (Fig. 1 et 2). Toutes ces cellules accumulent de grandes quantités de plomb. Très souvent on observe des infiltrats aux polynucléaires.

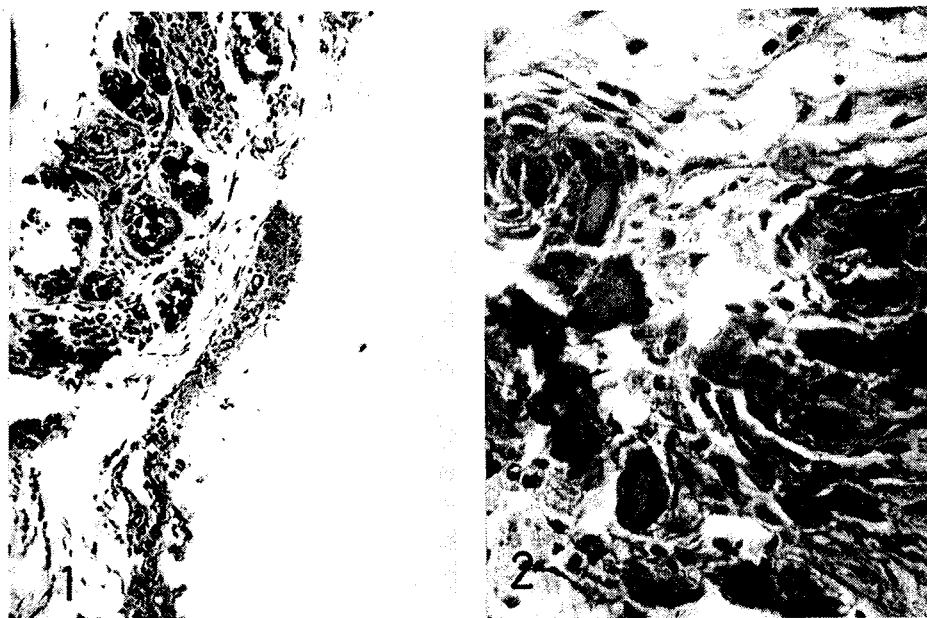


Fig. 1. — Structures granulomateuses dans le péritoine. Picro-Sirius red — H., 140 x.

Fig. 2. — Cellules géantes multinucléaires dans un granulome péritoneal. Perls — H., 560 x.

Les cellules mésothéliales sont chargées d'inclusions contenant du plomb qui se présentent sous forme de granules jaunâtres, sur les sections histologiques colorées par la méthode de Perls.

Le tissu conjonctif du mésothélium péritonéal est infiltré de cellules inflammatoires. De nombreux capillaires aux lumières dilatées traversent le tissu conjonctif (Fig. 3). Dans certaines régions, le péritoine est fibrosé à la suite d'activation des fibroblastes (Fig. 4).

L'étude au microscope électronique relève les détails de la structure ultrafine des cellules du péritoine du rat intoxiqué avec du plomb.

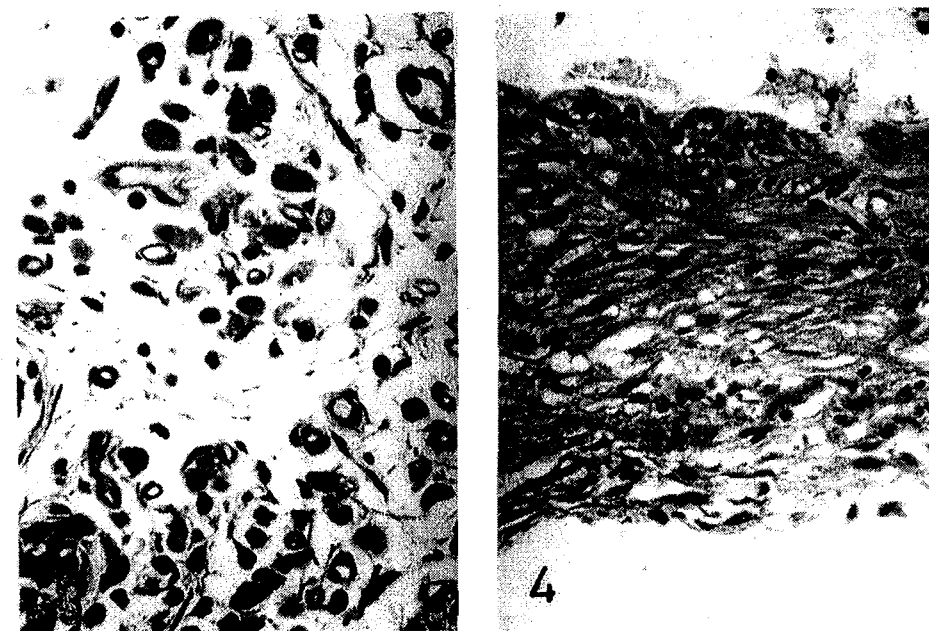


Fig. 3. — Vaisseaux capillaires et l'infiltrat inflammatoire dans le tissu conjonctif qui accompagne le mésothélium péritonéal. H.E., 560 x.

Fig. 4. — Le péritoine inflammé et fibrosé. Picro-Sirius red — H., 560 x.

Les cellules du mésothélium péritonéal sont de grandes cellules aplaties, avec de grands noyaux indentés, de nombreuses mitochondries allongées, le réticule endoplasmique granulaire (ergastoplasme) peu développé et les complexes Golgi situés auprès de noyau. On a observé de nombreuses granules électrodenses dispersées et aussi de grandes agglomérations des blocs électrodenses. Dans unes des cellules épithéliales on peut trouver des vacuoles contenant un matériel électrontransparent ou fin fibrillaire.

Les espaces entre les cellules épithéliales contiennent des filaments orientés parallèlement. Parmi ces faisceaux des filaments avec une structure dépourvue de périodicité sont de nombreuses agglomérations électrodense de plomb. (Fig. 5 et 6).

Les cellules de la série monocyte-macrophage qui participent à la constitution des granulomes sont très souvent lysées par l'action toxique du plomb. Les corps apoptotiques ont été observés fréquemment (Fig. 8). Les cellules épithélioïdes présentent un riche ergastoplasme (Fig. 7). Ces cellules syncyalisent en formant des cellules géantes multinucléaires. On observe le cytoplasme de deux cellules réciproquement indenté (Fig. 7).

Les fibroblastes sont une population cellulaire commune dans le péritoine des animaux témoins. Dans le péritoine inflammé à la suite de l'action toxique du

traitement avec acétate de plomb, des fibroblastes sont stimulés de synthétiser et de déposer le collagène.

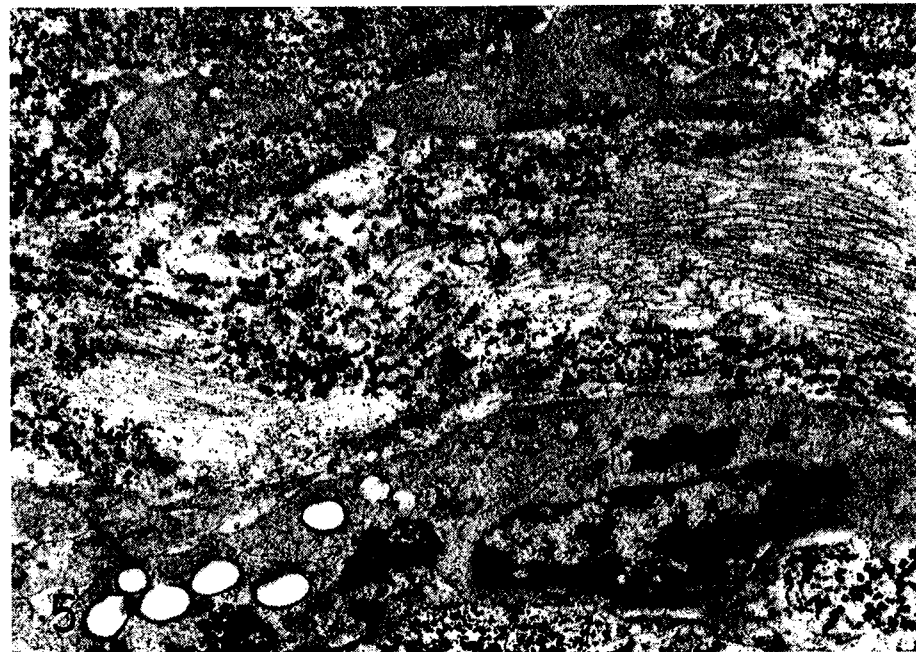


Fig. 5. — Cellules épithéliales péritonéales avec des accumulations importantes de matériel électrodense. Parmi les cellules on remarque des filaments de fibrine et des granules fines électrodenses. 11.000 x.

DISCUSSION

Le péritoine est le premier organe en contact avec la solution toxique d'acétate de plomb et il réagit comme une première barrière entre le toxique et l'organisme. La réaction immédiate de l'organisme face à la présence du toxique est la constitution de «tâches laiteuses» (4): des structures formées par l'agglomération des leucocytes neutrophiles, monocytes, macrophages et cellules multinucléaires géantes, concentrées sur ou entre les couches péritonéales.

Les données de littérature concernant la réaction des cellules de la série monocyte-macrophage sous l'influence des facteurs xénobiotiques présentent des descriptions détaillées sur la genèse et l'évolution des granulomes (5, 6, 7, 8, 9, 10).

La nécrose rapide des macrophages et des cellules géantes est très caractéristique pour la réaction du péritoine face à l'intoxication avec du plomb. Les granulomes péritonéaux constitués après les injections ip. avec du fer polymaltosé ont une existence beaucoup plus longue (11).



Fig. 8. – Monocyte et des corps apoptotiques. 11.000 x.

Pendant l'intoxication avec du plomb, le péritoine s'épaissit sous l'influence des infiltrats des cellules inflammatoires et grâce à l'augmentation de la perméabilité des capillaires péritonéaux qui déterminent l'imbibition excessive de cet organe. Ce processus se développe d'une manière similaire à une inflammation généralisée du péritoine (12). Ces éléments sont caractéristiques aussi pour l'état de la péritonite chronique, signalée dans le saturnisme (1).

Les agrégats de molécules de protéines complexés avec du plomb (13, 14), se concentrent dans le cytoplasme de cellules épithéliales du péritoine dans des formations électrodenses. Ce phénomène est lié à la diminution de l'effet toxique intracytoplasmique du plomb.

Les cellules les plus exposées à l'effet toxique du plomb sont les macrophages surchargées avec des inclusions contenant les complexes protéine-plomb. Les macrophages sont l'objet d'une lyse cellulaire rapide ou d'une apoptose cellulaire. La signification pathologique de l'apoptose, qui s'installe aussi dans l'intoxication avec thioacétamide (15), n'est pas encore assez claire.

La manière non inflammatoire d'élimination des cellules apoptotiques (16) représente un avantage pour le fonctionnement d'un tissu si fragile que le péritoine.

BIBLIOGRAPHIE

1. PAMBUCCIAN GR., 1980, „Morfopatogenia peritoneului” in: *Anatomia Patologică*, vol.2, ed. I, I. Moraru, Ed. Medicală, București, 329-330.

2. MUREȘAN E., BOGDAN A.T., GABOREANU M., BABA A. I., 1976, *Tehnici de Histochemie Normală și Patologică*, Ed. Ceres, București.
3. PUTT F.A., 1972, *Manual of Histopathologic Staining Methods*, John Wiley and Sons Inc., New York, Toronto, Sydney.
4. DOX K., ROUSE R.V., KYEWSKY B., 1986, *Eur. J. Immunol.*, **16** (8): 1029-1032.
5. CLINE M.J., LEHRER R.I., TERRITO M.C., GOLDE D.W., 1978, *Ann. Internat. Med.*, **88**, (1): 78-88.
6. VAN DER RHEE H.J., VAN DER BURGH C.P.M., DAEMS W.T., 1979, *Cell Tissue Res.*, **197** (3): 355-378.
7. PIERCE C.W., 1988: *Am. J. Pathol.*, **98** (1): 9-29.
8. PAPADIMITRIOU J.M., ROBERTSON T.A., 1980, *J. Pathol.*, **130** (2): 782.
9. BAUM H-P., THOENES W., 1985: *Virchow Arch. B, Cell Pathol.*, **50** (2): 181-193.
10. PAPADIMITRIOU J.M. VAN BRUGGEN I., 1986, *J. Pathol.*, **148** (2): 149-158.
11. PRUNESCU C-C., PRUNESCU P., 1988, *Rev Roum. Biochim.*, **25** (4): 355-365.
12. CHOMETTE G., AURIOL M., LE CHARPENTIER Y., LECLERC J.-P., TEREU Y., TRANBLOC P., 1982, *Anatomie Pathologique Speciale*, Tome 1, Edition Marketing, Elipse.
13. SCHOLMERICH J., OCHS A., 1991, “Trace elements” in: *Oxford Textbook of Clinical Pathology* vol. 1, N. McIntyre, J-F. Benhamou, J. Richter eds., Oxford University Press, 211-220.
14. ARTHUR M. J. P., 1992, “The metalloproteinases” in: *Cellular Aspects of Cirrhosis*, B. Clement, A. Guillouzo eds., Col. INSERM, John Libbey Eurotext, vol. 216, 235-244.
15. LEDDA-COLUMBANO G.M., CONI P., CURTO M., GIACOMINI L., 1991, *Am. J. Pathol.*, **139** (5): 1099-1109.
16. COHEN J.J., 1993, *Immunology Today*, **14** (3), 126-129.

*Institut de Biologie, 296 Splaiul Independenței
P.O.Box 56-53, Bucarest, Roumanie*

CORRIGENDA

In the paper of D. CURCĂ, published under the title of "Ascorbinemia and serum cholinesterase activity in industrial intensive system-raised suine", appeared in REV. ROUM. BIOL.-BIOL. ANIM., TOME 42, N^o 2, P. 193-200, BUCAREST, 1997, at page 196, caption of fig. 4, the reader is kindly requested to read:

- P: L, instead of p: L;
- S: F, instead of S: W.

AVIS AUX COLLABORATEURS

La «Revue roumaine de biologie – Série de biologie animale» publie des articles originaux d'un haut niveau scientifique de tous les domaines de la biologie animale: taxonomie, morphologie, physiologie, génétique, écologie, etc. Les sommaires des revues sont complétés par d'autres rubriques, comme: 1. La vie scientifique, qui traite des manifestations scientifiques du domaine de la biologie, symposiums, conférences, etc. 2. Comptes rendus des livres de spécialité.

Les auteurs sont priés de présenter leurs articles en double exemplaire imprimés, de préférence, sur une imprimante laser et espacés à double interligne. Le contenu des articles sera introduit sur de petites disquettes, dans un langage connu, préférentiellement Word 6.0. La composition et la mise en vedette seront faites selon l'usage de la revue – caractères de 11/13 points pour le texte, de 12/14 points pour le titre de l'article et de 9/11 pour les annexes (tableaux, bibliographie, explication des figures, notes, etc.) et le résumé, qui sera placé au début de l'article. Il est obligatoire que sur les disquettes il soit spécifié le nom des fichiers ainsi que le programme utilisé.

Le matériel graphique sera envoyé sur disquette, scanné, avec les mêmes spécifications. En l'absence d'un scanner, le matériel graphique sera exécuté en encre de Chine sur papier calque.

Les tableaux et les illustrations seront numérotés en chiffres arabes. La répétition des mêmes dans le texte, les tableaux et les graphiques sera évitée. Les tableaux et l'explication des figures seront imprimées sur des pages distinctes.

Les références seront citées dans le texte par des chiffres arabes et numérotés consécutivement dans l'ordre de l'apparition. Le nom des auteurs sera précédé des initiales. Les titres des revues seront abrégés conformément aux usages internationaux.

Les travaux seront accompagnés d'un court résumé en anglais de 10 lignes au maximum. Les textes ne doivent pas dépasser 7 pages (y compris les tableaux, la bibliographie et l'explication des figures).

La responsabilité pour le contenu des articles revient exclusivement aux auteurs.

La correspondance qui concerne les manuscrits sera envoyée à l'adresse du Comité de rédaction: P.O. Box 2-2, 78200 Bucarest 2, Roumanie.